STRUCTURE AND FUNCTION RELATIONSHIP OF PORCINE PYRIDOXAL KINASE

A thesis submitted to

The Hong Kong Polytechnic University

for the Degree of Master of Philosophy

in Biochemistry and Molecular biology

By

FUNG Long-yan

1999

TABLE OF CONTENTS

LIST OF FIGURES

LIST OF TABLES

LIST OF APPENDICES

DECLARATION

This thesis is written according to the experimental work undertaken solely by the candidate. It has not been accepted in any previous application for a degree.

All quotations have been distinguished by quotation marks and all sources of information have been acknowledged.

Signed

Long-yan Fung

ACKNOWLEDGMENTS

I would like to express my sincere thanks to my supervisors, Dr. Samuel Lo and Prof. Francis Kwok, for their excellent supervision, invaluable advice, constructive criticism, discussions and encouragement throughout my M.Phil. study.

I would like to give my deeply thanks to Dr. C.K Lau for his kind assistance, encouragement and enormous support over these years.

I would like to thank Prof. J.E. Churchich for his invaluable comments, suggestions, assistant and support in my project.

I would also like to thank the technicians in the Department of Applied Biology and Chemical Technology since they provided tremendous technical support in my project.

Finally I would like to thank my family for their endless support and encouragement.

LIST OF ABBREVIATIONS

ADP	Adenosine 5'-diphosphate
AP_4-PL	Adenosine Tetraphosphate Pyridoxal
ATP	Adenosine 5'-triphosphate
BSA	Bovine Serum Albumin
CD	Circular Dichroism
c^7dGTP	7-deaza-2'-deoxyguanosine 5'-triphosphate
dATP	2'3'-Deoxyadenosine 5'-triphosphate
dCTP	2'3'-Deoxycytidine 5'-triphosphate
ddATP	2'3'-Dideoxyadenosine 5'-triphosphate
ddCTP	2'3'-Dideoxycytidine 5'-triphosphate
ddGTP	2'3'-Dideoxyguanosine 5'-triphosphate
ddH_2O	Distilled Deionized Water
DDT	DL-Dithiothreitol
DMSO	Dimethyl Sulfoxide
DNA	Deoxyribonucleic Acid
dTTP	2'3'-Deoxythymidine 5'-triphosphate
ddTTP	2'3'-Dideoxythymidine 5'-triphosphate
DEAE	Diethylaminoethyl
EDTA	Ethylenediaminetetraacetic Acid
FMN	Flavin Mononucleotide
FPLC	Fast Perfomance Liquid Chromatography
GdnHCl	Guandinium hydrochloride

HPLC	High Pressure Liquid Chromatography
IAF	Iodecetamide Fluorescein
IDA	Iminodiacetic Acid
IPTG	Isopropyl β-D-thiogalactopyranoside
k_{cat}	Catalytic Constant
K_m	Michaelis constant
LB	Luria-Bertani
OPA+	One-Phor-All Buffer *PLUS*
4-PA	Pyridoxic Acid
PAGE	Polyacrylamide Gel
PCR	Polymerase Chain Reaction
PK	Pyridoxal Kinase
PL	Pyridoxal
PLP	Pyridoxal 5'-Phosphate
PM	Pyridoxamine
PMP	Pyridoxamine 5'-Phosphate
PN	Pyridoxine
PNP	Pyridoxine 5'-Phosphate
SDS	Sodium Dodecylsulphate
TBE	Tris-borate EDTA
TBS	Tris-Buffered Saline
TBST	Tris-Buffered Saline Tween-20
TCA	Trichloroacetic acid
TNP-ATP	Trinitrophenyl-ATP

WT	Wild-Type
X-Gal	5-Bromo-4-chloro-3-indolyl-β-D-galactopyranoside

SUMMARY

Recombinant truncated mutants of pyridoxal kinase lacking a series of amino acid residues at the N-terminal domain have been constructed. Deletion of 15 amino acid residues does not inactivate the kinase, whereas deletion of 16, 17, 18, and 21 or more amino acid residues, pertaining to the highly conserved sequence, RVLSIQHV, abolishes the catalytic function of the expressed enzyme. All species of recombinant pyridoxal kinase were purified using a method that a chain of histidine residues were tagged at the N-terminal of the protein. Wild-type, Δ15 and Δ16 variants of pyridoxal kinase were purified to homogeneity by two chromatographic steps including metal-chelating and DEAE ion exchange chromatographies. Purified enzymes were characterized by using circular dichroism (CD) and fluorescence spectroscopy with respect to the folding pattern of the protein. Results indicate that deletion of 16 amino acid residues initiates a misfolding pattern for the protein leading to subsequent loss of their ability to bind an ATP analogue, Trinitrophenyl-ATP (TNP-ATP), *in vitro*. The stability of wild-type and Δ15 mutant in the presence of guandinium hydrochloride (GdnHCl) was also examined using fluorescence spectroscopy. Results have shown that the unfolding process of the wild-type protein proceeds through a concerted reaction, whereas the denaturation process of the mutants (Δ15 and Δ16) endowed with and without catalytic activity shows a biphasic pattern of unfolding in GdnHCl. It is concluded that deletion mutants of pyridoxal kinase are not only less stable than the wild-type species, but they also follow different folding pathways.

CHAPTER ONE

LITERATURE REVIEW

I. LITERATURE REVIEW

1.1 INTRODUCTION

Vitamin B_6 is unique among the water-soluble vitamins with respect to the numerous functions it serves and its metabolism and chemistry. Figure 1 depicts the various forms of vitamin B_6, including the phosphorylated forms. The names and abbreviations commonly used for the three principal forms of vitamin B_6, their phosphoric esters, and analogues are as follows: pyridoxine, PN; pyridoxal, PL; pyridoxamine, PM; pyridoxine 5'-phosphate, PNP; pyridoxal 5'-phosphate, PLP; pyridoxamine 5'-phosphate; PMP; 4-pyridoxic acid, 4-PA. The coenzyme form of vitamin B_6, PLP, is found covalently bound to enzymes via a Schiff base with an ε-amino group of lysine in the protein. Figure 2 depicts the formation of a Schiff base with PLP and an amino acid. Due to the strong electron-attracting character of the pyridine ring, electrons are withdrawn from one of the three substituents (alkyl group, hydrogen, or carboxyl group) attached to the α-carbon of the substrate attached to PLP. This results in the formation of a quinonoid structure. PLP has been reported to be a coenzyme for over 100 enzymatic reactions (Sauberlich, 1985). Different types of enzymatic reactions catalyzed by PLP are classified according to whether the reactions occurring at the α-, β-, or γ-carbon as listed in Table I. The involvement of the active form of vitamin B_6, PLP, in such a wide

spectrum of enzymatic reactions is an indication of the importance of this vitamin.

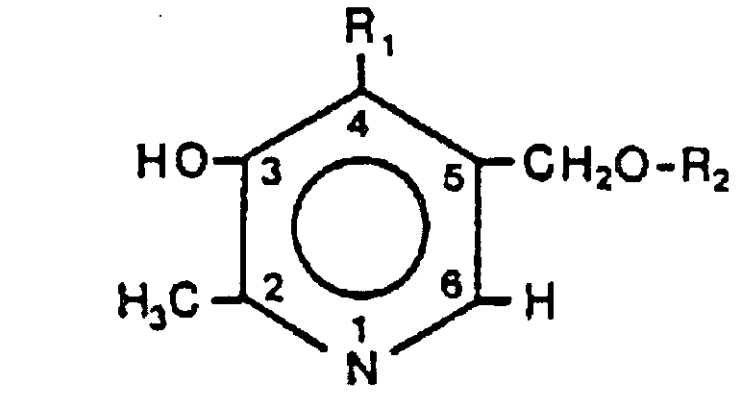

FIGURE 1: Structure of Vitamin B_6

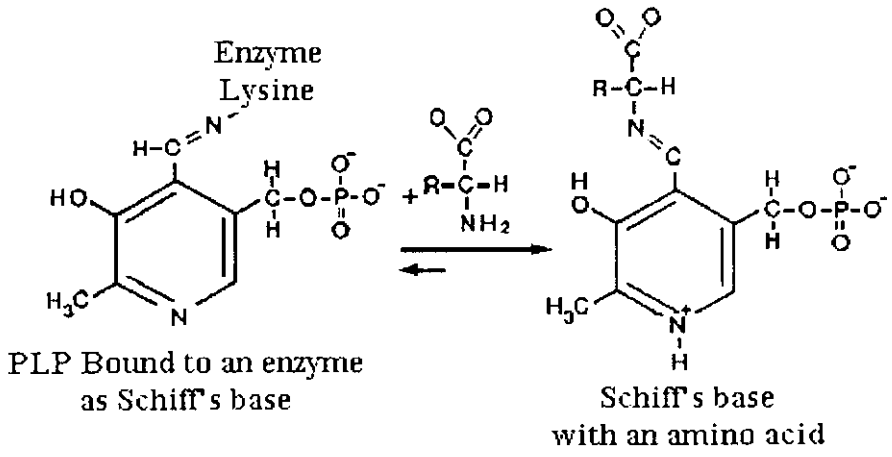

FIGURE 2: Schiff base formation between pyridoxal-5'-phosphate and an amino acid

TABLE I: Enzymatic Reactions Catalyzed by Pyridoxal 5'-Phosphate

Type of reaction	Typical reaction or enzyme
Reactions involving α-carbon	
Transamination	Alanine → pyruvate + PMP
Racemization	D-Amino acid $\rightleftarrows$ L-amino acid
Decarboxylation	5-OH Tryptophan → 5-OH tryptamine + CO_2
Oxidative deamination	Histamine → imidazole-4-acetaldehyde +NH_4^+
Loss of the side chain	THF + Serine → glycine + N5, 10-methylene THF
Reacitons involving β-carbon	
Replacement (exchange)	Cysteine synthetase
Elimination	Serine and threonine dehydratase
Reaction involving the γ-carbon	
Replacement (exchange)	Cystathionine → cysteine + homoserine
Elimination	Homocysteine desulfhydrase
Cleavage	Kynurenine → anthranilic acid

Extensive work by Lumeng and coworkers using on dogs (Lumeng *et al*, 1974) and rats (Lumeng and Li, 1980) has shown that the liver is the primary organ responsible for metabolism of vitamin B_6 and supplies the active form of vitamin B_6, PLP, to the circulation and other tissues. The primary interconversion of B_6 vitamins is depicted in Figure 3. Three nonphosphorylated forms are converted to their respective phosphorylated forms by pyridoxal kinase (ATP: pyridoxal 5'-phosphotransferase, EC 2.7.1.35). The two phosphorylated forms, pyridoxamine-5' phosphate and pyridoxine- 5'-phosphate, are converted to PLP via a flavin mononucleotide requiring oxidase (Wada and Snell, 1961). Dephosphorylation of the 5'-phosphate compound occurs by action of a phosphatase.

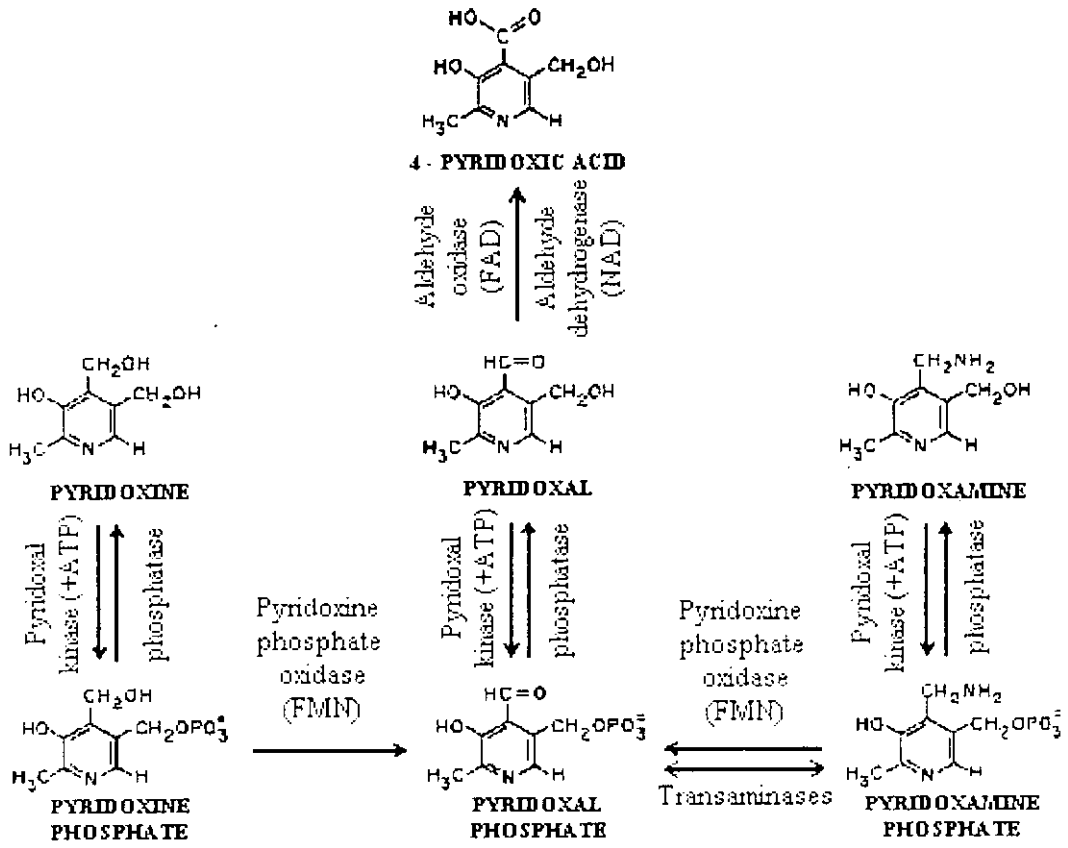

FIGURE 3: Metabolic interconversions of the B_6 vitamins

The involvement of PLP in a multiplicity of enzymatic reactions (Sauberlich, 1968) suggests that it would serve many functions in the body. Table II lists several of the known functions of PLP (Leklem, 1988). There are numerous diseases or pathological conditions such as coronary heart disease, premenstrual syndrome, sickle-cell anemia, asthma and carpal tunnel syndrome that will occur when vitamin B_6 metabolism is altered. Hence, controlling the metabolism of vitamin B_6, is necessary.

TABLE II: Cellular Processes Affected by Pyridoxal-5'-Phosphate

Cellular process or enzyme	Function/System influenced
1-carbon metabolism, hormone modulation	Immune function
Glycogen phosphorylase, transamination	Gluconeogenesis
Tryptophan metabolism	Niacin formation
Heme synthesis, transamination, O_2 affinity	Red cell metabolism and formation
Neurotransmitter synthesis, lipid metabolism	Nervous system
Hormone modulation, binding of PLP to lysine on hormone receptor	Hormone modulation

1.2 BACKGROUND OF RESEARCH

Pyridoxal kinase is an enzyme that catalyzes the formation of PLP from pyridoxal in the presence of ATP and a divalent ion. This enzyme has been found in many mammalian and bacterial sources. In 1961, McCormick *et al* conducted a detailed survey on the presence of pyridoxal kinase in various rat and bovine tissues and found that the brain is a rich source of this enzyme.

Several procedures for the purification of pyridoxal kinase were developed. From bovine brain, pyridoxal kinase was isolated with a 2000-fold purity (Neary and Diven, 1970), using a combination of ammonium sulphate fractionation, DEAE-cellulose chromatography, sephadex G-100 and ADP-agarose. Similar procedures were adopted to purify sheep liver pyridoxal kinase with a 1100- fold of purification (Karawya and Fonda, 1978). A different approach of purification steps involving ammonium sulphate fractionation, CM-sephadex chromatography, hydroxyapatite chromatography, sephadex G-100 and 4-deoxypyridoxyl sepharose was followed to purify pig brain pyridoxal kinase by Kwok and Churchich, (1979) with a 2000-fold purity. An affinity chromatographic step using pyridoxal-agarose was developed by Cash *et al* (1980). The pyridoxal group was linked onto ω-aminoctyl agarose through a Schiff base formation. The agarose gel, derivatized with a pyridoxyl group, displays binding to pyridoxal kinase via interaction between the pyridoxyl and the

substrate binding site of the enzyme. Pyridoxal kinase was purified 9000-fold from sheep brain by a procedure involving ammonium sulphate fractionation, DEAE-cellulose chromatography, pyridoxyl-agarose chromatography and gel filtration chromatography. Besides the mammalian sources, pyridoxal kinase was partially purified from bacterial sources (McCormick *et al*, 1961). Recently, pyridoxal kinase was purified 4300-fold from a parasitic protozoa, *Trypanosoma brucei*, using three chromatographic steps (Scott and Phillips, 1997) involving Resourace Q w/w, pyridoxal-agarose and phenyl superose 5/5.

Pyridoxal kinase is a homodimer with two identical subunits. Apparent molecular weights of pyridoxal kinase purified from different sources varied as shown in Table III. Kinetic parameters of its substrates, pyridoxal and ATP, are also shown in Table IV.

TABLE III: Molecular weight of pyridoxal kinase from various sources.

Sources	Molecular weight (Dalton)
Pig brain	60000[a]
Sheep brain	80000[b]
Bovine brain	80000[c]
Trypanosoma brucei	74000[d]

[a] Kwok and Churchich, 1979
[b] Kerry *et al*, 1986
[c] Sakurai *et al*, 1993
[d] Scott and Philips, 1997

TABLE IV: Kinetic values of various pyridoxal kinase, K_m values are expressed as μM

Compounds	Rat liver[a]	Pig brain[b]	Sheep brain[c]	Pig liver[d]	Bovine brain[e]	*Trypanosoma brucei*[f]
Pyridoxal	15	25	40	125	91	22
ATP	---	12	20	59	210	9

[a] McCormick and Snell, 1961
[b] Kwok and Churchich, 1979
[c] Kerry *et al*, 1986
[d] Tagaya *et al*, 1989
[e] Sakurai T *et al*, 1993
[f] Scott and Phillips, 1997

In the last twenty years, several experiments have been completed with respect to the catalytic mechanism and structural information on pyridoxal kinase. A study conducted by Neary *et al* (1970) showed that pyridoxal kinase required a divalent metal ion for enzymatic activity. Among metal ions including Zn^{2+}, Co^{2+}, Mn^{2+}, Mg^{2+}, and Fe^{2+}, zinc has been found to be the most effective ion in the kinase reaction *in vitro*. The role of zinc ions in this reaction involves the formation of a $ZnATP^{2-}$ complex with ATP. This complex serves as the phosphate donor in the phosphorylation of vitamin B_6 compounds. In most tissues, zinc is associated with metal-binding ligands such as metallothionein. Churchich *et al* (1989) reported on the relationship between metallothionein and zinc bound to the pyridoxal kinase. No interaction between metallothionein and pyridoxal kinase in the mechanism of activation was shown. However, ATP was shown to promote the release of Zn^{2+} from metallothionein. This suggests that Zn^{2+} -metallothionein may act as a mediator of pyridoxal

kinase activity by providing a reservoir of transferrable Zn^{2+} that serves as a source of $ZnATP^{2-}$ for the kinase reaction.

The substrate binding sites of pyridoxal kinase were characterized previously by many laboratories in the past. The interactions between pyridoxal and the kinase was investigated by means of emission anisotropy (Kwok and Churchich, 1979a). Results revealed that pyridoxal was not rigidly trapped by the protein matrix. The fluorescence probe, *N*-dansyl-2-oxopyrrolidine which is a competitive inhibitor with respect to ATP was shown to be immobilized by strong interactions at a hydrophobic portion of the protein, indicating that the nucleotide binding site of pyridoxal kinase was highly hydrophobic. Results were further confirmed by the primary sequence of the kinase.

Irradiation of the kinase in the presence of riboflavin leads to irreversible loss of catalytic activity (Kwok and Churchich, 1979). Results have found that histidine is involved in the binding of the substrate ATP to the catalytic site of pyridoxal kinase, since histidine and to a certain extent tyrosine and tryptophan are more susceptible to chemical modification upon illumination in the presence of flavins. Amino acid analysis indicated a progressive decrease in the histidine content but no change in the cysteine, tyrosine, and tryptophan content of inactiviated samples has occurred during the photooxidation process. Furthermore, the rate of photoinactivation of pyridoxal kinase is influenced by the presence of

substrate ATP but no protection against photoinactivation is affected by the substrate pyridoxal.

Other experimental results indicated that an essential tyrosine residue is present at the pyridoxal-binding site of pyridoxal kinase (Scholz and Kwok, 1989). Photoirradiation of pyridoxal kinase was performed in the presence of 4-benzoylbenzoic acid which is a competitive inhibitor to pyridoxal kinase and resulted in an irreversible loss of enzymatic activity. This photoinactivation was prevented by the presence of pyridoxal. Amino acid analysis and reaction with tetranitromethane revealed that one tyrosine residue per subunit was modified during photoinactivation.

Pyridoxal kinase purified from sheep brain by Kerry *et al* (1986) revealed that there are two domains per subunits in this dimeric enzyme by means of high magnification electron microscopy. Results showed that a 'cleft', which trapped negative-staining material, was observed running across the protein mass of one subunit of the pyridoxal kinase, indicating that each subunit contains a cleft that splits the monomer into two domains. When pyridoxal kinase was exposed to 2M GdnHCl, it dissociated into two subunits with the catalytic activity conserved. Moreover, pyridoxal kinase treated with crosslinking reagent 4,4' dimaleimidestilbene 2,2' disulfonic acid, which is specific for SH groups, the catalytic function of the kinase was shown not to be impaired. Hence, the two subunits function

independently during catalysis and monomeric species are catalytically competent (Kwok *et al.*, 1987).

Each of the two identical subunits of pyridoxal kinase contained two domains that were expected to contain binding sites for different substrates, e.g. ATP, pyridoxal. Limited chymotryptic digestion of pyridoxal kinase yields two fragments of proteins (Dominici *et al*, 1988, 1989 and Churchich, 1990). This was based on the assumption that cleavage of pyridoxal kinase by limited proteolysis was restricted to sites on the flexible polypeptide chain connecting two structural domains. If the immediate environment surrounding the substrate binding sites remain intact, binding experiments of substrate analogues can be performed on these two protein fragments to locate the substrate binding sites in which domains. Both fragments of 24 and 16 kDa were shown concomitant loss of catalytic activity. Fragments separated by chromatographic techniques were examined for interaction with ATP analogue, trinitrophenyl-ATP (TNP-ATP) using fluorescence spectroscopy (Dominici *et al*, 1989). The emission band of TNP-ATP is significantly enhanced upon the addition of 24 kDa fragment, suggesting that the nucleotide binding site is located at the 24 kDa fragment, and proteolysis has not perturbed the topography of the nucleotide binding site.

Effect of proteolysis on the binding of each fragment to pyridoxal analogues was tested by affinity chromatography and emission

spectroscopy. In affinity chromatography, AH-Sepharose 4B derivatized with pyridoxal was found to retain native pyridoxal kinase. In marked contrast to the native enzyme, none of the fragments is retained by pyridoxal-Sepharose (Dominici *et al*, 1989). After mixing pyridoxaloxime with the native kinase, the fluorescence of the oxime is 80 % quenched. Under similar experimental conditions, about 10 % quenching of pyridoxal oxime was observed in the presence of the fragment of 24 kDa, but no quenching effect was detected in the presence the 16 kDa fragment (Churchich *et al*, 1990). Furthermore, pyridoxal is the only substrate that exerts a protective effect against proteolysis. Results strongly suggest that cleavage of some chemical bonds joining the two structural domains of the kinase is essential for opening the conformation of the pyridoxal binding site on the protein. Therefore, possibility exists that the pyridoxal binding site comprises of amino acid residues that are located in the flexible polypeptide chain that is susceptible to chymotryptic attack and not on the other two domains.

The nucleotide affinity label, adenosine tetraphosphate pyridoxal (AP_4-PL), was used to locate amino acid residues involved in the binding of pyridoxal, and ATP (Dominici *et al*, 1988). The affinity label probed a peptide fragment and was purified by HPLC using a reverse phase column. The fragment was subjected to protein sequencing by Edmand degradation. The amino acid composition of the fragment was VDAVVGAGDLAAMLLATXHKF which was localized in the 24 kDa

fragment of chymotryptic digestion (Dominici *et al*,1989). The X labeled on the peptide sequence corresponded to a lysine residue derivated by AP_4-PL. Thus, AP_4-PL inactivated the kinase by reacting specifically with one lysyl residue. It is postulated that the modified lysyl residue is involved in direct interactions with phosphoryl groups of ATP.

Owing to the fact that neither ATP nor pyridoxal bind to the 16 kDa fragment, the functional role of this fragment remains unknown. However, a small peptide that belonged to the 16 kDa fragment was probed by iodoacetamide fluoresceine (IAF) (Churchich, 1990). IAF binds to a specific cysteinyl residue of this fragment. The fragment was isolated and sequenced by Edman degradation. The amino acid sequence is TVSAMXHVLQR, where X corresponds to the cysteinyl residue.

Stability of the pyridoxal kinase in the presence of denaturing agents was investigated (Pineda and Churchich, 1993) by incubating with lower concentration range (0-2 M) of GdnHCl. It revealed that pyridoxal kinase underwent a cooperative structural transition in solutions containing 0.2–1.5 M GdnHCl. This transition alters the secondary structure of the protein. The denaturation of pyridoxal kinase by GdnHCl is a reversible process, and the catalytic activity is completely restored upon refolding of the protein by dialyzing away the GdnHCl. By using fluorescent analogs of ATP and pyridoxal to bind to the enzyme in the presence of GdnHCl, it was revealed that the two structural domains of the enzyme pyridoxal

kinase differ in their stability with respect to GdnHCl, the nucleotide domain is more stable than the pyridoxal domain of the kinase.

1.3 AIMS AND OBJECTIVES

Despite results of studies described previously which revealed some aspects of the tertiary structure of pyridoxal kinase, little is known about the chemical nature of the amino acid residues participating in the catalytic events. Identification and characterization of cDNAs encoding pyridoxal kinase from bacteria (Yang *et al*, 1996) and mammals (Hanna *et al.*, 1997 and Gao *et al.*, 1998) have been reported by several laboratories in the last three years. Identification of the pyridoxal kinase gene now permits detailed analysis of the enzyme function at the molecular level. Mutagenesis, deletion and replacement of specific amino acid residues, will help to define the role played by the structural domains of pyridoxal kinase. Sequence comparisons of three mammalian sources of pyridoxal kinase revealed highly conserved sequences of the protein (Figure 4). However, the N-terminal region of pig brain pyridoxal kinase contained large extensions of polypeptide as compared with its eukaryotic homologues. In order to investigate if the N-terminal region of pyridoxal kinase is essential for catalysis or protein folding mechanism, it is aimed to prepare truncated pyridoxal kinase at the N-terminal region and investigate the effects on enzyme activity and folding of the tertiary structure. Using site-directed mutagenesis, various pyridoxal kinases with deleted N-terminal regions could be produced and examined.

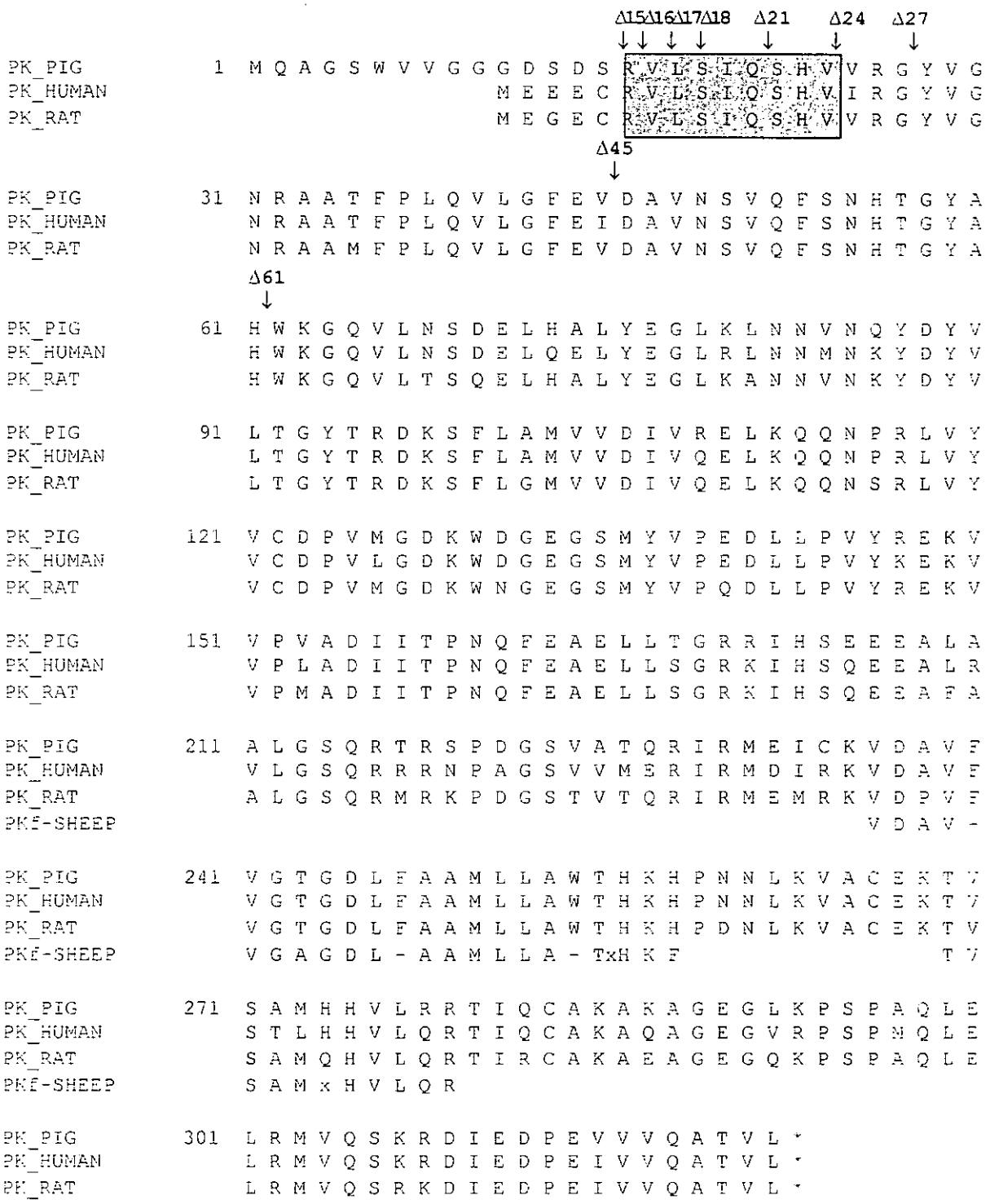

FIGURE 4: Alignment of pyridoxal kinase sequences. DNA sequence alignment of pig brain cortex (PK_PIG, AF041255[a]), human (PK_HUMAN, U89606[b]), Norway rat liver (PK_RAT, AF020346[c]) pyridoxal kinase and two pieces of sheep fragment sequence (PKf_SHEEP). The position of each deletion mutants is shown by an arrow. The grayed region is the highly conserved sequence at the N-terminus. [a,b,c]GenBank Accession number.

1.4 STRATEGIES AND METHODS USED

Polymerase chain reaction was used to construct a series of N-terminal truncated mutants with specific 5'-end primer and one universal 3'-end primer (Figure 5). The constructed mutants were expressed in *E.coli.* Expressed mutant proteins were purified to homogeneity by two chromatographic steps including metal-chelating and DEAE-chromatographies. The purified mutant proteins were examined by using activity assay, circular dichroism and fluoresence spectroscopy.

(A)

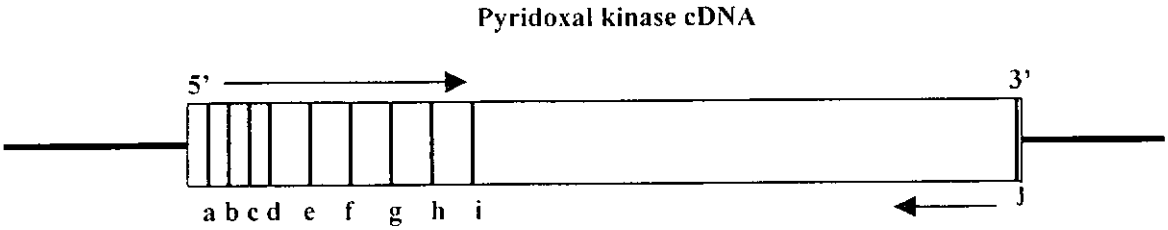

(B)

		Mutants	Primer sequence
5' primers	a	Δ15	5'GGC *AAG CTT* CGG GTG CTC TCC ATT C3'
	b	Δ16	5'GGC *AAG CTT* GTG CTC TCC ATT CAG3'
	c	Δ17	5'GGC *AAG CTT* CTC TCC ATT CAG AGC3'
	d	Δ18	5'GGG *AAG CTT* TCC ATT CAG AGC CAC3'
	e	Δ21	5'GGG *AAG CTT* AGC CAC GTC GTC CGC3'
	f	Δ24	5'GGG *AAG CTT* GTC CGC GGC TAC GTG3'
	g	Δ27	5'GGG *AAG CTT* TAC GTG GGC AAC CGA3'
	h	Δ45	5'GGG *AAG CTT* GAT GCA GTG AAT TCT GTC3'
	i	Δ61	5'GGG *AAG CTT* TGG AAG GGG CAG GTG3'
	j	3'primer	5'GGG ATC GAT CAC AGC ACC GTG GC3'

FIGURE 5: Schematic diagrams of pyridoxal kinase cDNA (A) and the primers used for mutagenesis (B). The *Hin*dIII site is shown in italic type. The sequence primed on the pyridoxal kinase cDNA is underlined.

CHAPTER TWO

EXPERIMENTAL PROCEDURES

II. EXPERIMENTAL PROCEDURES

Useless stated, otherwise all the standard procedures for molecular biology were performed according to Sambrook et al., 1989. The reagents and solutions with * were listed in Appendix I.

2.1 CONSTRUCTION OF PYRIDOXAL KINASE N-TERMINAL MUTANTS

N-terminally truncated mutagenesis of pig brain pyridoxal kinase was carried out by polymerase chain reaction (PCR) methodology (Vallette *et al.*, 1989, Kadowaki *et al.*, 1989). Expand™ High Fidelity PCR System (Boehringer Mannheirm, USA) was used in the PCR.

2.1.1 Preparation of primer

Primers were synthesized by Integrated DNA Technologies (U.S.A.) with standard purification. The primers were resuspended in sterilized distilled deionized water (ddH_2O) to a final concentration of 100 μM as a stock solution and stored in –20°C until use. 20 μM working primer solution was prepared from the stock by diluting 5 fold and stored in –20°C.

2.1.2 Operation of the Expand™ High Fidelity PCR system

The procedure was performed according to the manufacturer's instructions. Two master mixes were set up. Each final volume was 25 μl made up by ddH_2O. The master mix One contained 200 μM

each of dATP, dCTP, dGTP and dTTP, 300 nM each of downstream and up stream primers and about 0.1 μg template DNA. Concentration of DNA was measured by A_{260}. One unit of absorbance represented 50 μg of double stranded DNA. The construct, PK-pAED4, (Appendix II) containing the pyridoxal kinase gene was used as template for PCR. The master mix Two contained 10 μl 10X Expand HF buffer with 15 mM $MgCl_2$ and 2.6 U Expand™ High Fidelity PCR system enzyme mix. During operation, all the reagents were kept on ice except enzyme mix that was always stored at –20°C. 25 μl master mix One was transferred to a sterilized thin-walled PCR tube and placed in the Perkin Elmer GenAmp 9600 Thermocycler (U.S.A.). A hot start and touch down program was performed as follows. Initial denaturation of master mix One was performed for 5 min at 95°C. Subsequently, 25 μl of master mix Two was added immediately. Thirty amplification cycles each of (95°C for 45s, 60°C for 45s, 72°C for 90s) were performed with a 0.3°C decrease at each cycle. Final extension was carried out at 72°C for 10 min. The reaction was stopped at 4°C and the PCR product was subjected to agarose gel electrophoresis.

2.2 AGAROSE GEL PREPARATION

0.8 % agarose gel electrophoresis was used to check the homogeneity of the PCR product. Powdered agarose (0.8 g) was added to 100 ml of electrophoresis buffer (0.5x TBE)* in an Erlenmeyer flask. The slurry was heated in a microwave oven until the agarose melted. The solution was cooled to 60°C and ethidium bromide at a final concentration of 0.5 μg/ml was added and mixed thoroughly. With the comb in place, the warm agarose was poured into the mold. After the gel was completely set, it was placed in the electrophoresis tank. Enough electrophoresis buffer was filled into the electrophoresis tank to cover the gel to a depth of about 1 mm above the agarose gel. Samples were mixed with the gel-loading buffer III (0.25 % bromophenol blue, 0.25 % xylene cyanol FF, 30 % glycerol in water). The mixture was slowly loaded into the well of the submerged gel. Marker DNAs of known sizes were loaded into the slots on the right or left sides of the gel. Constant voltage of 100 v was applied. When the bromophenol blue and xylene cyanol FF had migrated about half of the length of the gel, electrophoresis was stopped. The gel was removed and examined under ultraviolet light. Three types of molecular weight markers were used in the agarose gel electrophoresis. DNA Molecular Weight Marker III (0.12-21.2 kbp) was purchased from Boehringer Maninheim (Appendix III), 100 Base-Pair Ladder was purchased from Pharmacia Biotech, U.S.A. (Appendix IV) and λDNA *Hin*dIII digested fragment was prepared as follows.

2.3 PREPARATION OF λDNA *Hin*dIII DIGESTED MARKER

50 μg of λDNA was mixed with 100 units of *Hin*dIII restriction enzyme in One-Phor-All Buffer *PLUS* (OPA+) (Appendix V). The reaction mixture was incubated at 37°C for 6 hour. One μl of the reaction mixture was used in 0.8 % agarose gel electrophoresis to confirm complete digestion. Then the completely digested reaction mixture was heated at 85°C to inactivate the *Hin*dIII restriction enzyme. Gel-loading buffer III (0.25 % bromophenol blue, 0.25 % xylene cyanol FF, 30 % glycerol in water) was added and kept at 4°C until use.

2.4 RECOVERY OF THE DNA FROM LOW-MELTING TEMPERATURE AGAROSE GEL

2.4.1 Preparation of Phenol

Hydroxyquinoline to a final concentration of 0.1 % was added to liquified phenol at 68°C. An equal volume of 0.5 M Tris buffer (pH8.0) was added to the molten phenol. The mixture was stirred for 15 minutes and allowed to stand. When the two phases were separated, the upper aqueous phase was discarded. An equal volume of 0.1 M Tris (pH8.0) was added to the phenol. The mixture was stirred for another 15 minutes and the upper aqueous phase was again discarded. The extraction was repeated until pH of the phenolic phase was greater than 7.8. After the phenol was equilibrated and the final aqueous phase has been removed, 0.1 volume of 0.1 M Tris (pH8.0) containing 0.2 % β-mercaptoethanol

was added. The phenol solution was stored in this manner under 100 mM Tris (pH8.0) in a light-tight bottle at 4°C for periods of up to 1 month.

2.4.2 Preparation of Chloroform

Twenty-four parts of chloroform were mixed with one part of isoamyl alcohol and stored in brown bottle at room temperature.

2.4.3 DNA recovery from Low-melting temperature agarose gel

Preparation of 0.8 % low-melting temperature agarose gel was the same as the procedure mentioned in Section 2.2. Electrophoresis was performed at 4°C to ensure that the gel does not melt during the run. Electrophoresised DNA fragments were cut from the 0.8 % low-melting temperature agarose gel and mixed with 5 volumes (w/v) of 20 mM Tris (pH8.0) containing 1 mM EDTA. The mixture was allowed to melt at 65°C for 5 minutes. Buffered phenol was added in a 1:1 fraction and the mixture vortexed for 20 seconds. The aqueous phase was recovered by centrifugation at 4000 x g for 10 minutes at 20°C. The aqueous layer was washed with one volume phenol:chloroform (1:1) mixture and then subsequently with another volume of chloroform. Two volumes of ice-cold absolute ethanol were added and kept at –20°C for 30 minutes. The mixture was centrifuged at 15,000 x g for 10 minutes at 4°C. One ml of ice-cold 70 % ethanol was used to wash the pellet and the pellet was dried by

vacuum for 5 minutes. DNA recovered was dissolved in 20 μl of ddH_2O.

2.5 OPERATION OF THE PGEM-T EASY VECTOR SYSTEM

The pGEM-T vector (Promega, U.S.A.) is a convenient vector for the cloning of PCR product and performing sequencing by M13-40 universal primer and M13 reverse primer. These primers were supplied in the AutoCycle™ sequencing kit (Pharmacia Biotech) which was used to check the sequence of cloned PCR product. Operation of the pGEM-T Easy Vector System was divided into two parts, Ligation and Transformation. All the procedures were performed according to the instructions of the manufacturers.

2.5.1 Ligating the PCR product to pGEM-T Vector

The pGEM-T Vector was briefly centrifuged. Ligation reactions were set up by mixing 1 μl T4 DNA Ligase 10X buffer (300 mM Tris containing 100 mM $MgCl_2$, 100 mM DTT and 10 mM ATP, pH7.8), 1 ul pGEM-T vector (50ng/μl), 7 μl recovered PCR product and 1 μl T4 DNA Ligase (3 Weiss units/μl). Reaction mixtures were incubated overnight at 4°C.

2.5.2 Transformations using the pGEM-T Vector Ligation Reactions

The bacterial strain used for transformation was JM109 High Efficiency Competent Cells supplied in the system. The genotype of

JM109 is *rec*A1, *end*A1, *gyr*A96, *thi*, *hsd*R17 (r_{K^-},m_{K+}), *rel*A1, *sup*E44, Δ(*lac-pro*AB), [F', *tra*D36, *pro*AB, *lac*$I^qZ\Delta M15$] (Messing *et al.*, 1981). The tube containing the ligation reaction was centrifuged to collect contents at the bottom of the tube. 2 μl of each ligation reaction was added to a 1.5 ml sterile microcentrifuge tube on ice. A tube of frozen JM109 High Efficiency Competent Cells was removed from –70°C storage and placed in an ice bath until just thawed. The tube was mixed by gentle flicking. 50 μl of cells were transferred to the tube containing 2 μl ligation reaction mixture. Contents of the tube was mixed by gentle flicking and placed on ice for 20 minutes. Contents of the tube was heat shocked by placing in a 42°C water bath for 50 seconds and then returned to ice immediately for 2 minutes. 950 μl of SOC medium* at room temperature was added to the tubes containing cells transformed with ligation reaction. The tube was incubated for 1.5 hours at 37°C with 150 rpm shaking. 100 μl of each transformation culture was plated on LB/ampicillin/IPTG/X-Gal plates*. The plate was incubated overnight at 37°C.

2.6 EXTRACTION AND PURIFICATION OF PLASMID DNA

2.6.1 Preparation of bacterial culture transformed plasmid DNA

A single bacterial colony was transferred into 3 ml of LB medium* containing 50 μg/ml ampicillin* in a loosely capped 15-ml tube. The culture was incubated overnight at 37°C with 300 rpm shaking.

2.6.2 Minipreparations of plasmid DNA was prepared by the alkaline lysis method

3 ml of the culture was poured into a microcentrifuge tube and centrifuged at 12,000 x g for 30 seconds at 4°C in a KUBOTA 1300 microcentrifuge using a RA-150AM rotor. The broth was removed and the bacterial pellet was dried. The bacterial pellet was resuspended in 100 μl of ice-cold Solution I* by vigorous vortexing. 200 μl of freshly prepared Solution II* was added to the tube. The tube was closed tightly and the contents mixed by inverting the tube rapidly five times. 150 μl of ice-cold Solution III* was added. The tube was closed and vortexed gently in an inverted position for 10 seconds to disperse Solution III through the viscous bacterial lysate. The tube was left on ice for 5 minutes. Subsequently, the tube was centrifuged at 12,000 x g for 2 minutes at 4°C in a microcentrifuge. The supernatant was transferred to a fresh tube. Equal volume of phenol:chloroform (1:1) was added and mixed by vortexing. The tube was centrifuged at 12,000 x g for 2 minutes at 4°C in a microcentrifuge, and the supernatant was transferred to a fresh

tube. Double-stranded DNA was precipitated with 2 volumes of absolute ethanol at –20°C for 30 minutes. The tube was centrifuged at 12,000 x g for 5 minutes at 4°C. The supernatant was removed and the tube was allowed to stand in an inverted position on a paper towel to allow total drainage of the fluid. The pellet of double-stranded DNA was rinsed with 1 ml of 70 % ethanol at 4°C. The supernatant was removed by centrifugation. The pellet was dried under vacuum.

2.6.3 Plasmid DNA purification by Wizard™ Plus Minipreps DNA Purification Systems (Promega)

The procedure was performed according to the manufacturer's instruction and the composition of reagents was shown in Appendix VI. 3 ml of cells was pelleted by centrifugation for 2 minutes at 10,000 x g in a microcentrifuge. The supernatant was poured off and the tube was blotted upside-down on a paper towel to remove excess media. The cell pellet was resuspended in 200 µl of Cell Resuspension Solution. 200 µl of Cell Lysis Solution was added and mixed by inverting the tube 4 times. 200 µl of Neutralization Solution was added and mixed by inverting the tube 4 times. The lysate was centrifuged at 10,000 x g in a microcentrifuge for 5 minutes. 1 ml of the resuspended resin was pipetted into each barrel of the Minicolumn/Syringe assembly. All of the cleared lysate from each miniprep was carefully removed and transferred to the barrel of the

Minicolumn/Syringe assembly containing the resin. The syringe plunger was carefully inserted and the slurry gently pushed into the Minicolumn. The syringe was detached from the Minicolumn and the plunger removed from the Syringe Barrel. 2 ml of Column Wash Solution was pipetted into the barrel of the Minicolumn/syringe assembly. The plunger was inserted again into the syringe and the Column Wash Solution gently pushed through the Minicolumn. The syringe was removed and the Minicolumn was transferred to a 1.5 ml microcentrifuge tube. The Minicolumn was centrifuged at 10,000 x g in a microcentrifuge for 2 minutes to dry the resin. The Minicolumn was transferred to a new 1.5 ml microcentrifuge tube. 50 µl of water was applied to the Minicolumn and waited for 1 minute. The Minicolumn attached to the 1.5 ml microcentrifuge tube was centrifuged at 10,000 x g for 20 seconds to elute the DNA. The plasmid DNA was stored in the microcentrifuge tube at -20^{0}C.

2.7 SEQUENCING TECHNIQUES

Two commercial kits were used for DNA sequencing depending on the vectors used. AutoCycle™ Sequencing Kit (Pharmacia Biotech) is designed to perform cycle sequencing reactions. The cycle sequencing is a PCR-like reaction. M13-40 universal primer and M13 reverse primer were provided in the kit for sequencing the DNA cloned into the pGEM-T vector. AutoRead Sequencing Kit (Pharmacia Biotech) combined with Fluore-dATP Labelling Mix (Pharmacia Biotech) was used for internal labelling sequencing reaction by T7 polymerase. This was used for sequencing of our DNA which was cloned into the expression vector, pAED4, which cannot use the M13 universal primer for sequencing.

2.7.1 AutoCycle™ Sequencing Kit

The procedure was performed according to the manufacturer's instruction and the reagents used was listed in Appendix VII. The sequencing DNA sample was purified by Wizard™ *Plus* Minipreps DNA purification Systems as mentioned at Section 2.6.3. The reagents used in the reaction were provided from the kit and kept at 4°C during processing. Four microcentrifuge tubes were labeled 'A', 'C', 'G' and 'T' for each template. 2 µl of the appropriate stock ddNTP Solution was added to each tube. A master mix was prepared by mixing the following components to a microcentrifuge tube in the order indicated.

1.	DNA Template resupended in 5 μl ddH_2O	0.2-4 μg
2.	Reaction Buffer	2 μl
3.	dNTP Solution	5 μl
4.	DMSO	2 μl
5.	A.L.F. Primer (1-10 pmol)	2 μl

Taq DNA polymerase was diluted to 1.25 units per μl by Enzyme dilution buffer. 2 μl of diluted Taq DNA polymerase was added to the master mix and mixed gently. The mixed component was centrifuged briefly to collect the contents at the bottom of the tube. 4 μl of the master mix was added to each of the four labelled microcentrifuge tubes containing a stock ddNTP solution. The tubes were mixed and centrifuged briefly. The tubes were placed in a Perkin-Elmer GenAmp 9600 ThermoCycler. The reactants underwent initial denaturation (94°C for 2 min), followed by 36 amplification cycles (94°C for 15s, 54°C for 15s and 72°C for 40s) and final extension (72°C for 10 min) and the temperature was held at 4°C for adding 4 μl Stop Solution to each reaction. Each reaction was heated at 95°C for 3 minutes and then placed in an ice-bath.

2.7.2 AutoRead™ Sequencing Kit by using Fluore-dATP Labelling Mix Standard

Procedures were performed according to the instruction of manufacturers and the composition of reagents were listed in Appendix VIII.

2.7.2.1 Annealing of Primer to Double-Stranded Template

32 μl of 15 μg DNA was used in the reaction. The concentration of DNA was measured by A_{260}. 8 μl of 2 M NaOH was mixed with 32 μl DNA in a 0.5 ml microcentrifuge tube and incubated at room temperature for 10 minutes. 7 μl of 3 M sodium acetate (pH4.8) and 4 μl of ddH_2O was added after incubation. 120 μl of 100 % ethanol was added to the tube and placed in –20°C for 30 minutes. The DNA precipitated was collected by centrifugation for 15 minutes with 15,000 x g. The supernatant was discarded. The pellet was rinsed with 70 % ethanol. The tube was centrifuged for 10 minutes and the supernatant was discarded and dried under vacuum. The pellet was resuspended with 12 μl of ddH_2O. 20 pmol of T7PR primer, 5'TTA ATA CGA CTC ACT ATA CC3', which complementary to the T7 promoter region of pAED4 expression vector and 2 μl annealing buffer was added to the resuspended pellet. The tube was vortexed gently and centrifuged briefly. The tube was incubated at 65°C for 5

minutes. Then the tube was placed immediately in a 37°C water bath for 10 minutes incubation. After that, the tube was placed at room temperature for at least 5 minutes.

2.7.2.2 Sequencing Reaction

2.7.2.2a Essential Preliminaries for Sequencing Reactions

8 units/μl of the stock of T7 DNA Polymerase stock was diluted by Enzyme Dilution Buffer to final concentration of 8 units/2 μl. Four microcentrifuge tubes 'A', 'C', 'G' and 'T' was labeled. 3 μl of the 'A' Mix, 'C' Mix, 'G' Mix and 'T' Mix was added into the corresponding tube.

2.7.2.2b Labelling Reaction

The tube containing the annealed template and primer was added to 1 μl of the Fluore-dATP Labelling. 2 μl of diluted T7 DNA Polymerase was added to the tube. The tube was incubated for 10 minutes at 37°C. The four sequencing mixes were preheated when the incubation of the Labelling Reaction was nearly completed. After 10 minutes incubation of the Labelling Reaction, 1 μl of Extension Buffer and 3.5 μl of DMSO was added to each labelling reaction and mixed well.

2.7.2.2c Termination Reactions

5.4 μl of the labelling reaction was added to the four appropriate preheated sequencing reactions. The reactions were incubated for 5 minutes at 37°C. 6 μl of Stop Solution was added to the reaction. Then the reactions were heated at 85°C for 3 minutes and immediately quenched on ice and loaded to the sequencing gel set in the A.L.F. DNA Sequencer (Pharmacia Biotech).

2.7.3 Operation of A.L.F. DNA Sequencer

50 ml of ReadyMix Gel, A.L.F. grade (Pharmacia Biotech) mixed with 300 μl of 10 % (w/v) ammonium persulphate was used to prepare 6 % (w/v) polyacrylamide gels on a thoroughly cleaned gel cassette. The molded gel was assembled to the A.L.F. DNA sequencer. The sequencing reaction of each template were loaded into the slots of the gel carefully with the order A, C, G and T. The whole running process was kept at 40°C and a 1000 v constant voltage was applied. There was light emitted when the laser beam excited the fluorescein label on the DNA molecule which was detected by photodetectors on the sequencer. The result was analysed by the A.L.F. computer system (A.L.F. Manager version 2.5 software).

2.8 CONSTRUCTION OF EXPRESSION VECTOR

A construct, 6xHis-PK-pAED4, (Appendix IX) containing the pyridoxal kinase gene inserted into pAED4 expression vector with methoinine followed by six histidine (His-tag) engineered to the N-terminal of the gene was kindly prepared by Dr. Z.G. Gao of our group. Mutant expression vectors were constructed by replacing of *Hin*dIII-*Sac*I fragment of pyridoxal kinase gene to the truncated one.

*2.8.1 Hin*dIII *and Sac*I *Restriction Enzymes Digestion*

Plasmid DNA of each mutant cloned into pGEM-T vector and 6xHis-PK-pAED4 were prepared and purified by the alkaline lysis method (Section 2.6.2). 2 μg of each plasmid DNA was mixed individually with 8 units *Hin*dIII and *Sac*I in OPA+ buffer (Appendix V). Final volume of digestion mixture was made up to 10 μl by ddH_2O. The mixture was incubated at 37°C for 3 hours. Successful digestion were checked by 0.8 % agarose gel electrophoresis (Section 2.2).

2.8.2 Ligation

Digested fragments were purified by the low-melting temperature method (Section 2.4). Ligation reactions were set up by mixing 0.5 μg of purified *Hind*III-*Sac*I fragment of mutants and 0.5 μg of purified *Hind*III-*Sac*I 6xHis-PK-pAED4 fragment. 3 Weiss units of T4 DNA Ligase was added to the mixture and incubated overnight at 4°C.

Then the ligation reaction was transformed to JM109 competent cell (Section 2.5.2).

2.8.3 *Hin*dIII *and Pvu*II *Restriction Enzymes Digestion*

Plasmid DNA of the constructed 6xHis-Mutant-pAED4 was prepared by the procedure mentioned at Section 2.6.1 and the DNA was purified by the alkaline lysis method (Section 2.6.2). 2 μg of purified DNA was mixed with 8 units *Hin*dIII restriction enzyme in OPA+ buffer (Appendix V). Final volume of digestion mixture was made up to 10 μl by ddH_2O. The mixture was incubated at 37°C for 3 hours. Then the completely digested reaction mixture was heated at 85°C to inactivate the enzyme activity. Digested DNA was purified by the alkaline lysis method and sujected to *Pvu*II restriction enzyme digestion. 8 units of *Pvu*II restriction enzyme in OPA+ buffer with 50 mM NaCl was added to the purified *Hin*dIII digested DNA. Final volume of digestion mixture was made up to 10 μl by ddH_2O. The mixture was incubated at 37°C for 3 hours. Successful digestion were checked by 0.8 % agarose gel electrophoresis (Section 2.2).

2.9 EXPRESSION OF THE RECOMBINANT PYRIDOXAL KINASE

2.9.1 Transformation

The recombinant pyridoxal kinase expression vectors were transformed into BL21(DE3)pLysS bacteria strain (F', *omp*T, *hsd*S_B (r_B^-, m_B^-), *dcm*, *gal*, (DE3), pLysS, Cm^r). A tube of frozen BL21(DE3)pLysS competent Cells was removed from –70°C storage and placed in an ice bath until just thawed. The tube was mixed by gentle flicking. 50 µl of cells were transferred to the tube. 1 µl plasmid was added to the cells. The tube was mixed by gentle flicking and placed on ice for 20 minutes. The tube was heat shocked by placing in a 42°C water bath for 50 seconds and then returned to ice immediately for 2 minutes. 950 µl room temperature SOC medium was added to the tubes containing cells transformed with plasmid. The tubes were incubated for 1.5 hours at 37°C with 150 rpm shaking. 100 µl of each transformation culture was plated on LB/ampicillin plates. The plate was incubated overnight at 37°C.

2.9.2 Glycerol Stock of Expressed Recombinant Cell Preparation

A single colony of each mutant strains were isolated from LB/ampicillin plate and inoculated in 3 ml LB medium containing 100 µg/ml ampicillin with 300 rpm shaking at 37°C overnight. Three sets of each mutant glycerol stocks were prepared by mixing 850 µl of the overnight culture and 150 µl 100 % sterilized glycerol solution. The glycerol stocks were kept at –70°C.

2.9.3 Expression of Recombinant Pyridoxal Kinase

A small amount of recombinant pyridoxal kinase bacterial strain was isolated from glycerol stock by sterilized loop. It was inoculated to 3 ml LB medium containing 100μg/ml ampicillin. The medium were grown at 37°C overnight with 300 rpm shaking. 0.5 ml overnight culture was transferred to a new 50 ml LB medium in a 250 ml flask containing 100 μg/ml ampicillin and grown continuously at the same condition. Absorbance at 600 nm was monitored at half an hour materials until the reading reached 0.6. IPTG* to a final concentration of 0.4 mM was added to induce the cell and the culture was further grown for 5 hours.

2.9.4 Extraction of Protein from Bacterial Culture

The cell was harvested by centrifugation at 5000 x g for 10 minutes at 4°C. The pellet was resuspened in 20 mM Tris containing 100 mM NaCl at pH8.0. Lysozyme to a final concentration 0.75 mg/ml was added to the resuspended pellet and incubated at 30°C for 20 minutes. Sonication was performed by Soniprep 150 sonicator at 14 amplitude microns with 3 pulses for 10 seconds. The sample was clarified by centrifugation at 5000 x g for 30 minutes at 4°C to pellet any insoluble material.

2.10 PURIFICATION OF RECOMBINANT PYRIDOXAL KINASE

2.10.1 Ammonium Sulphate Precipitation

40 % ammonium sulphate precipitation was performed by adding 243 g/L of ammonium sulphate slowly to the cell lysate with stirring. After stirring for 30 minutes, the suspension was centrifuged at 5000 x g for 30 minutes and the precipitate was discarded. Ammonium sulphate concentration of the supernatant was raised to 60 % by adding 132 g/L ammonium sulphate slowly with stirring for another 30 min at 4°C. The suspension was centrifuged at 5000 x g for 30 minutes. The precipitate obtained from the 40-60 % cut was dissolved in a minimal amount of 5 mM potassium phosphate at pH7.4 and dialysed against 1L of the same buffer overnight with one change of buffer.

2.10.2 Affinity Chromatography

2.10.2.1 Preparation of Pyridoxyl-Agarose

The method employed was modified from that of Cash *et al.* (1980). 20 ml commercially available ω-aminooctyl agarose was supported in 0.1 M $NaHCO_3$ pH8.0 and 2 g solid pyridoxal hydrochloride was added to the slurry with stirring. After the pH of the slurry was adjusted to 8 by 2 M NaOH, it was gently shaken for 16 hours in the dark at 37°C. Then the slurry was cooled by placing its container in an ice bath and 100 mg solid sodium borohydride was added until all traces of yellow colour

had disappeared. The slurry was washed thoroughly with ddH_2O to remove excess sodium borohydride and was stored in 0.5 M NaCl pH7.0 at 4^{0}C before being used.

2.10.2.2 Pyridoxyl-Agarose Chromatography

Dialysed sample after ammonium sulphate fractionation was applied to a column (2 x 2 cm) of pyridoxal-agarose previously equilibrated with 5 mM potassium phosphate at pH7.4. The sample was loaded onto the column and was washed by 0.4 M KCl in 5 mM potassium phosphate at pH7.4. After the washing step, the column was eluted with 50 mM pyridoxal at pH4.0. Samples were collected into 0.5 M potassium phosphate at pH7.4 in a ratio of 4:1 (v/v). The collected sample was concentrated to approximately 1 ml by a Diaflo membrane concentrator (Amicon) which had been fitted with a PM-30 membrane.

2.10.3 Metal-Chelating Chromatography

2.10.3.1 Preparation of Nickel-Chelating Iminodiacetic Acid (IDA) Agarose

Ten ml of commercially available IDA agarose was used to chelate the nickel ions. The storage buffer of the IDA agarose was discarded by filtration. The agarose was resuspended into two volumes of 50 mM $NiSO_4 \cdot 6H_2O$ solution with four changes

of the same solution. Then the column was washed thoroughly with ddH_2O to remove the unbound nickel ions. The nickel-chelated IDA agarose was stored in 20 mM Tris containing 100 mM NaCl pH8.0 at 4^0C before being used.

2.10.3.2 Nickel-chelating IDA Chromatography

The cell lysate prepared from Section 2.9.4 was loaded onto a nickel-chelating IDA column (2 x 4 cm) previously equilibrated with 20mM Tris containing 100 mM NaCl at pH8.0 (Buffer A). The column was washed with 20 mM imidazole in Buffer A. After the washing step, the column was eluted with 100 mM imdazole in Buffer A. A sample with pyridoxal kinase activity was pooled and dialysed against 5 mM potassium phosphate at pH7.4.

2.10.4 DEAE Chromatography was performed using a FPLC system

The dialysed sample was transferred to a previously cooled 50 ml sample loop. The loop was attached at an injection position of FPLC system (Pharmacia Biotech). The TSK DEAE 5pW column (8 x 75 mm, LKB) was equilibrated with 5 mM potassium phosphate, pH7.4. The sample was injected into the column with the flow rate at 0.5 ml/min. The column was then washed with 5 mM potassium phosphate buffer until no protein was detected by the UV monitor at wavelength 280 nm. The sample was eluted

with a 0-200 mM NaCl gradient and 1 ml fractions were collected. The elution profiles were monitored by recording absorbance at 280 nm.

2.11 PURIFIED SAMPLE PREPARATION

The purified samples with pyridoxal kinase activity were pooled together and dialysed against 5 mM potassium phosphate (pH7.0). The dialysed samples were freeze dried by Flexi-Dry™ μP freeze-dryer (FTS systems, USA). The sample was redissolved into ddH_2O as a 10mg/ml stock solution and kept at –20°C.

2.12 ENZYMATIC ASSAY

0.2 mM ATP and 0.2 mM pyridoxal solution were freshly prepared by dissolving in assay buffer (70 mM potassium phosphate buffer containing 100 μM $ZnCl_2$ at pH6.4). 10 μl of the 0.2 mM ATP and 10 μl of 0.2 mM pyridoxal were mixed with 100 μl of sample in a 1.5 ml microcentrifuge tube. The final volume of assay reaction was made up to 1 ml by assay buffer. The sample was incubated at 37°C for 30 minutes with a control. The control was performed without addition of ATP. 100 μl 100 % TCA was added to terminate the reaction. The assay mixture was clarified by centrifugation at 15,000 x g for 5 minutes at 4°C. The supernatant was subjected to a phenylhydrazine reaction (Wada and Snell, 1961) to measure the amount of PLP formed. 1 ml of supernatant was mixed with 1 ml of assay buffer and 100 μl of phenylhydrazine in 12N H_2SO_4 acid was

added. The solution was mixed by inverting. The change in absorbance at 410 nm within 2 minutes interval was measured by a Hitachi UV-3210 UV-visible spectrophotometer. The amount of PLP formed in the reaction was determined from a calibration curve using PLP as standard. One unit of enzymatic activity is equivalent to the formation of 1 nmol of PLP formed per minutes when the enzyme is saturated by ATP and pyridoxal.

The initial velocity data were fitted by a least-square method to the Lineweaver-Burk transformation of equation (1)

$$V = V[S]/K_m + [S] \qquad (1)$$

where [S] represents the concentration of the varied substrate and K_m represents the Michaelis constant.

2.13 PROTEIN DETERMINATION

The protein concentration of sample was assayed by Bradford Method (Bradford, 1976). 200 μl of Bradford dye reagent concentrate (Bio-Rad) was mixed with 800 μl of sample. The range of protein that can be detected was limited to 0-20 μg/ml. The absorbance at 595 nm was measured by a Hitachi UV-3210 UV-visible spectrophotometer after allowing the mixture to stand at room temperature for 5 minutes. Protein concentration was determined from a calibration curve using bovine serum albumin as a protein standard.

2.14 POLYACRYLAMIDE GEL ELECTROPHORESIS

2.14.1 Sodium dodecylsulphate (SDS) / polyacrylamide gel

SDS polyacrylamide gel was carried out according to the method developed by Laemmli (1970). The reagents used was listed in Appendix X. A 12 % acrylamide separating gel (pH8.8) and 4 % stacking gel (pH6.8) containing 0.1 % sodium dodecyl sulphate (SDS) were prepared. Samples from collected fractions were diluted 1:4 with sample buffer which contained 2 % SDS, 5 % β-mercaptoethanol, 10 % glycerol and 1.25 x 10^{-3} % bromophenol blue. After heating this mixture at 100°C for 5 minutes. 15 µl of this mixture was applied to the sample slot. The electrophoresis was carried out at a constant voltage 150 v for about 1 hour. Gels were stained for 1 hour with Coomassie Brilliant Blue R–150 dissolved in a solution of 40 % methanol and 10 % acetic acid. Finally, the gels were destained in 40 % methanol and 10 % acetic acid.

2.14.2 Non-denaturing 8-15 % gradient polyacrylamide gel

A non-denaturing 8-15 % gradient polyacrylamide gel electrophoresis was performed according to the method of Blackshear (1984). A linear gradient gel was prepared with increasing acrylamide concentration from 8 % to 15 %. A gradient mixer and peristaltic pump were used in the preparation. Two concentration of acrylamide solution were prepared. 2 ml of

15 % acrylamide separating gel solution (pH8.8) was transferred to the gradient mixer chamber near the outlet. 8 % acrylamide separating gel solution (pH8.8) was transferred into next chamber away from the outlet. The outlet of the gradient mixer was connected to the peristaltic pump which uniformly introduces the acrylamide solution between the glass plate assembly of Mini-PROTEAN II (Bio-Rad). Once all of the acrylamide mixture has been introduced, water-saturated n-butanol was overlayed on the gel and left to polymerize. After the gel has polymerized, 4 % stacking gel (pH6.8) was added on the top of the gradient separating gel with the inserted well comb. Samples were diluted 1:4 with sample buffer without addition of SDS and β-mercaptoethanol. 15 μl of this mixture was applied to the sample slot. The electrophoresis was carried out at a constant current 5 mA for 5 hours at 4°C. Gels were stained for 1 hour with Coomassie Brilliant Blue R–150 dissolved in a solution of 40 % methanol and 10 % acetic acid. Finally, the gels were destained in 40 % methanol and 10 % acetic acid.

2.15 WESTERN IMMUNOBLOTTING

2.15.1 Electrophoretical Separation of Proteins by Gel Electrophoresis

Components in the cell extracts were separated by 12 % SDS/PAGE with prestained marker. The procedure for performing 12 % SDS/PAGE was mentioned in Section 2.14.1.

2.15.2 Transfer of the Proteins from the Gel to a Suitable Membrane

The electrophoresised 12 % SDS/PAGE was immersed in pre-cooled transfer buffer (25 mM Tris, 192 mM glycine, 20 % v/v methanol) for 15 minutes. The gel was assembled with the nitrocellulose membrane and submerged in transfer buffer in a Mini Trans-Blot Cell (Bio-Rad). Proteins separated by SDS/PAGE were electrotransferred onto a nitrocellulose membrane at a constant voltage 100 v for 1 hour at 4°C.

2.15.3 Blocking of Non-specific Binding Sites

The transblotted membrane was blocked by 1 % BSA in Tris-buffered Saline (TBS, 50mM Tris containing 150 mM NaCl at pH7.5) for 2 hours at room temperature. Then the membrane was washed three times with TBS-Tween 20 (TBST, TBS with 0.1 % Tween 20) for 10 minutes each.

2.15.4 Primary Antibody Reaction

The primary antibody is anti-pig brain pyridoxal kinase antibody raised from the mouse. The antibody is a gift from Dr. S. Y. Choy, Hallym University, Korea and was diluted 10 times by antibody buffer (0.1 % BSA in TBST). The membrane was incubated with diluted primary antibody for 2 hours at room temperature. Then, the membrane was washed three times with TBST for 10 minutes each.

2.15.5 *Second Antibody Reaction*

BM chromgenic Western Blotting Kit (Boehringer Mannheim) was used to perform the second antibody reaction and chromogenic detection on Western blots. The second antibody supplied from BM Chromogenic Western Blotting Kit is anti-mouse Ig/anti-rabbit IgG-AP mixture. Membrane was incubated with the anti-mouse Ig/anti-rabbit IgG-AP mixture at a recommended concentration 800 mU/ml for 30 minutes at room temperature. The membrane was washed twice with TBST for 10 minutes each and then washed twice with TBS for 10 minutes each.

2.15.6 *The chromogenic detection of alkaline phosphatase-labeled antibodies on Western blots*

2 ml of AP substrate solution (NBT/X-phosphate solution) supplied from the kit was added to the membrane until the desired band intensity was attained and the membrane was thoroughly washed by ddH_2O.

2.16 CIRCULAR DICHROISM SPECTRA

For Circular Dichroism (CD) experiment, the sample was diluted from a stock solution (Section 2.11) to 0.5 mg/ml by 10 mM potassium phosphate at pH7.0. Circular dichroism measurements were carried out on a Jasco-720A spectropolarimeter using cuvettes of 0.2 cm path length. Each CD spectrum represents the average of four scans. Spectra were acquired over the range 250–190 nm under constant N_2 flush. The instrument was regularly calibrated with a 1 mg/ml solution of 10-camphorsulfonic acid. The CD data are expressed in terms of ellipiticity, the mean residue ellipiticity $[\theta]mrw,\lambda$ at a wavelength λ is quoted in units of $deg.cm^2.dmol^{-1}$ and is given by :

$$[\theta]mrw,\lambda = \frac{MRW\ \theta}{10\ dc}$$

where $[\theta]mrw,\lambda$ is the observed ellipticity, d is the path length (0.2 cm) and c is the concentration (g/ml), MRW is the means residue weight.

On the basis of the sizes of the CD signals at 222 nm , fairly reliable estimates of the α-helix contents of proteins can be made using the following equation :

$$\%\ \alpha\text{-helix} = \frac{([\theta]_{222}-3000)}{(-39{,}000)} \times 100\ \%$$

2.17 FLUORESCENCE SPECTROSCOPY

Emission spectra were recorded in a Perkin-Elmer Ls50B luminescence spectrometer. The samples were dissolved in 5 mM potassium phosphate at pH7.4. The absorbance of the samples at the 280 nm were 0.1. Intrinsic tryptophan fluorescence of recombinant pyridoxal kinase was measured by excitation at 295 nm. The spectra were collected from 300 to 500 nm. The excitation and emission band widths were 2.5 nm.

For TNP-ATP binding experiment, 2.5 μM protein sample was titrated with 7.5 μM TNP-ATP. The fluorescence was excited at 410 nm and the spectra was collected from 500 nm to 600 nm. The excitation and emission band widths were 2.5 nm. In this experiment 25 μM ATP mixed with the mixture of TNP-ATP and recombinant pyridoxal kinase was performed to observe the competitive inhibition effect of ATP respected to TNP-ATP.

2.18 DENATURATION EXPERIMENTS

For denaturation studies, each sample was prepared by diluting 0.2 ml of stock solutions (Section 2.11) to 2 ml with GdnHCl containing 10 mM potassium phosphate at pH7.0. The concentration of GdnHCl was performed in a range of 0 to 2 M. All fluoroscence measurements were carried out at 25°C with 30 minutes incubation in the presence of GdnHCl. Control experiments indicated that this time of incubation was sufficient to achieve equilibrium. The incubated solution was subjected to fluorometric measurement at excitation wavelength of 295 nm.

CHAPTER THREE

RESULTS

III. RESULTS

3.1 CONSTRUCTION OF N-TERMINAL TRUNCATED PYRIDOXAL KINASE MUTANTS

In order to analyse the function of the N-terminal region in pyridoxal kinase, a series of truncated mutant were constructed. The cDNA fragment, specified with one 5'-end oligonucleotide and one universal 3'-end oligonucleotide as shown in Figure 5, were synthesized using PCR. A *Hin*dIII restriction site was added into the 5'-end primer to facilitate subcloning of the fragment into expression vectors. As shown in Figure 5B, all the 5'-end primers containing 15-19 nucleotides are complementary to the pyridoxal kinase gene. This design can increase the efficiency of priming during PCR. Purity of each cDNA fragment constructed was tested using 0.8 % agarose electrophoresis. One single band was observed in all the samples (Figure 6A-D). Molecular size of each fragment matched with the calculated molecular weights (Table V) from the DNA sequence. Each cDNA fragment was subcloned separately into pGEM-T vectors which were used for subsequent DNA sequencing. In order to confirm that accurate deletion was attained, DNA sequencing was performed for each sample with the A.L.F. DNA sequencer. The deduced sequences are shown in Figure 7A-I.

(A)

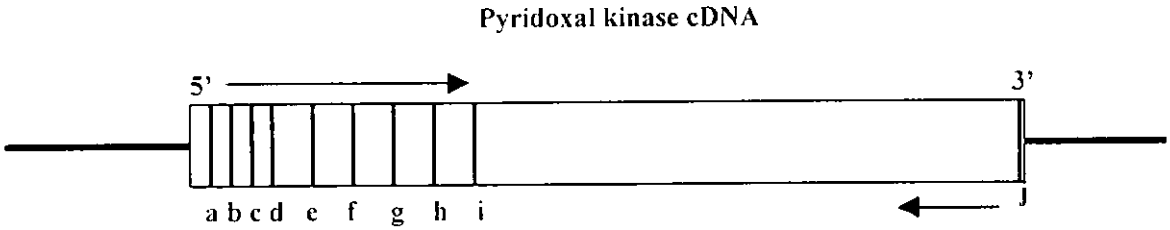

(B)

		Mutants	Primer sequence
5' primers	a	Δ15	5'GGC *AAG CTT* CGG GTG CTC TCC ATT C3'
	b	Δ16	5'GGC *AAG CTT* GTG CTC TCC ATT CAG3'
	c	Δ17	5'GGC *AAG CTT* CTC TCC ATT CAG AGC3'
	d	Δ18	5'GGG *AAG CTT* TCC ATT CAG AGC CAC3'
	e	Δ21	5'GGG *AAG CTT* AGC CAC GTC GTC CGC3'
	f	Δ24	5'GGG *AAG CTT* GTC CGC GGC TAC GTG3'
	g	Δ27	5'GGG *AAG CTT* TAC GTG GGC AAC CGA3'
	h	Δ45	5'GGG *AAG CTT* GAT GCA GTG AAT TCT GTC3'
	i	Δ61	5'GGG *AAG CTT* TGG AAG GGG CAG GTG3'
	j	3'primer	5'GGG ATC GAT CAC AGC ACC GTG GC3'

FIGURE 5: **Schematic diagram of pyridoxal kinase cDNA (A) and the primers used for mutagenesis (B).** The *Hin*dIII site is shown in italic type. The sequence primed on the pyridoxal kinase cDNA is underlined.

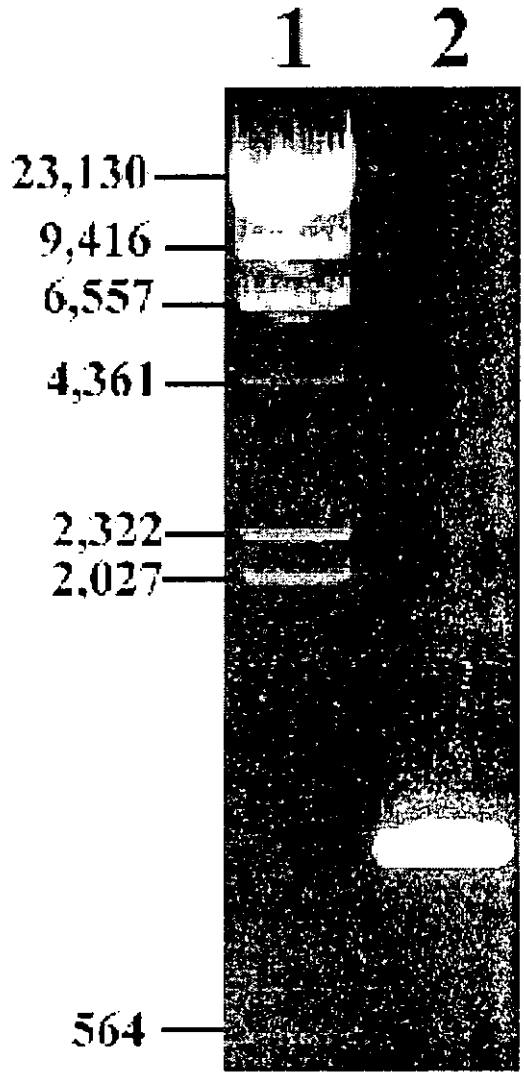

FIGURE 6A: PCR product of mutant Δ15 shown in 0.8 % agarose gel electrophoresis. Lane 1, λDNA *Hin*dIII marker, molecular weight in base pairs are indicated; Lane 2, PCR product of Δ15.

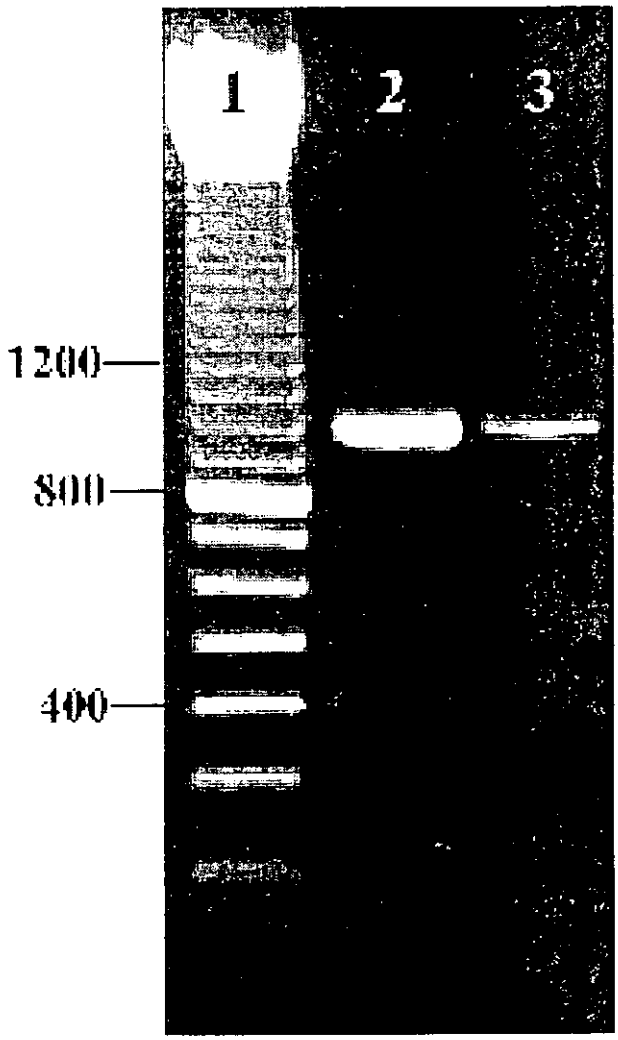

FIGURE 6B: PCR products of mutants (Δ16 and Δ17) shown in 0.8 % agarose gel electrophoresis. Lane 1, 100 Base-Pair Ladder, molecular weight in base pairs are indicated; Lane 2, PCR product of Δ16; Lane 3, PCR product of Δ17.

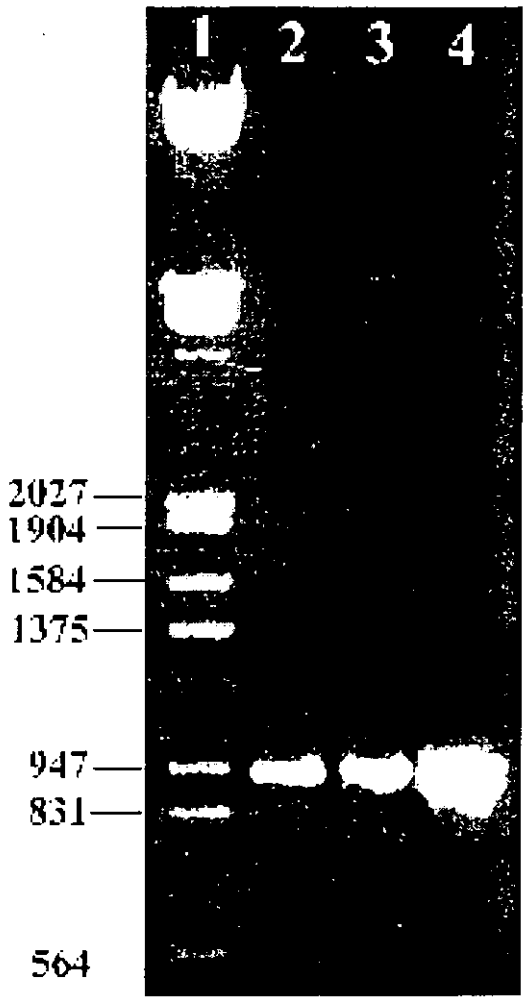

FIGURE 6C: PCR products of mutants (Δ18, Δ21 and Δ24) shown in 0.8 % agarose gel electrophoresis. Lane 1, DNA Molecular weight Marker III, molecular weight in base pairs are indicated; Lane 2, PCR product of Δ18; Lane 3, PCR product of Δ21; Lane 4, PCR product of Δ24.

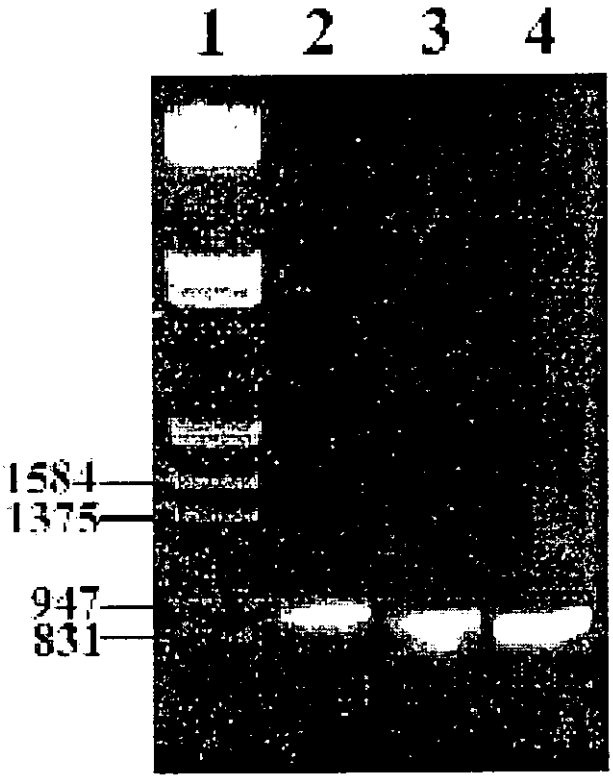

FIGURE 6D: **PCR products of mutants (Δ27, Δ45 and Δ61) shown in 0.8% agarose gel electrophoresis.** Lane 1, DNA molecular weight marker III, molecular weight in base pairs are indicated; Lane 2, PCR product of Δ27; Lane 3, PCR product of Δ45; Lane 4, PCR product of Δ61.

```
5'    TA  CGC  CAA  GCT  ATT  TAG  GTG  ACA  CTA  TAG  AAT  ACT  CAA  GCT

ATG  CAT  CCA  ACG  CGT  TGG  GAG  CTC  TCC  GAT  ATG  GTC  GAC  CTG  CAG

GCG  GCC  GCA  CTA  GTG  ATT  GGC  AAG  CTT  CGG  GTG  CTC  TCC  ATT  CAG
                                          R    V    L    S    I    Q
AGC  CAC  GTC  GTC  CGC  GGC  TAC  GTG  GGC  AAC  CGA  GCT  GCA  ACG  TTC
 S    H    V    V    R    G    Y    V    G    N    R    A    A    T    F
CCG  CTG  CAG  GTT  CTG  GGG  TTC  GAG  GTC  GAT  GCA  GTG  AAT  TCT  GTC
 P    L    Q    V    L    G    F    E    V    D    A    V    N    S    V
CAG  TTT  TCA  AAC  CAC  ACA  GGC  TAC  GCG  CAC  TGG  AAG  GGG  CAG  GTG
 Q    F    S    N    H    T    G    Y    A    H    W    K    G    Q    V
CTG  AAC  TCG  GAC  GAG  CTG  CAC  GCG  CTG  TAC  GAG  GGG  CTG  AAG  CTG
 L    N    S    D    E    L    H    A    L    Y    E    G    L    K    L
AAC  AAC  GTA  AAT  CAG  TAC  GAT  TAT  GTG  CTC  ACG  GGT  TAC  ACG  AGA
 N    N    V    N    Q    Y    D    Y    V    L    T    G    Y    T    R
GAC  AAG  TCC  TTC  CTG  GCC  ATG  GTG  GTG  GAC  ATC  GTG  CGG  GAG  CTG
 D    K    S    F    L    A    M    V    V    D    I    V    R    E    L
AAG  CAG  CAG  AAC  CCG  AGG  CTG  GTG  TAC  GTG  TGC  GAC  CCG  GTG  ATG
 K    Q    Q    N    P    R    L    V    Y    V    C    D    P    V    M
GGA  GAC  AAG  TGG  GAT  GGA  GAA  GGC  TCC  ATG  TAC  GTC  CCC  GAG  GAC
 G    D    K    W    D    G    E    G    S    M    Y    V    P    E    D
CTC  CTT  CCA  GTT  TAC  AGA  GAG  AAG  GTC  GTG  CCC  GTG  GCA  GAC  ATC
 L    L    P    V    Y    R    E    K    V    V    P    V    A    D    I
ATA  ACC  CCC  AAC  CAG  TTT  GAG  GCG  GAG  TTG  CTG  ACC  GGC  AGG  AGG
 I    T    P    N    Q    F    E    A    E    L    L    T    G    R    R
ATC  CAC  AGT  GAG  GAA  GAA  GCC  TTG  GCG  GTG  ATG  GAC  ATG  CTG  CAC
 I    H    S    E    E    E    A    L    A    V    M    D    M    L    H
GCA  ATG  GGC  CCG  GAC  ACG  GTG  GTC  ATC  ACG  AGC  TCG
 A    M    G    P    D    T    V    V    I    T    S    S
```

FIGURE 7A: Deduced sequence of PCR product of mutant Δ15 inserted into pGEM-T vector. **The greyed region is the part of pGEM-T vector sequence (Appendix XI). The bolded region is the Δ15 N'-terminal primer sequence. The *Hin*dIII (AAGCTT) and *Sac*I (GAGCTC) restriction sites were shown in bold and italic type.**

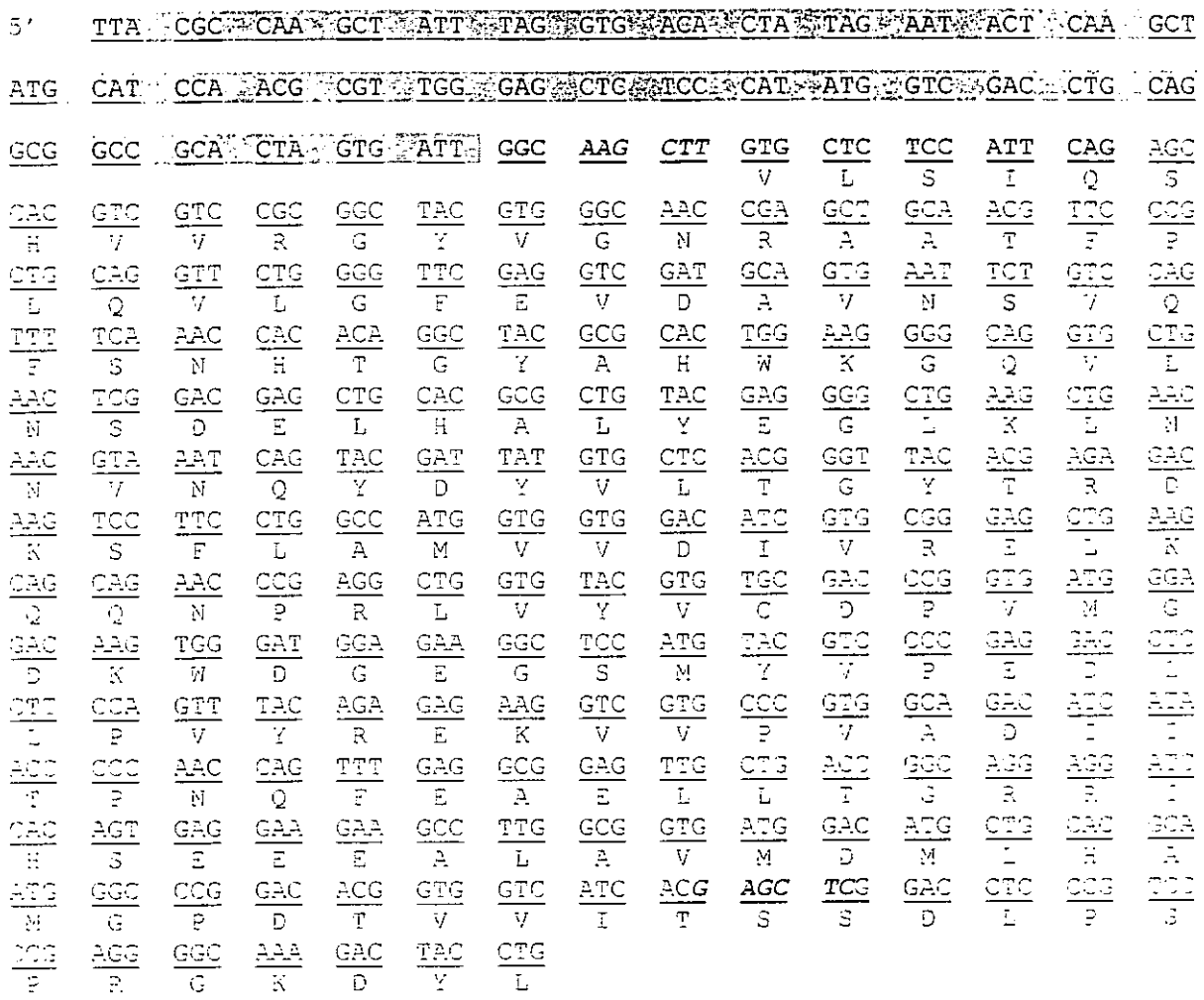

FIGURE 7B: **Deduced sequence of PCR product of mutant Δ16 inserted into pGEM-T vector.** The greyed region is the part of pGEM-T vector sequence (Appendix XI). The bolded region is the Δ16 N'-terminal primer sequence. The *Hin*dIII (AAGCTT) and *Sac*I (GAGCTC) restriction sites were shown in bold and italic type.

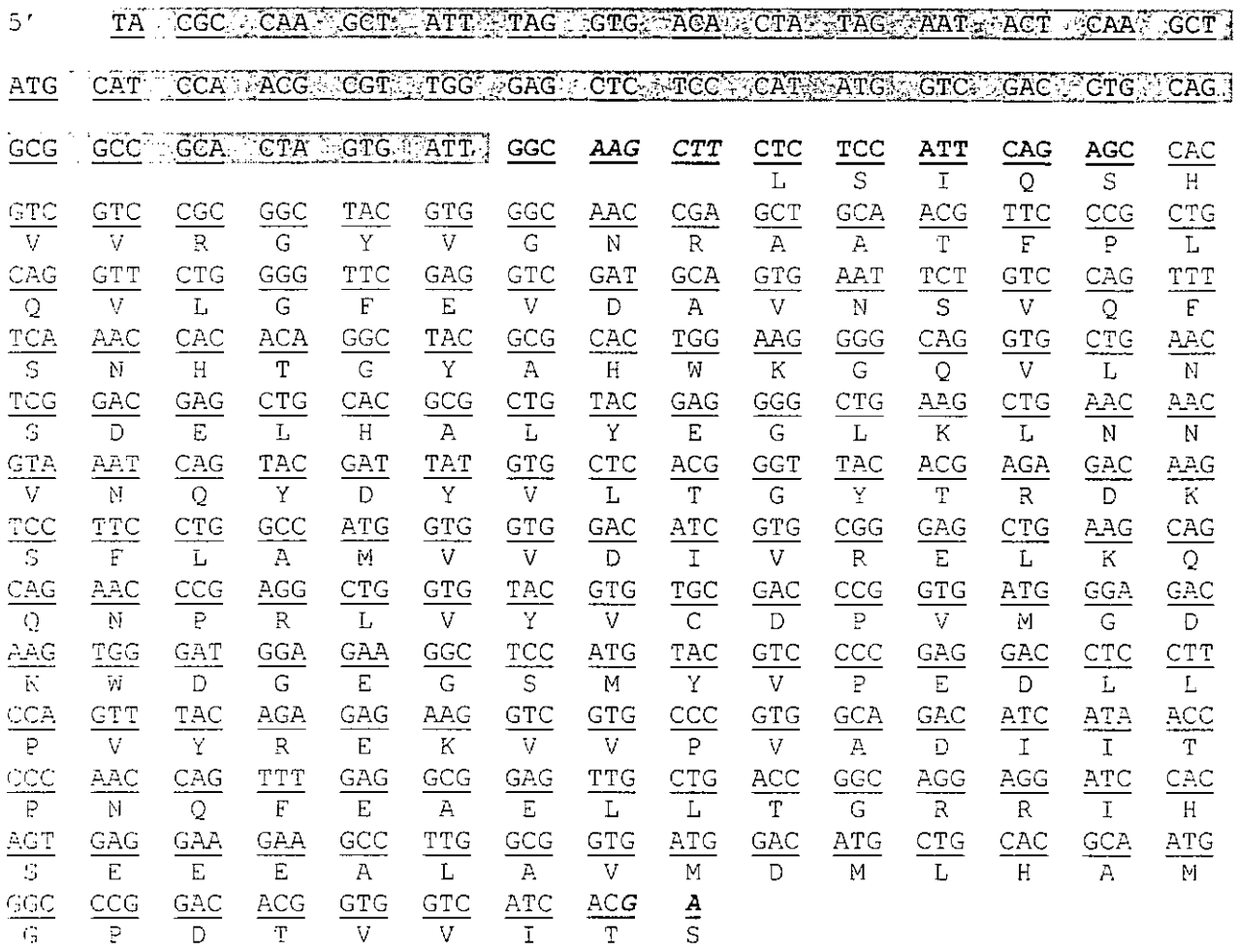

FIGURE 7C: Deduced sequence of PCR product of mutant Δ17 inserted into pGEM-T vector. The greyed region is the part of pGEM-T vector sequence (Appendix XI). The bolded region is the Δ17 N'-terminal primer sequence. The *Hin*dIII (AAGCTT) and *Sac*I (GAGCTC) restriction sites were shown in bold and italic type.

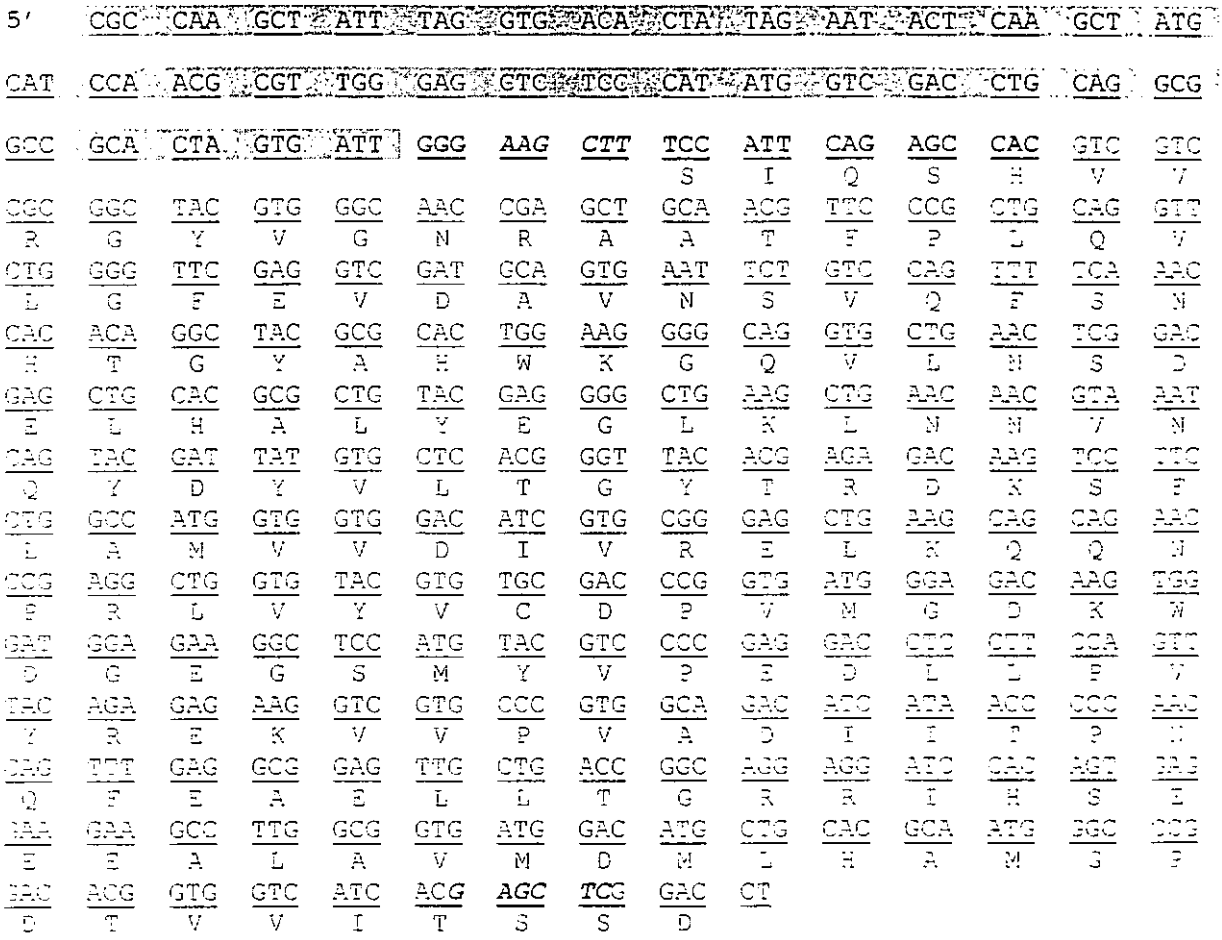

FIGURE 7D: **Deduced sequence of PCR product of mutant Δ18 inserted into pGEM-T vector.** The greyed region is the part of pGEM-T vector sequence (Appendix XI). The bolded region is the Δ18 N'-terminal primer sequence. The *Hin*dIII (AAGCTT) and *Sac*I (GAGCTC) restriction sites were shown in bold and italic type.

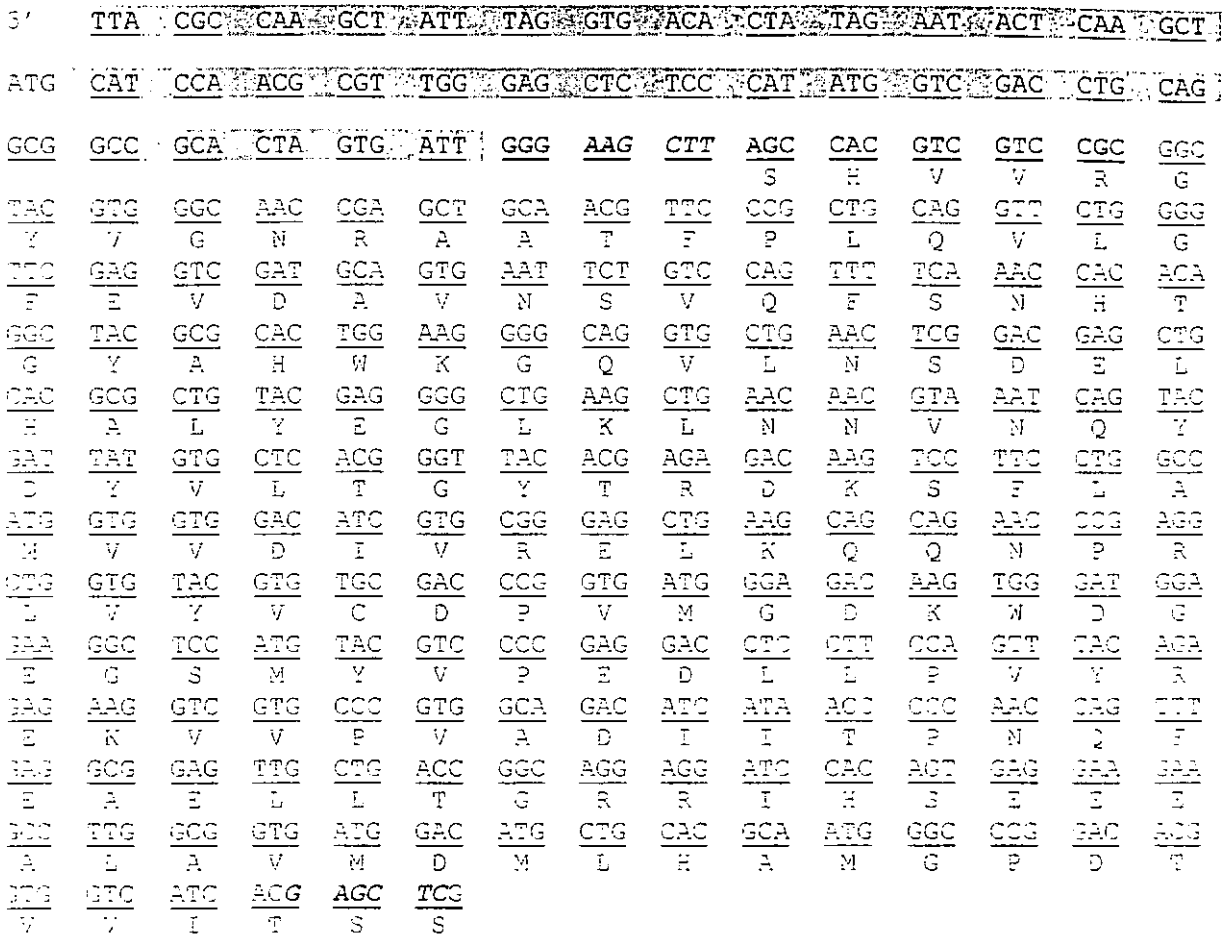

FIGURE 7E: **Deduced sequence of PCR product of mutant Δ21 inserted into pGEM-T vector.** The greyed region is the part of pGEM-T vector sequence (Appendix XI). The bolded region is the Δ21 N'-terminal primer sequence. The *Hin*dIII (AAGCTT) and *Sac*I (GAGCTC) restriction sites were shown in bold and italic type.

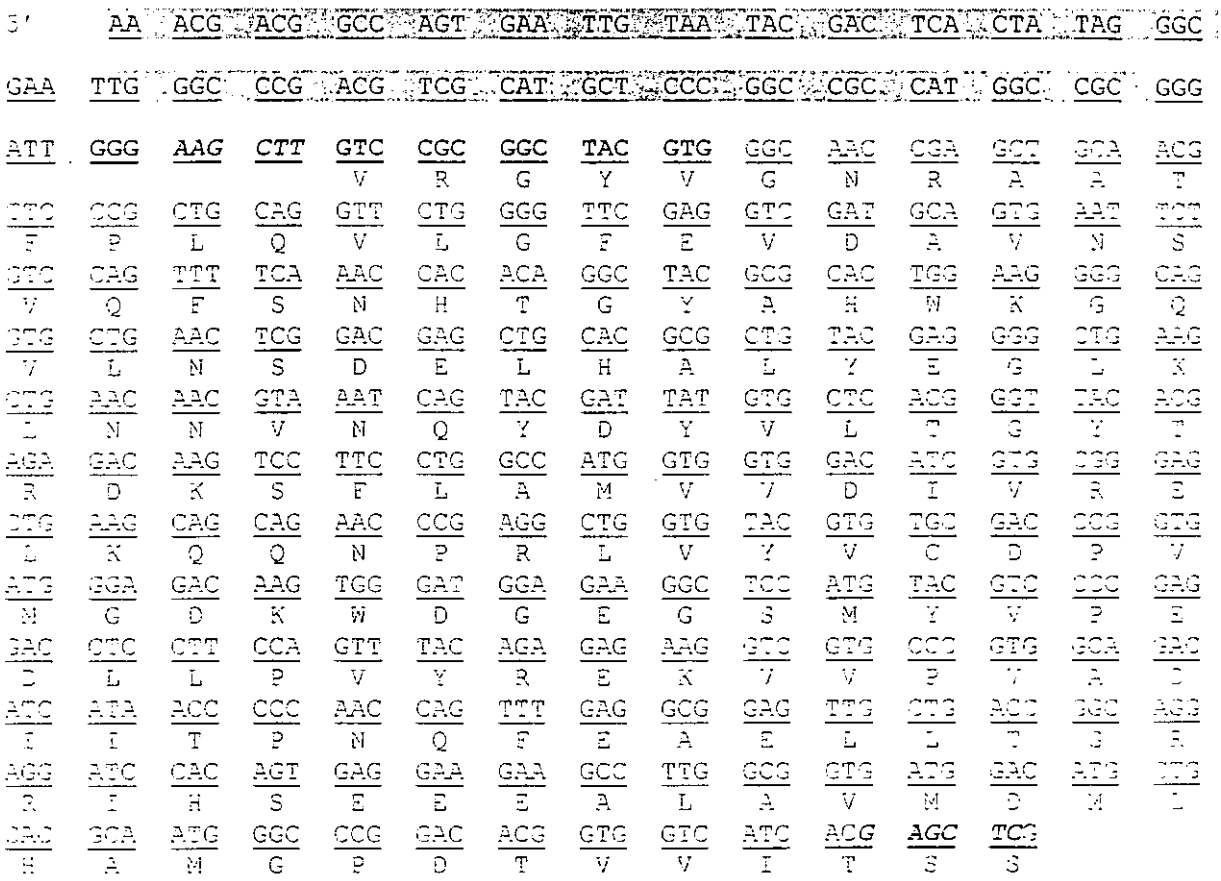

FIGURE 7F: **Deduced sequence of PCR product of mutant Δ24 inserted into pGEM-T vector.** The greyed region is the part of pGEM-T vector sequence (Appendix XI). The bolded region is the Δ24 N'-terminal primer sequence. The *Hin*dIII (AAGCTT) and *Sac*I (GAGCTC) restriction sites were shown in bold and italic type.

```
5'  AA ACG ACG GCC AGT GAA TTG TAA TAC GAC TCA GTA TAG GGC
GAA TTG GGC CCG ACG TCG CAT GCT CCC CGC CGC CAT GGC CGC GGG

ATT GGG AAG CTT TAC GTG GGC AAC CGA GCT GCA ACG TTC CCG CTG
      Y   V   G   N   R   A   A   T   F   P   L
CAG GTT CTG GGG TTC GAG GTC GAT GCA GTG AAT TCT GTC CAG TTT
Q   V   L   G   F   E   V   D   A   V   N   S   V   Q   F
TCA AAC CAC ACA GGC TAC GCG CAC TGG AAG GGG CAG GTG CTG AAC
S   N   H   T   G   Y   A   H   W   K   G   Q   V   L   N
TCG GAC GAG CTG CAC GCG CTG TAC GAG GGG CTG AAG CTG AAC AAC
S   D   E   L   H   A   L   Y   E   G   L   K   L   N   N
GTA AAT CAG TAC GAT TAT GTG CTC ACG GGT TAC ACG AGA GAC AAG
V   N   Q   Y   D   Y   V   L   T   G   Y   T   R   D   K
TCC TTC CTG GCC ATG GTG GTG GAC ATC GTG CGG GAG CTG AAG CAG
S   F   L   A   M   V   V   D   I   V   R   E   L   K   Q
CAG AAC CCG AGG CTG GTG TAC GTG TGC GAC CCG GTG ATG GGA GAC
Q   N   P   R   L   V   Y   V   C   D   P   V   M   G   D
AAG TGG GAT GGA GAA GGC TCC ATG TAC GTC CCC GAG GAC CTC CTT
K   W   D   G   E   G   S   M   Y   V   P   E   D   L   L
CCA GTT TAC AGA GAG AAG GTC GTG CCC GTG GCA GAC ATC ATA ACC
P   V   Y   R   E   K   V   V   P   V   A   D   I   I   T
CCC AAC CAG TTT GAG GCG GAG TTG CTG ACC GGC AGG AGG ATC CAC
P   N   Q   F   E   A   E   L   L   T   G   R   R   I   H
AGT GAG GAA GAA GCC TTG GCG GTG ATG GAC ATG CTG CAC GCA ATG
S   E   E   E   A   L   A   V   M   D   M   L   H   A   M
GGC CCG GAC ACG GTG GTC ATC ACG AGC TCG GAC CTC CCG TCC CCG
G   P   D   T   V   V   I   T   S   S   D   L   P   S   P
AGG GGC AAA GAC TAC CTG ATC GCG CTG GGG AGC CAG AGG
R   G   K   D   Y   L   I   A   L   G   S   Q   R
```

FIGURE 7G: Deduced sequence of PCR product of mutant Δ27 inserted into pGEM-T vector. The greyed region is the part of pGEM-T vector sequence (Appendix XI). The bolded region is the Δ27 N'-terminal primer sequence. The *Hin*dIII (AAGCTT) and *Sac*I (GAGCTC) restriction sites were shown in bold and italic type.

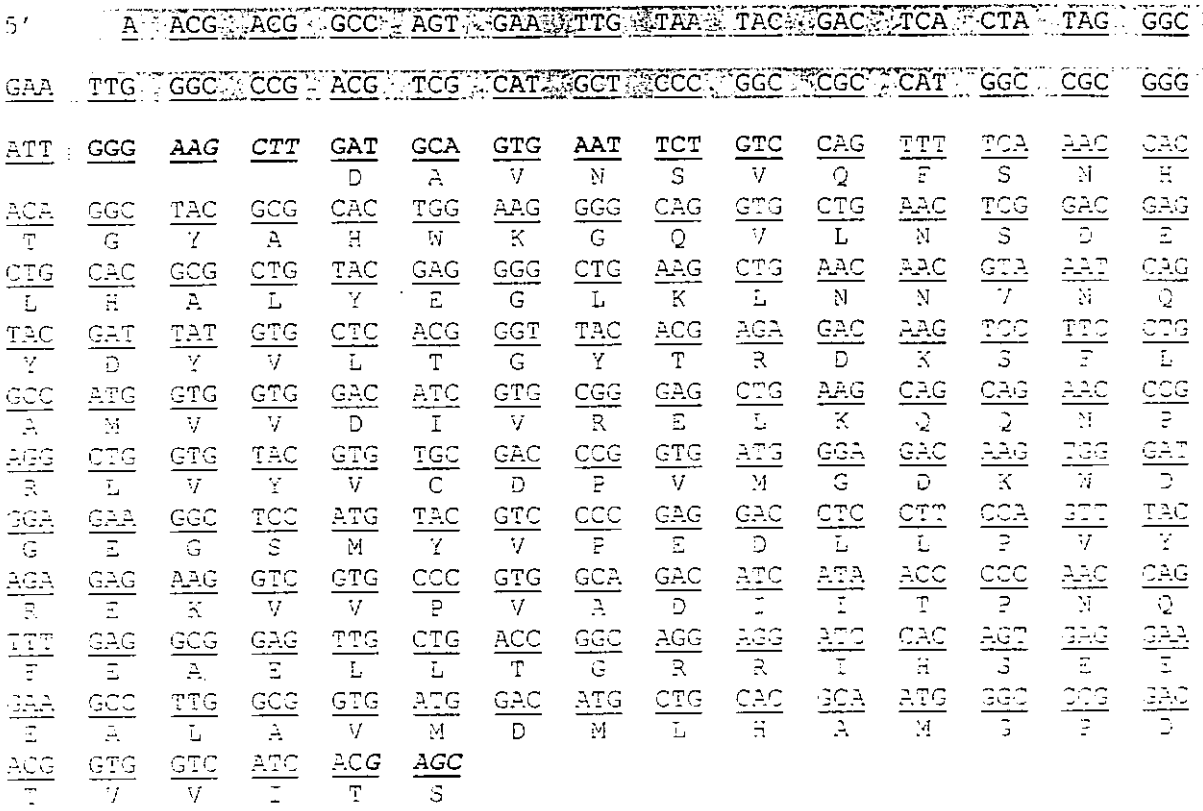

FIGURE 7H: Deduced sequence of PCR product of mutant Δ45 inserted into pGEM-T vector. The greyed region is the part of pGEM-T vector sequence (Appendix XI). The bolded region is the Δ45 N'-terminal primer sequence. The *Hin*dIII (AAGCTT) and *Sac*I (GAGCTC) restriction sites were shown in bold and italic type.

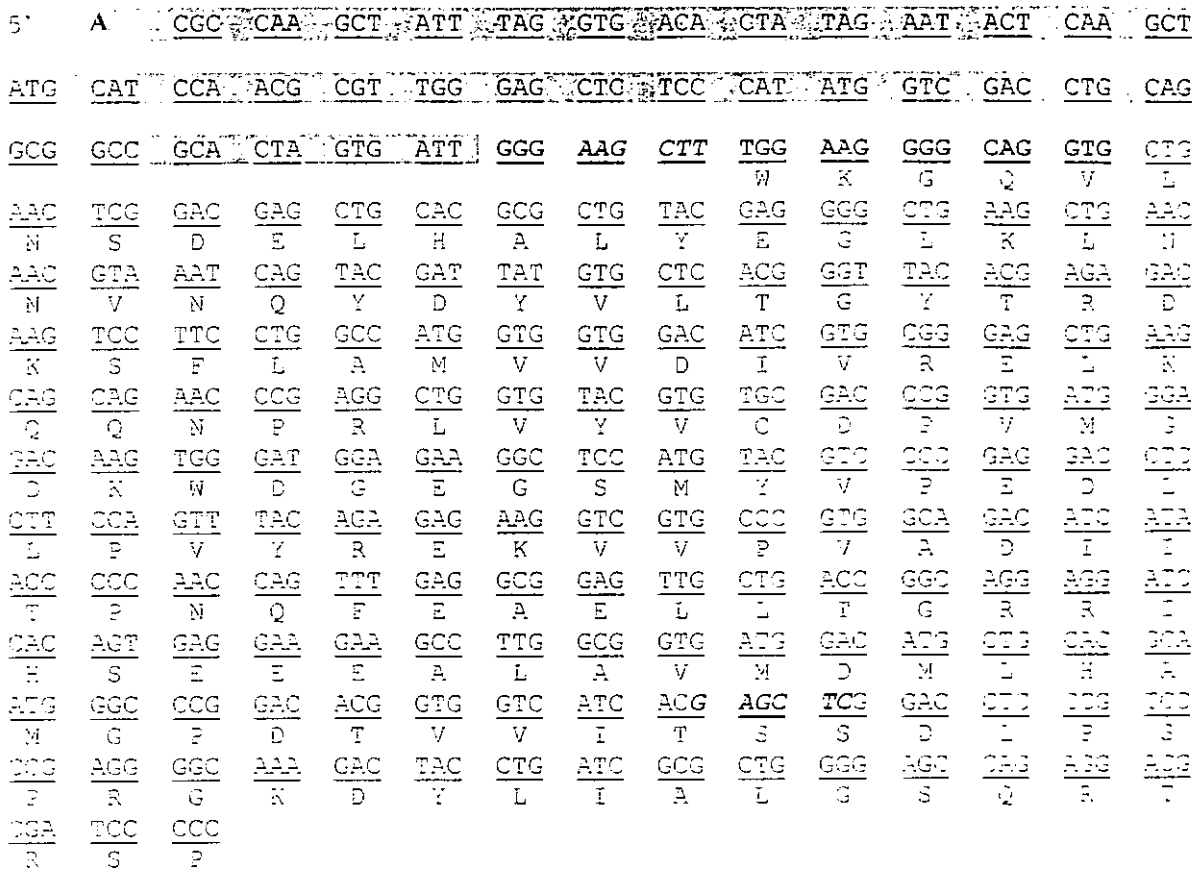

FIGURE 7I: Deduced sequence of PCR product of mutant Δ61 inserted into pGEM-T vector. The greyed region is the part of pGEM-T vector sequence (Appendix XI). The bolded region is the Δ61 N'-terminal primer sequence. The *Hin*dIII (AAGCTT) and *Sac*I (GAGCTC) restriction sites were shown in bold and italic type.

TABLE V: The fragment size of mutants in PCR, *Hin*dIII-*Sac*I digestion and *Hin*dIII-*Pvu*II digestion. The molecular weight was expressed in base pair (bp).

Mutant	*PCR product (bp)*	*HindIII-SacI (bp)*	*HindIII-PvuII (bp)*
Δ15	941	552	855
Δ16	938	549	852
Δ17	935	546	849
Δ18	932	543	846
Δ21	923	534	837
Δ24	914	525	828
Δ27	905	516	819
Δ45	851	462	765
Δ61	803	414	717

3.2 CONSTRUCTION OF THE RECOMBINANT EXPRESSION VECTORS

The truncated pyridoxal kinase cDNA was digested with *Hin*dIII and *Sac*I restriction enzymes. The *Hin*dIII site was located at the 5'-end. The *Sac*I site was located inside the pyridoxal kinase gene sequence. The restriction map of pyridoxal kinase is shown in Appendix IX. Molecular weights of *Hin*dIII-*Sac*I fragments of each mutant were listed in Table V. Successful digestion of fragments was monitored on agarose gel electrophoresis (Figure 8A-C). Two fragments were observed in all mutants digestion except mutants Δ24, Δ27 and Δ45. Three fragments were seen in these three mutants because cloning of these mutants into pGEM-T vector was

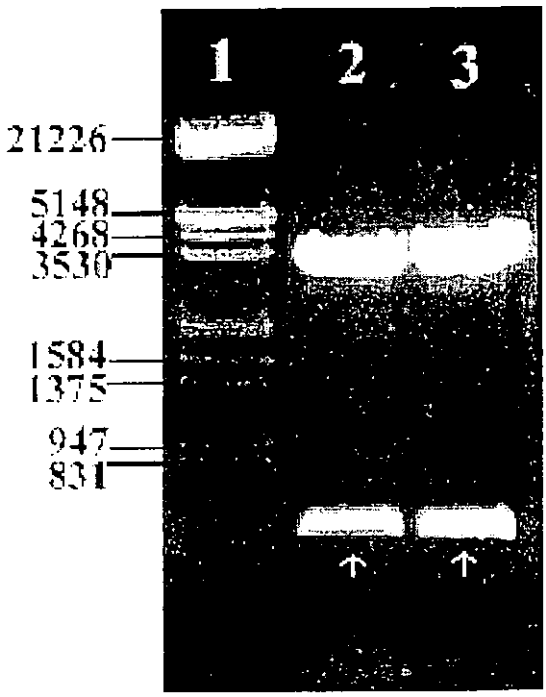

FIGURE 8A: *Hin*dIII and *Sac*I digested fragments of mutants (Δ16 and Δ17) inserted into pGEM-T vector shown in 0.8 % agarose gel electrophoresis. Lane 1, DNA molecular weight marker III, molecular weight in base pairs are indicated; Lane 2, Δ16; Lane 3, Δ17. The arrows indicated the fragments that were inserted into the pAED4 expression vectors.

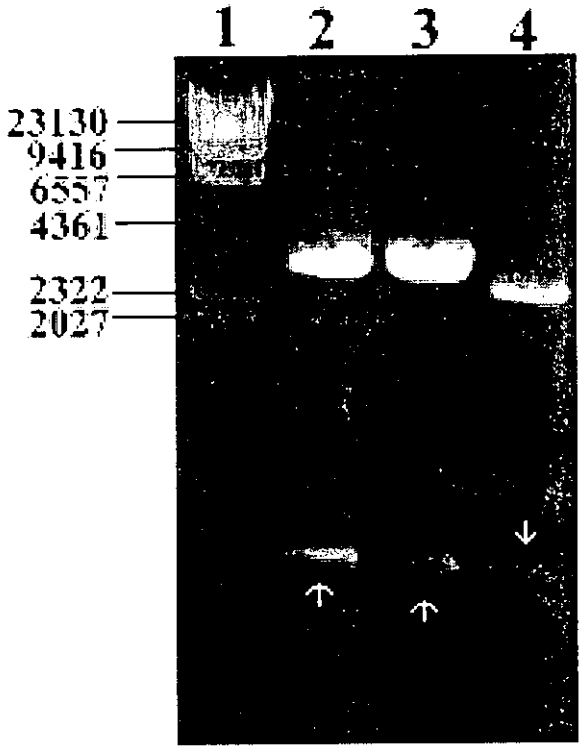

FIGURE 8B: *Hin*dIII and *Sac*I digested fragments of mutants (Δ18, Δ21 and Δ24) inserted into pGEM-T vector shown in 0.8 % agarose gel electrophoresis. Lane 1, λDNA *Hin*dIII marker, molecular weight in base pairs are indicated; Lane 2, Δ18; Lane 3, Δ21; Lane 4, Δ24. The arrows indicated the fragments that were inserted into the pAED4 expression vectors.

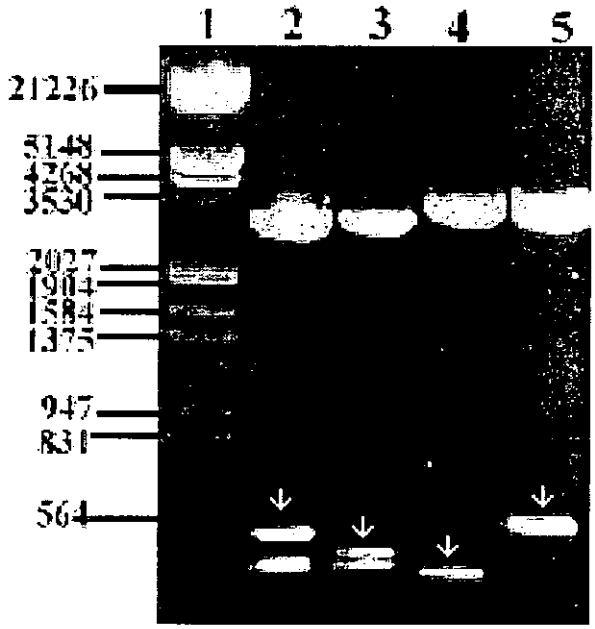

FIGURE 8C: *Hin*dIII and *Sac*I digested fragments of mutants (Δ27, Δ45, Δ61 and Δ15) inserted into pGEM-T vector shown in 0.8 % agarose gel electrophoresis. Lane 1, DNA molecular weight marker III, molecular weight in base pairs are indicated; Lane 2, Δ27; Lane 3, Δ45; Lane 4, Δ61 and Lane 5, Δ15. The arrows indicated the fragments that were ligated into the pAED4 expression vectors.

bidirectional (Appendix XII). The other mutants were inserted in the correct direction as indicated in Appendix XIIB. Both directions would generate three fragments but of different molecular sizes. However, as shown in Appendix VIIB, the smallest fragment (47 bp) is too small to be seen in the agarose gel. The cDNA fragment between *Hin*dIII-*Sac*I sites were purified and ligated with linear 6xHis-PK-pAED4 treated with the same restriction enzymes. *Hin*dIII and *Pvu*II digestion was used to check the success of ligation for each constructed mutant expression vector. The digestion results are shown after agarose gel electrophoresis (Figure 9A-B). *Hin*dIII-*Pvu*II fragments of these mutants showed a gradual reduction in molecular weights with an increasing number of N-terminal amino acid deletion. Apparent molecular weights of these digested fragments observed were in agreement with that calculated using the DNA sequence (Table V). cDNA inserted in this plasmid vector (Appendix XI) is under the control of a T7 promoter and in frame with a sequence that have six histidine residues in the N-terminal fusion peptide. This was confirmed in DNA sequencing analysis. The deduced sequences show that the start codon (ATG) was followed by the six histidine-tag at the N-terminal (Figure 10A-E). This His-tag functions as a metal-binding site on the fusion protein, hence allowing purification of the recombinant proteins by immobilized metal-affinity chromatography (Lu *et al.*, 1993).

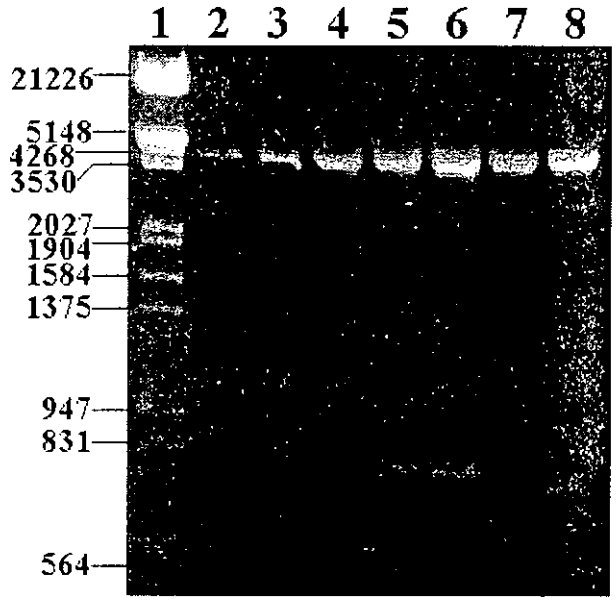

FIGURE 9A: *Hin*dIII and *Pvu*II digested fragments of recombinant pyridoxal kinase expression vector constructs (6xHis-PK, Δ15, Δ16, Δ17, Δ18, Δ21 and Δ24-pAED4). Lane 1, DNA molecular weight marker III, molecular weight in base pairs are indicated; Lane 2, 6xHis-PK-pAED4; Lane 3, 6xHis-Δ15-pAED4; Lane 4, 6xHis-Δ16-pAED4; Lane 5, 6xHis-Δ17-pAED4; Lane 6, 6xHis-Δ18-pAED4; Lane 7, 6xHis-Δ21-pAED4; Lane 8, 6xHis-Δ24-pAED4.

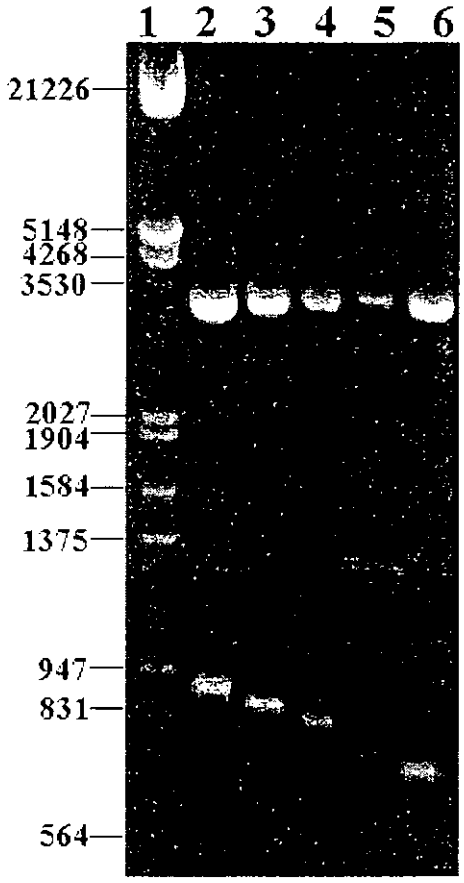

FIGURE 9B: *Hin*dIII and *Pvu*II digested fragments of recombinant pyridoxal kinase expression vector constructs (6xHis-PK, Δ15, Δ27, Δ45 and Δ61-pAED4). Lane 1, DNA molecular weight marker III, molecular weight in base pairs are indicated; Lane 2, 6xHis-PK-pAED4; Lane 3, 6xHis-Δ15-pAED4; Lane 4, 6xHis-Δ27-pAED4; Lane 5, 6xHis-Δ45-pAED4; Lane 6, 6xHis-Δ61-pAED4.

```
5'   CAA  CGG  TTT  CCC  TCT  AGA  AAT  AAT  TTT  GTT  TAA  CTT  TAA  GAA

GGA  GAT  ATA  CAT  ATG  CAT  CAT  CAT  CAT  CAT  CAT  AAG  CTT  CGG  GTG
                  M    H    H    H    H    H    H    K    L    R    V
CTC  TCC  ATT  CAG  AGC  CAC  GTC  GTC  CGC  GGC  TAC  GTG  GGC  AAC  CGA
 L    S    I    Q    S    H    V    V    R    G    Y    V    G    N    R
GCT  GCA  ACG  TTC  CCG  CTG  CAG  GTT  CTG  GGG  TTC  GAG  GTC  GAT  GCA
 A    A    T    F    P    L    Q    V    L    G    F    E    V    D    A
GTG  AAT  TCT  GTC  CAG  TTT  TCA  AAC  CAC  ACA  GGC  TAC  GCG  CAC  TGG
 V    N    S    V    Q    F    S    N    H    T    G    Y    A    H    W
AAG  GGG  CAG  GTG  CTG  AAC  TCG  GAC  GAG  CTG  CAC  GCG  CTG  TAC  GAG
 K    G    Q    V    L    N    S    D    E    L    H    A    L    Y    E
GGG  CTG  AAG  CTG  AAC  AAC  GTA  AAT  CAG  TAC  GAT  TAT  GTG  CTC  ACG
 G    L    K    L    N    N    V    N    Q    Y    D    Y    V    L    T
GGT  TAC  ACG  AGA  GAC  AAG  TCC  TTC  CTG  GCC  ATG  GTG  GTG  GAC  ATC
 G    Y    T    R    D    K    S    F    L    A    M    V    V    D    I
GTG  CGG  GAG  CTG  AAG  CAG  CAG  AAC  CCG  AGG  CTG  GTG  TAC  GTG  TGC
 V    R    E    L    K    Q    Q    N    P    R    L    V    Y    V    C
GAC  CCG  GTG  ATG  GGA  GAC  AAG  TGG  GAT  GGA  GAA  GGC  TCC  ATG  TAC
 D    P    V    M    G    D    K    W    D    G    E    G    S    M    Y
GTC  CCC  GAG  GAC  CTC  CTT  CCA  GTT  TAC  AGA  GAG  AAG  GTC  GTG  CCC
 V    P    E    D    L    L    P    V    Y    R    E    K    V    V    P
GTG  GCA  GAC  ATC  ATA  ACC  CCC  AAC  CAG  TTT  GAG  GCG  GAG  TTG  CTG
 V    A    D    I    I    T    P    N    Q    F    E    A    E    L    L
ACC  GGC  AGG  AGG  ATC  CAC  AGT  GAG  GAA  GAA  GCC  TTG  GCG  GTG  ATG
 T    G    R    R    I    H    S    E    E    E    A    L    A    V    M
GAC  ATG  CTG  CAC  GCA  ATG  GGC  CCG  GAC  ACG  GTG  GTC  ATC  ACG  AGC
 D    M    L    H    A    M    G    P    D    T    V    V    I    T    S
TCG  GAC  CTC  CCG  TCC  CCG  AGG
 S    D    L    P    S    P    R
```

FIGURE 10A: Deduced sequence of mutant Δ15 cDNA inserted into pAED4 expression vector. The greyed region is six histidine tag. The ATG start codon (bold italic type) is located at upstream of the histidine tag. The *Nde*I (CATATG), *Hin*dIII (AAGCTT) and *Sac*I (GAGCTC) restriction sites are shown in italic type. The sequence in red colour is part of pAED4 sequence.

```
5′      A  CAA  CGG  TTT  CCC  TCT  AGA  AAT  AAT  TTT  GTT  TAA  CTT  TAA

GAA  GGA  GAT  ATA  CAT  ATG  CAT  CAT  CAT  CAT  CAT  CAT  AAG  CTT  GTG
                       M    H    H    H    H    H    H    K    L    V
CTC  TCC  ATT  CAG  AGC  CAC  GTC  GTC  CGC  GGC  TAC  GTG  GGC  AAC  CGA
 L    S    I    Q    S    H    V    V    R    G    Y    V    G    N    R
GCT  GCA  ACG  TTC  CCG  CTG  CAG  GTT  CTG  GGG  TTC  GAG  GTC  GAT  GCA
 A    A    T    F    P    L    Q    V    L    G    F    E    V    D    A
GTG  AAT  TCT  GTC  CAG  TTT  TCA  AAC  CAC  ACA  GGC  TAC  GCG  CAC  TGG
 V    N    S    V    Q    F    S    N    H    T    G    Y    A    H    W
AAG  GGG  CAG  GTG  CTG  AAC  TCG  GAC  GAG  CTG  CAC  GCG  CTG  TAC  GAG
 K    G    Q    V    L    N    S    D    E    L    H    A    L    Y    E
GGG  CTG  AAG  CTG  AAC  AAC  GTA  AAT  CAG  TAC  GAT  TAT  GTG  CTC  ACG
 G    L    K    L    N    N    V    N    Q    Y    D    Y    V    L    T
GGT  TAC  ACG  AGA  GAC  AAG  TCC  TTC  CTG  GCC  ATG  GTG  GTG  GAC  ATC
 G    Y    T    R    D    K    S    F    L    A    M    V    V    D    I
GTG  CGG  GAG  CTG  AAG  CAG  CAG  AAC  CCG  AGG  CTG  GTG  TAC  GTG  TGC
 V    R    E    L    K    Q    Q    N    P    R    L    V    Y    V    C
GAC  CCG  GTG  ATG  GGA  GAC  AAG  TGG  GAT  GGA  GAA  GGC  TCC  ATG  TAC
 D    P    V    M    G    D    K    W    D    G    E    G    S    M    Y
GTC  CCC  GAG  GAC  CTC  CTT  CCA  GTT  TAC  AGA  GAG  AAG  GTC  GTG  CCC
 V    P    E    D    L    L    P    V    Y    R    E    K    V    V    P
GTG  GCA  GAC  ATC  ATA  ACC  CCC  AAC  CAG  TTT  GAG  GCG  GAG  TTG  CTG
 V    A    D    I    I    T    P    N    Q    F    E    A    E    L    L
ACC  GGC  AGG  AGG  ATC  CAC  AGT  GAG  GAA  GAA  GCC  TTG  GCG  GTG  ATG
 T    G    R    R    I    H    S    E    E    E    A    L    A    V    M
GAC  ATG  CTG  CAC  GCA  ATG  GGC  CCG  GAC  ACG  GTG  GTC  ATC  ACG  AGC
 D    M    L    H    A    M    G    P    D    T    V    V    I    T    S
```

FIGURE 10B: Deduced sequence of mutant Δ16 cDNA inserted into pAED4 expression vector. The greyed region is six histidine tag. The ATG start codon (bold italic type) is located at upstream of the histidine tag. The *Nde*I (CATATG), *Hin*dIII (AAGCTT) and *Sac*I (GAGCTC) restriction sites are shown in italic type. The sequence in red colour is part of pAED4 sequence.

5′	TTT	CCC	TCT	AGA	AAT	AAT	TTT	GTT	TAA	CTT	TAA	GAA	GGA	GAT
ATA	CAT	ATG	CAT	CAT	CAT	CAT	CAT	CAT	AAG	CTT	CTC	TCC	ATT	CAG
		M	H	H	H	H	H	H	K	L	L	S	I	Q
AGC	CAC	GTC	GTC	CGC	GGC	TAC	GTG	GGC	AAC	CGA	GCT	GCA	ACG	TTC
S	H	V	V	R	G	Y	V	G	N	R	A	A	T	F
CCG	CTG	CAG	GTT	CTG	GGG	TTC	GAG	GTC	GAT	GCA	GTG	AAT	TCT	GTC
P	L	Q	V	L	G	F	E	V	D	A	V	N	S	V
CAG	TTT	TCA	AAC	CAC	ACA	GGC	TAC	GCG	CAC	TGG	AAG	GGG	CAG	GTG
Q	F	S	N	H	T	G	Y	A	H	W	K	G	Q	V
CTG	AAC	TCG	GAC	GAG	CTG	CAC	GCG	CTG	TAC	GAG	GGG	CTG	AAG	CTG
L	N	S	D	E	L	H	A	L	Y	E	G	L	K	L
AAC	AAC	GTA	AAT	CAG	TAC	GAT	TAT	GTG	CTC	ACG	GGT	TAC	ACG	AGA
N	N	V	N	Q	Y	D	Y	V	L	T	G	Y	T	R
GAC	AAG	TCC	TTC	CTG	GCC	ATG	GTG	GTG	GAC	ATC	GTG	CGG	GAG	CTG
D	K	S	F	L	A	M	V	V	D	I	V	R	E	L
AAG	CAG	CAG	AAC	CCG	AGG	CTG	GTG	TAC	GTG	TGC	GAC	CCG	GTG	ATG
K	Q	Q	N	P	R	L	V	Y	V	C	D	P	V	M
GGA	GAC	AAG	TGG	GAT	GGA	GAA	GGC	TCC	ATG	TAC	GTC	CCC	GAG	GAC
G	D	K	W	D	G	E	G	S	M	Y	V	P	E	D
CTC	CTT	CCA	GTT	TAC	AGA	GAG	AAG	GTC	GTG	CCC	GTG	GCA	GAC	ATC
L	L	P	V	Y	R	E	K	V	V	P	V	A	D	I
ATA	ACC	CCC	AAC	CAG	TTT	GAG	GCG	GAG	TTG	CTG	ACC	GGC	AGG	AGG
I	T	P	N	Q	F	E	A	E	L	L	T	G	R	R
ATC	CAC	AGT	GAG	GAA	GAA	GCC	TTG	GCG	GTG	ATG	GAC	ATG	CTG	CAC
I	H	S	E	E	E	A	L	A	V	M	D	M	L	H
GCA	ATG	GGC	CCG	GAC	ACG	GTG	GTC	ATC	ACG	AGC	TCG	GAC		
A	M	G	P	D	T	V	V	I	T	S	S	D		

FIGURE 10C: Deduced sequence of mutant Δ17 cDNA inserted into pAED4 expression vector. The greyed region is six histidine tag. The ATG start codon (bold italic type) is located at upstream of the histidine tag. The *Nde*I (CATATG), *Hin*dIII (AAGCTT) and *Sac*I (GAGCTC) restriction sites are shown in italic type. The sequence in red colour is part of pAED4 sequence.

5′	CGG	TTT	CCC	TCT	AGA	AAT	AAT	TTT	GTT	TAA	CTT	TAA	GAA	GGA
GAT	ATA	*CAT*	***ATG***	CAT	CAT	CAT	CAT	CAT	CAT	*AAG*	*CTT*	TCC	ATT	CAG
			M	H	H	H	H	H	H	K	L	S	I	Q
AGC	CAC	GTC	GTC	CGC	GGC	TAC	GTG	GGC	AAC	CGA	GCT	GCA	ACG	TTC
S	H	V	V	R	G	Y	V	G	N	R	A	A	T	F
CCG	CTG	CAG	GTT	CTG	GGG	TTC	GAG	GTC	GAT	GCA	GTG	AAT	TCT	GTC
P	L	Q	V	L	G	F	E	V	D	A	V	N	S	V
CAG	TTT	TCA	AAC	CAC	ACA	GGC	TAC	GCG	CAC	TGG	AAG	GGG	CAG	GTG
Q	F	S	N	H	T	G	Y	A	H	W	K	G	Q	V
CTG	AAC	TCG	GAC	GAG	CTG	CAC	GCG	CTG	TAC	GAG	GGG	CTG	AAG	CTG
L	N	S	D	E	L	H	A	L	Y	E	G	L	K	L
AAC	AAC	GTA	AAT	CAG	TAC	GAT	TAT	GTG	CTC	ACG	GGT	TAC	ACG	AGA
N	N	V	N	Q	Y	D	Y	V	L	T	G	Y	T	R
GAC	AAG	TCC	TTC	CTG	GCC	ATG	GTG	GTG	GAC	ATC	GTG	CGG	GAG	CTG
D	K	S	F	L	A	M	V	V	D	I	V	R	E	L
AAG	CAG	CAG	AAC	CCG	AGG	CTG	GTG	TAC	GTG	TGC	GAC	CCG	GTG	ATG
K	Q	Q	N	P	R	L	V	Y	V	C	D	P	V	M
GGA	GAC	AAG	TGG	GAT	GGA	GAA	GGC	TCC	ATG	TAC	GTC	CCC	GAG	GAC
G	D	K	W	D	G	E	G	S	M	Y	V	P	E	D
CTC	CTT	CCA	GTT	TAC	AGA	GAG	AAG	GTC	GTG	CCC	GTG	GCA	GAC	ATC
L	L	P	V	Y	R	E	K	V	V	P	V	A	D	I
ATA	ACC	CCC	AAC	CAG	TTT	GAG	GCG	GAG	TTG	CTG	ACC	GGC	AGG	AGG
I	T	P	N	Q	F	E	A	E	L	L	T	G	R	R
ATC	CAC	AGT	GAG	GAA	GAA	GCC	TTG	GCG	GTG	ATG	GAC	ATG	CTG	CAC
I	H	S	E	E	E	A	L	A	V	M	D	M	L	H
GCA	ATG	GGC	CCG	GAC	ACG	GTG	GTC	ATC	*ACG*	*AGC*				
A	M	G	P	D	T	V	V	I	T	S				

FIGURE 10D: Deduced sequence of mutant Δ18 cDNA inserted into pAED4 expression vector. The greyed region is six histidine tag. The ATG start codon (bold italic type) is located at upstream of the histidine tag. The *Nde*I (CATATG), *Hin*dIII (AAGCTT) and *Sac*I (GAGCTC) restriction sites are shown in italic type. The sequence in red colour is part of pAED4 sequence.

```
5'      A  CGG  TTT  CCC  TCT  AGA  AAT  AAT  TTT  GTT  TAA  CTT  TAA  GAA

GGA  GAT  ATA  CAT  ATG  CAT  CAT  CAT  CAT  CAT  CAT  AAG  CTT  AGC  CAC
                  M    H    H    H    H    H    H    K    L    S    H
GTC  GTC  CGC  GGC  TAC  GTG  GGC  AAC  CGA  GCT  GCA  ACG  TTC  CCG  CTG
 V    V    R    G    Y    V    G    N    R    A    A    T    F    P    L
CAG  GTT  CTG  GGG  TTC  GAG  GTC  GAT  GCA  GTG  AAT  TCT  GTC  CAG  TTT
 Q    V    L    G    F    E    V    D    A    V    N    S    V    Q    F
TCA  AAC  CAC  ACA  GGC  TAC  GCG  CAC  TGG  AAG  GGG  CAG  GTG  CTG  AAC
 S    N    H    T    G    Y    A    H    W    K    G    Q    V    L    N
TCG  GAC  GAG  CTG  CAC  GCG  CTG  TAC  GAG  GGG  CTG  AAG  CTG  AAC  AAC
 S    D    E    L    H    A    L    Y    E    G    L    K    L    N    N
GTA  AAT  CAG  TAC  GAT  TAT  GTG  CTC  ACG  GGT  TAC  ACG  AGA  GAC  AAG
 V    N    Q    Y    D    Y    V    L    T    G    Y    T    R    D    K
TCC  TTC  CTG  GCC  ATG  GTG  GTG  GAC  ATC  GTG  CGG  GAG  CTG  AAG  CAG
 S    F    L    A    M    V    V    D    I    V    R    E    L    K    Q
CAG  AAC  CCG  AGG  CTG  GTG  TAC  GTG  TGC  GAC  CCG  GTG  ATG  GGA  GAC
 Q    N    P    R    L    V    Y    V    C    D    P    V    M    G    D
AAG  TGG  GAT  GGA  GAA  GGC  TCC  ATG  TAC  GTC  CCC  GAG  GAC  CTC  CTT
 K    W    D    G    E    G    S    M    Y    V    P    E    D    L    L
CCA  GTT  TAC  AGA  GAG  AAG  GTC  GTG  CCC  GTG  GCA  GAC  ATC  ATA  ACC
 P    V    Y    R    E    K    V    V    P    V    A    D    I    I    T
CCC  AAC  CAG  TTT  GAG  GCG  GAG  TTG  CTG  ACC  GGC  AGG  AGG  ATC  CAC
 P    N    Q    F    E    A    E    L    L    T    G    R    R    I    H
AGT  GAG  GAA  GAA  GCC  TTG  GCG  GTG  ATG  GAC  ATG  CTG  CAC  GCA  ATG
 S    E    E    E    A    L    A    V    M    D    M    L    H    A    M
GGC  CCG  GAC  ACG  GTG  GTC  ATC  ACG  AGC  TCG  GAC  CTC  CCG  TCC  CCG
 G    P    D    T    V    V    I    T    S    S    D    L    P    S    P
AGG  GGC  AAA  GAC  TAC  CTG  ATC  GCG
 R    G    K    D    Y    L    I    A
```

FIGURE 10E: Deduced sequence of mutant Δ21 cDNA inserted into pAED4 expression vector. The greyed region is six histidine tag. The ATG start codon (bold italic type) is located at upstream of the histidine tag. The *Nde*I (CATATG), *Hin*dIII (AAGCTT) and *Sac*I (GAGCTC) restriction sites are shown in italic type. The sequence in red colour is part of pAED4 sequence.

3.3 EXPRESSION

The His-tagged wild type and various deletion mutants of pyridoxal kinase were successfully expressed. Up to 0.2 mg/ml of protein was detected in bacterial lysate using Bradford method. Samples were analysed by SDS/PAGE (Figure 11), immunoblotting by using monoclonal antibody against native pig brain pyridoxal kinase (Figure 12A-B) and pyridoxal kinase activtiy assay. All the recombinant pyridoxal kinase proteins have the expected sizes and listed in Table VI.

TABLE VI: Molecular weight of pyridoxal kinase calculated from SDS/PAGE and Western blots

Mutants	Molecular weight in Dalton
Wild-type	38,173
Δ15	36,545
Δ16	36,352
Δ17	36,344
Δ18	36,121
Δ21	35,865
Δ24	35,461
Δ27	35,001
Δ45	34,903
Δ61	33,413
Pig brain PK	37,265

Molecular weight of the His-tagged recombinant pyridoxal kinase was slightly higher than that of the native pig brain pyridoxal kinase. The

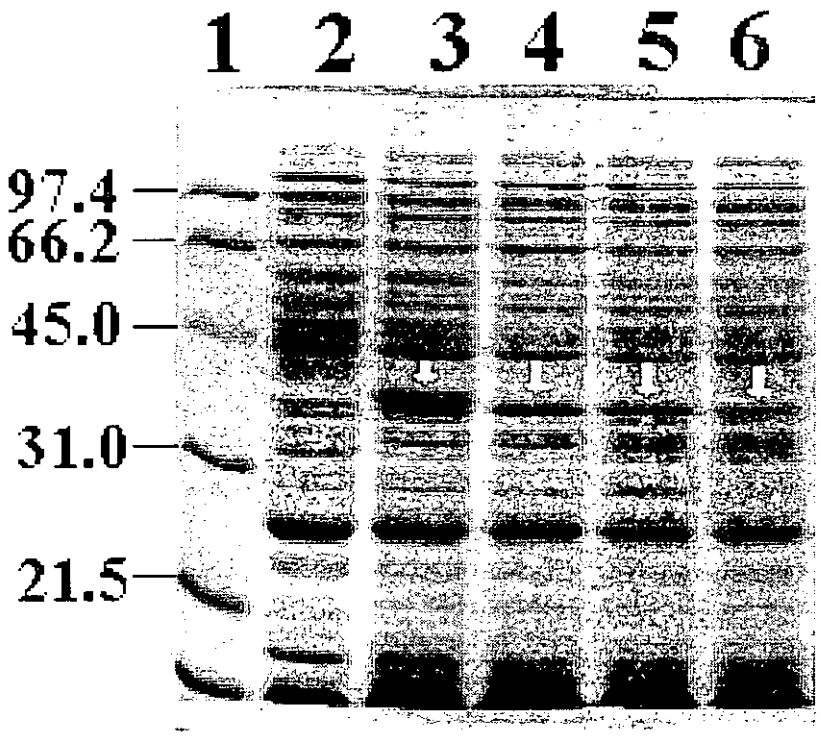

FIGURE 11: **SDS/PAGE of expressed protein in cell lysate.** Lane 1 molecular mass standards, molecular masses in kilodaltons are indicated; Lane 2, Control, *E.coli* strain with pAED4; Lane 3, wild-type, *E.coli* strain with 6xHis-PK-pAED4; Lane 4, Δ15, *E.coli* strain with 6xHis-Δ15-pAED4; Lane 5, Δ16, *E.coli* strain with 6xHis-Δ16-pAED4; Lane 6, Δ17, *E.coli* strain with 6xHis-Δ17-pAED4. The arrows indicates the target proteins.

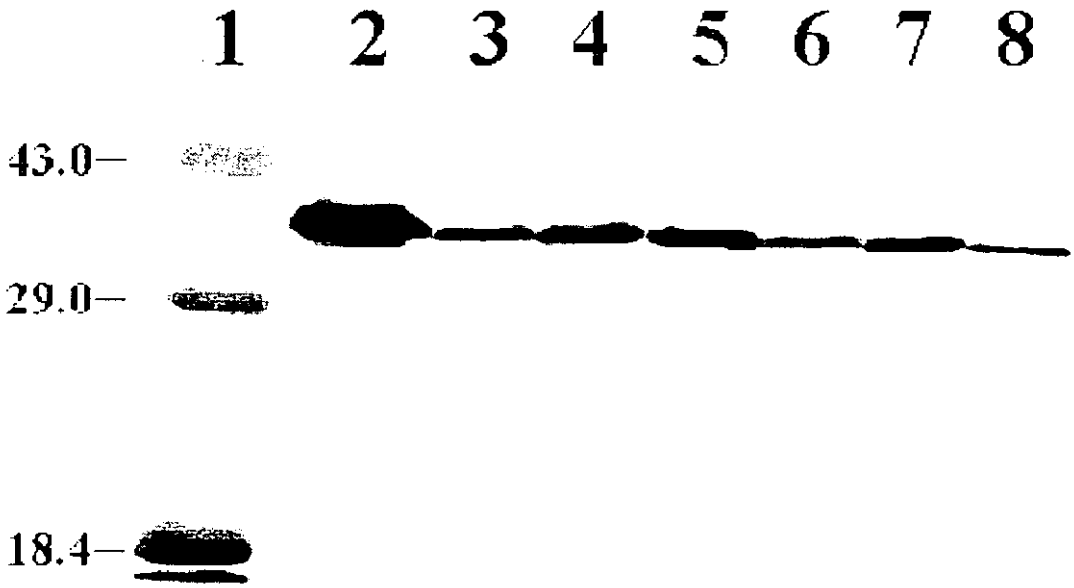

FIGURE 12A: Western blots analysis of expressed cell lysate (6xHis-PK, Δ15, Δ16, Δ17, Δ18, Δ21 and Δ24). Lane 1, molecular mass standards, molecular masses in kilodaltons are indicated; Lane 2, 6xHis-PK (500ng); Lane 3, 6xHis-Δ15 (500ng); Lane 4, 6xHis-Δ16 (10μg); Lane 5, 6xHis-Δ17 (500ng); Lane 6, 6xHis-Δ18 (10μg); Lane 7, 6xHis-Δ21 (10μg); Lane 8, 6xHis-Δ24 (10μg). The monoclonal antibody is anti-pig brain pyridoxal kinase raised from the mouse.

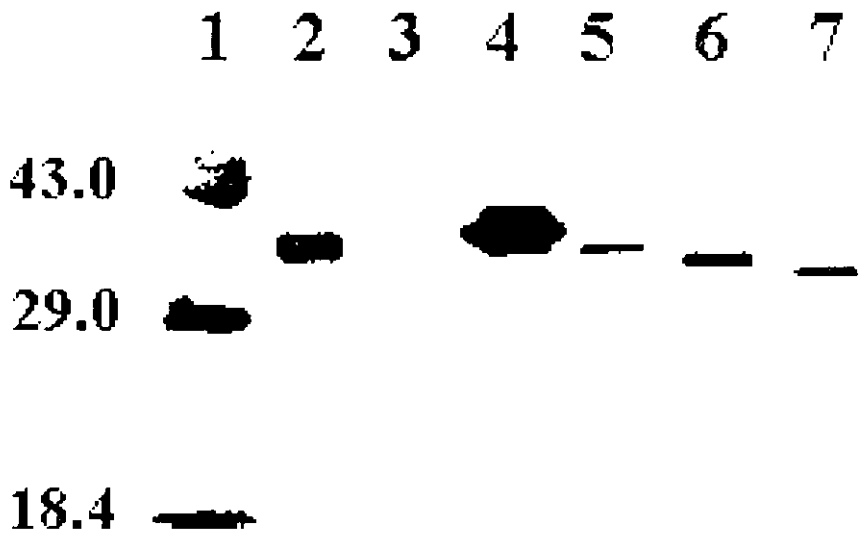

FIGURE 12B: Western blots analysis of expressed cell lysate (6xHis-PK, Δ27, Δ45 and Δ61). Lane 1, molecular mass standards, molecular masses in kilodaltons are indicated; Lane 2, native pig brain pyridoxal kinase; Lane 3, pAED4 (500ng); Lane 4, 6xHis-PK (500ng); Lane 5, 6xHis-Δ27 (10μg); Lane 6, 6xHis-Δ45 (10μg); Lane 7, 6xHis-Δ61 (10μg). The monoclonal antibody is anti-pig brain pyridoxal kinase raised from the mouse.

excess molecular weight was probably due to the histidine tail. About 10 % of His-tagged protein was expressed in the total bacterial lysate as observed using SDS/PAGE (Figure 11). Both of the immunoblot and SDS/PAGE showed that the level of expression of truncated mutants was reduced. For mutants Δ15, Δ16, and Δ17, the expression level of mutant protein were similar, but about half when compared with the non-truncated pyridoxal kinase protein. Cell lysate of mutants with 18 amino acids or more deleted were barely detectable on immunoblots when compared with wild type using similar total protein level. When a 20 folds more concentrated mutant cell lysate was loaded into the immunoblot, comparable intensity with the wild type was seen. Pyridoxal kinase activity was measured in each expressed bacterial protein. A summary of activity measurements is shown in Table VII.

TABLE VII: Summary of activity measurement of expressed recombinant pyridoxal kinase in cell lysate

Sample	Specific activity (nmole PLP min^{-1} mg^{-1})
Control Stain	0
Wild-type	4.23
Δ15	2.88
Δ16	1.42
Δ17	0
Δ18	0
Δ21	0
Δ24	0
Δ27	0
Δ45	0
Δ61	0

No pyridoxal kinase activity was found in the control (*E.coli* strain with vector, but without the pyridoxal kinase cDNA insert). The pyridoxal kinase activity was detected in His-tagged recombinant wild-type, Δ15 and Δ16 but not in the other mutants. There were 68 % and 33 % specific activity retained in Δ15 and Δ16 respectively when compared to the wild-type. When the mutant Δ17 with one more amino acid, valine, was deleted the catalytic activity was lost totally.

3.4 PURIFICATION

In order to investigate the relationship of structural change with the catalytic activity lost of recombinant pyridoxal kinase by some biophysical experimentation, purification was performed on three expressed proteins, His-tagged wild type, Δ15 and Δ16. Preliminary studies on several purification steps were done to optimize the purification procedures and conditions. Ammonium sulphate precipitation and pyridoxal-agarose chromatography were tried. They were the routine steps involved in pig brain pyridoxal kinase purification (Kerry *et al.*, 1986). The His-tagged pyridoxal kinase was purified three folds (Table VIII) after treatment with 40-60 % ammonium sulphate fractionation. The sample was dialysed against 5 mM potassium phosphate buffer and analyzed by SDS/PAGE (Figure 13). The dialysed sample was loaded onto a pyridoxyl-agarose column (2 x 2 cm). The kinase was eluted by 50 mM pyridoxal at pH4.0. There was a 50 % decrease in the specific activity of the eluted protein. The activity lost was probably due to the stringent elution condition.

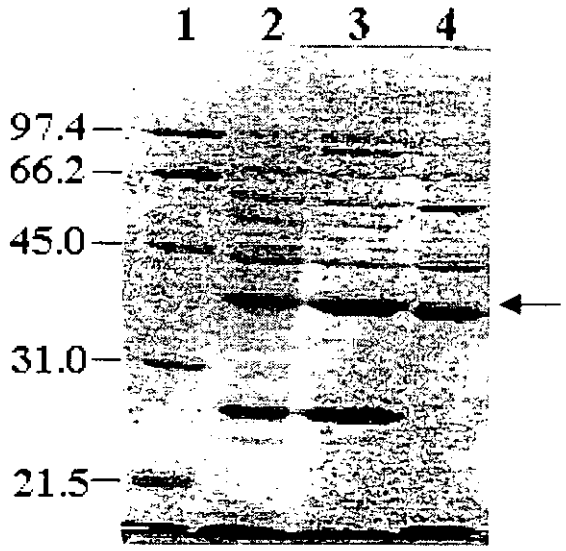

FIGURE 13: **SDS/PAGE of recombinant pyridoxal kinase purified by 40-60% ammonium sulphate fractionation and pyridoxyl-agarose affinity chromatography.** Lane 1, molecular mass standards, molecular masses in kilodaltons are indicated; Lane 2, Total cellular protein of 6xHis-PK; Lane 3, sample after 40-60% ammonium sulphate fractionation; Lane 4, sample after pyridoxyl-agarose affinity chromatography. The arrow indicates the target protein.

TABLE VIII: Summary of purification included 40-60 % ammonium sulphate fractionation and pyridoxyl-agarose affinity chromatography

Treatment	Total Protein (mg)	Total Activity (nmole PLP min^{-1})	Specific Activity (nmole PLP min^{-1} mg^{-1})	Purification (Fold)	Yield (%)
WT in cell lysate	10	68	6.8	1	100
40-60 % Ammonium sulphate fractionation	1.98	44.7	22.6	3.3	65.7
Pyridoxyl-agarose affinity chromatography	0.72	8.2	11.4	0.5	12

A nickel-chelated IDA chromatography was tried to purify the recombinant pyridoxal kinase taking advantage of the fusion peptide at the N-terminal. The sample loaded onto the column was eluted by 100 mM imidazole. The recombinant pyridoxal kinase was purified four folds and the SDS/PAGE result is shown in Figure 14. Compared with the purification performance of ammonium sulphate precipitation and

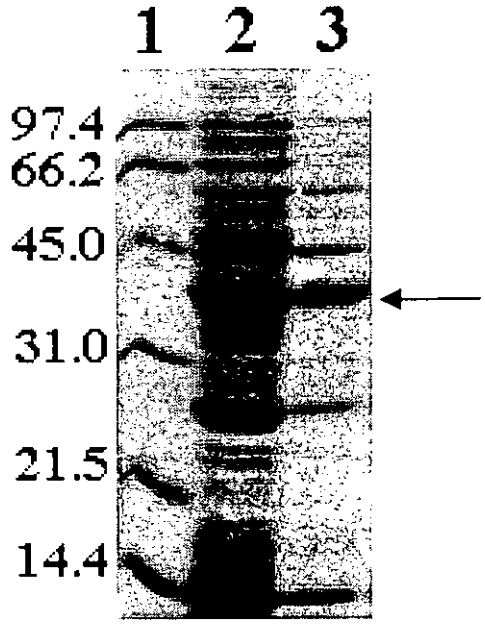

FIGURE 14: SDS/PAGE of recombinant pyridoxal kinase purified by nickel-chelating chromatography using 100 mM imidazole elution. Lane 1, molecular mass standards, molecular masses in kilodaltons are indicated; Lane 2, Total cellular protein of 6xHis-PK (Specific activity is 9.6 nmole PLP min^{-1} mg^{-1}); Lane 3, Sample eluted by 100 mM imidazole with 38 nmole PLP min^{-1} mg^{-1} specific activity. The arrow indicates the target protein.

pyridoxal agarose, this single step (nickel-chelating IDA chromatography) was the most successful approach in purifying active His-tagged pyridoxal kinase. The purity of eluted protein from nickel-chelating IDA column can be further improved by washing with 20 mM imidazole before elution. The bound His-tagged protein was eluted by 100 mM imidazole. It was because the 20 mM imidazole wash can remove large amount of contaminants and with minimal lost of pyridoxal kinase activity. The SDS/PAGE of protein eluted by a series concentration of imidazole are shown Figure 15. The His-tagged pyridoxal kinase eluted by this method was purified 7 fold (Table IX) and the purity of the eluted protein was analysed by SDS/PAGE (Figure 16).

TABLE IX: Summary of purification of non-truncated recombinant pyridoxal kinase

Treatment	Total Protein (mg)	Total Activity (nmole PLP min^{-1})	Specific Activity (nmole PLP min^{-1} mg^{-1})	Purification (Fold)	Yield (%)
WT in cell lysate	154	1478.4	9.6	1	100
Ni^{2+}-chelating chromatography	17	1164.5	68.5	7.14	78.8
DEAE chromatography	4.12	1021.76	248.0	25.8	69.1

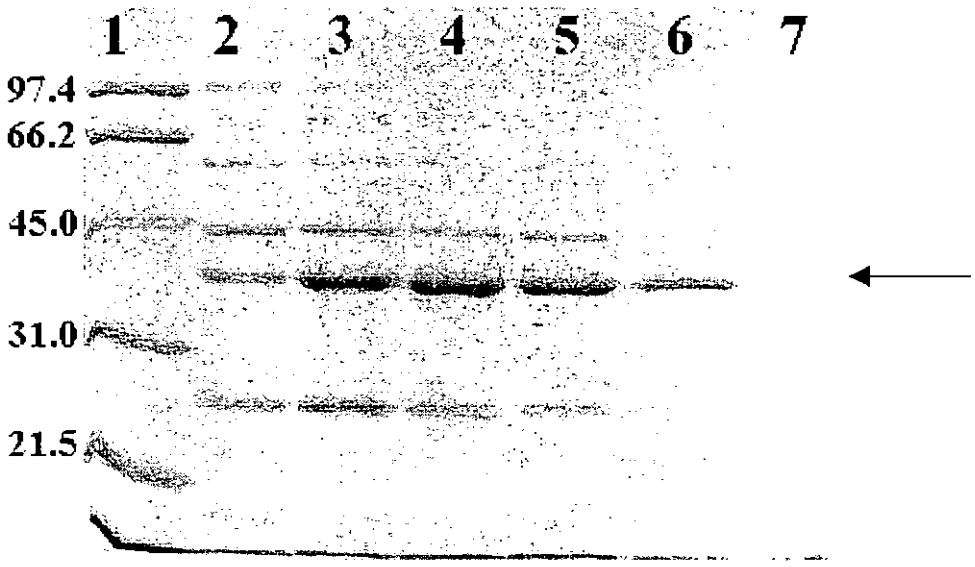

FIGURE 15: SDS/PAGE of recombinant pyridoxal kinase eluted from nickel-chelating chromatography by a series concentration of imidazole (20-500 mM). Lane 1, molecular mass standards, molecular masses in kilodaltons are indicated; Lane 2, sample (3.3 U) eluted by 20 mM imidazole; Lane 3, sample (25.3 U) eluted by 40 mM imidazole; Lane 4, sample (30.2 U) eluted by 60 mM imidazole; Lane 5, sample (25.4 U) eluted by 80 mM imidazole; Lane 6, sample (24,4 U) eluted by 100 mM imidazole; Lane 7, sample (0 U) eluted by 500 mM imidazole. The total activity (U is total nmole PLP formed per min) of each eluted fraction was indicated in the bracket. The arrow indicates the target protein.

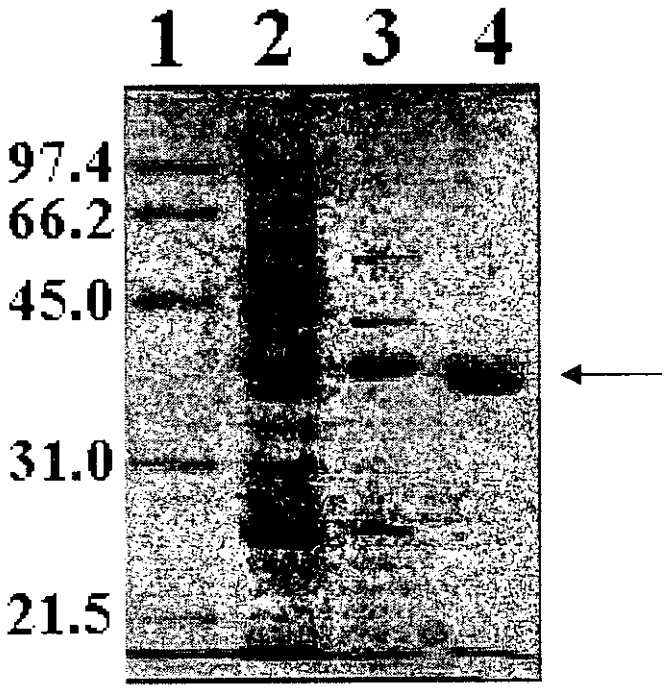

FIGURE 16: SDS/PAGE of purified recombinant pyridoxal kinase. Lane 1, molecular mass standard, molecular masses in kilodaltons are indicated; Lane 2, Total cellular protein of 6xHis-PK; Lane 3, Sample after nickel-chelating chromatography; Lane 4, Sample after DEAE. The arrow indicates the target protein.

The partially purified protein was subjected to an anion exchanger, DEAE, under the control of a FPLC system. The sample was eluted by a 0-200 mM NaCl gradient as detailed in Section 2.10.4 of experimental procedures. The elution profile of DEAE is shown in Figure 17. There was three major protein peaks observed. The first peak eluted at 174 mM NaCl and the other two peaks eluted at 181 mM NaCl and 183 mM NaCl respectively. Only the first protein peak had detectable pyridoxal kinase activity. By these two step purification, the protein can be purified 25 fold (Table IX) and the SDS/PAGE is shown in Figure 16.

Mutant Δ15 and Δ16 were purified using the same methodology as the wild type. The elution profile of DEAE chromatography is shown in Figure 18. Interestingly, Δ15 was eluted as one major protein peak and at a lower concentration of NaCl (102 mM) compared to the elution profile of wild-type enzyme. The purification table of Δ15 is shown in Table X.

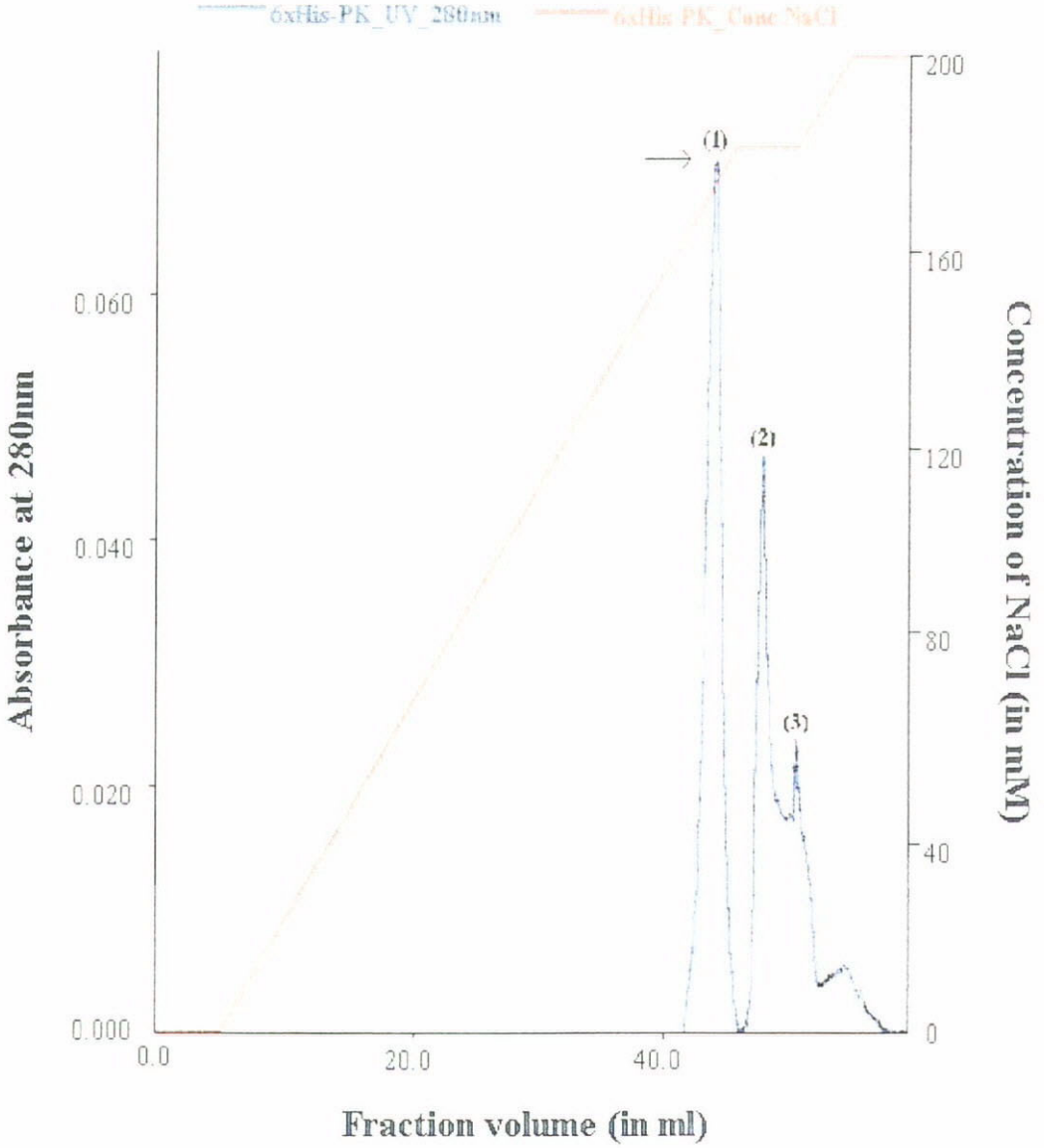

FIGURE 17: DEAE chromatography elution profile of non-truncated recombinant pyridoxal kinase. Peak (1) eluted at 174 mM NaCl. Peak (2) and Peak (3) eluted at 181 mM and 183 mM NaCl. The peak with pyridoxal kinase activity was indicated by an arrow. The orange line represents the NaCl gradient ant the blue line represents the protein concentration measured at absorbance 280 nm.

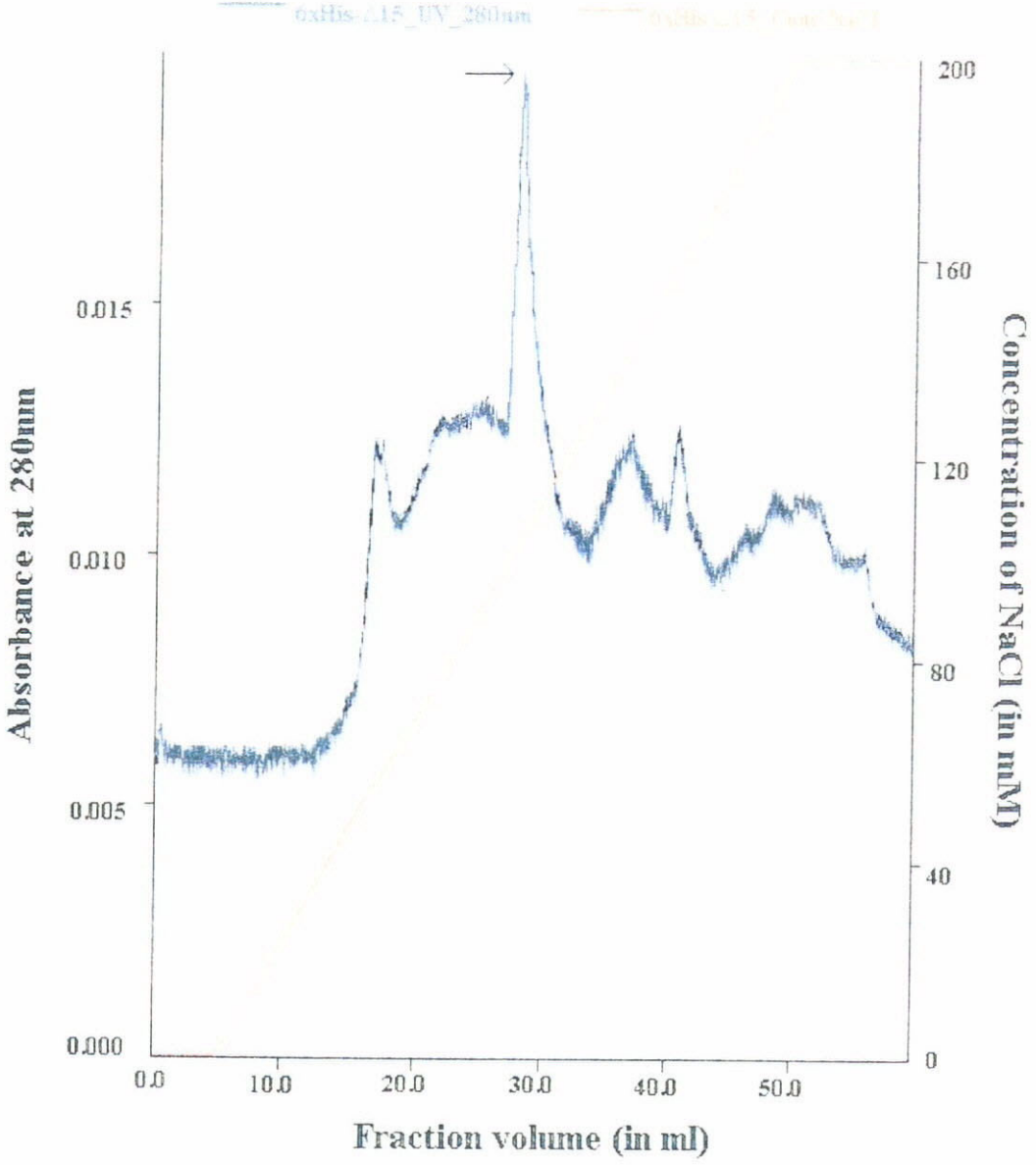

FIGURE 18: DEAE chromatography elution profile of mutant Δ15. The mutant Δ15 was eluted at 102 mM NaCl and indicated by an arrow. The orange line represents the NaCl gradient ant the blue line represents the protein concentration measured at absorbance 280 nm.

TABLE X: Summary of purification of mutant Δ15

Treatment	Total Protein (mg)	Total Activity (nmole PLP min^{-1})	Specific Activity (nmole PLP min^{-1} mg^{-1})	Purification (Fold)	Yield (%)
Δ15 in cell lysate	148	843.6	5.7	1	100
Ni^{2+}-chelating chromatography	13	534.17	41.09	7.2	63.32
DEAE chromatography	2.1	289.11	137.67	24.15	34.27

For the mutant Δ16, the same purification procedures were taken. The pyridoxal kinase activity was totally lost after passed through the nickel-chelating IDA Chromatography. All the eluted sample was pooled and dialysed against the 5 mM potassium phosphate buffer and loaded onto the DEAE chromatography. The elution profile of DEAE chromatography is shown in Figure 19. There are several protein peaks observed in the profile. Because the mutant proteins have no pyridoxal kinase catalytic activities, mutant proteins in the DEAE eluate were identified by Western blotting using monoclonal antibodies against pyridoxal kinase. As shown in Western blots (Figure 20), the second peak eluted at 174 mM NaCl is the targeted mutant (Δ16) protein. The three recombinant pyridoxal kinase was purified to homogeneity (Figure 21) and have positive result on Western blots (Figure 22). The purified wild-type and mutant Δ15 was

subjected to 8-15 % gradient native gel electrophoresis (Figure 23) to confirm that they ae in dimeric structure.

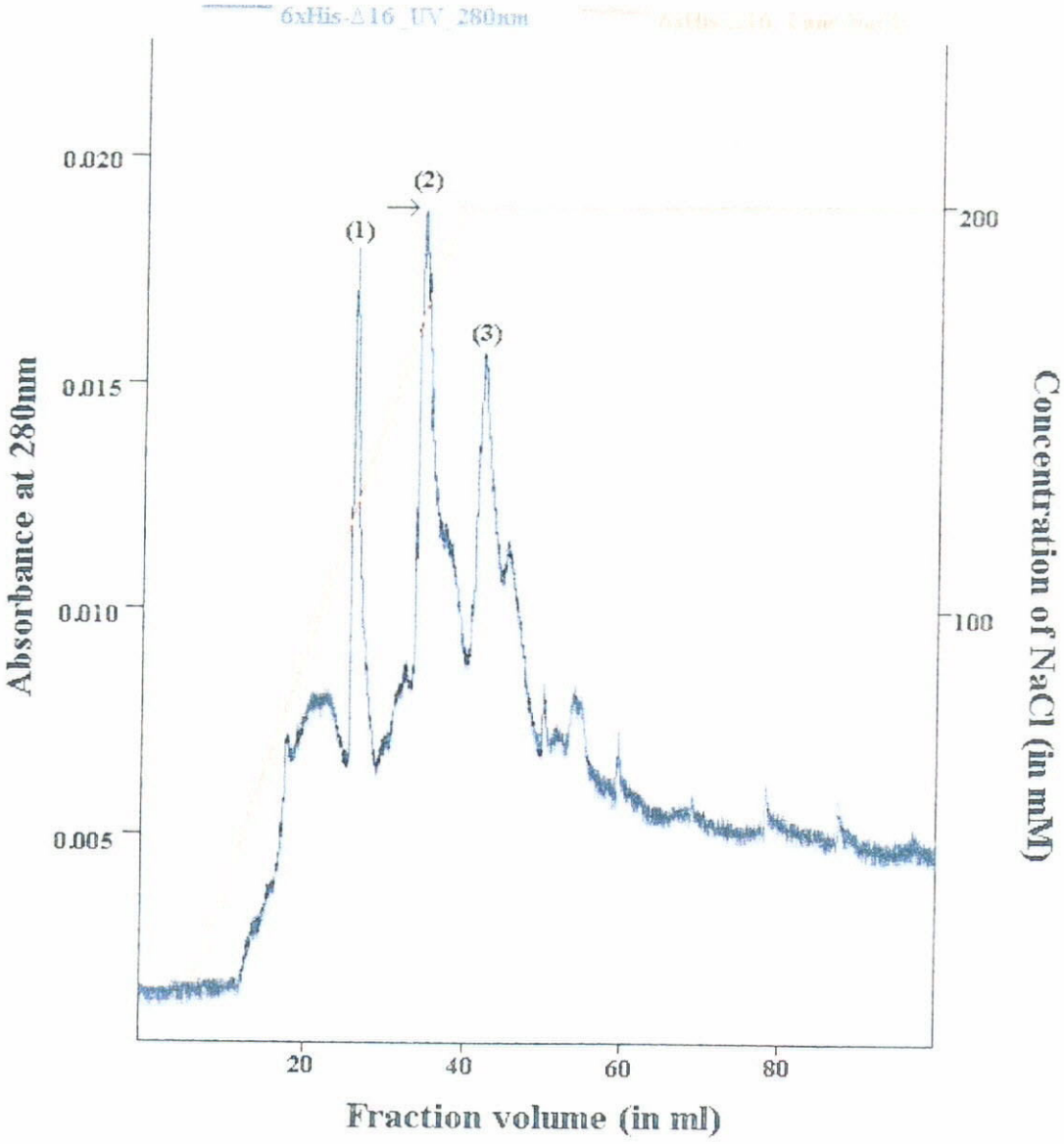

FIGURE 19: DEAE chromatography elution profile of mutant Δ16. The sample was eluted at 174 mM NaCl and indicated by an arrow. The orange line represents the NaCl gradient ant the blue line represents the protein concentration measured at absorbance 280 nm.

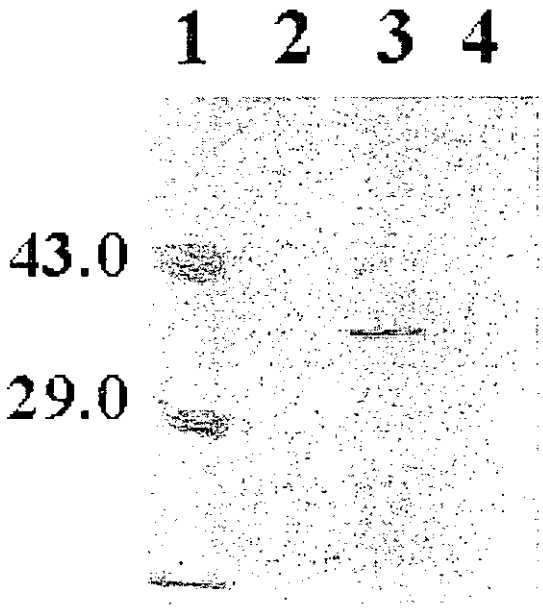

FIGURE 20: Western blots of mutant Δ16 eluted from DEAE chromatography. Lane 1, molecular mass standards, molecular masses in kilodaltons are indicated; Lane 2, first protein peak; Lane 3, second protein peak; Lane 4, third protein peak; from DEAE chromatography (Figure 19).

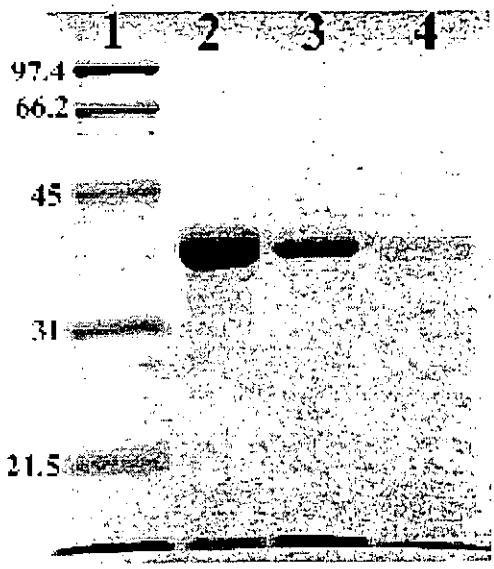

FIGURE 21: SDS/PAGE of purified recombinant pyridoxal kinase (WT, Δ15 and Δ16). Lane 1, molecular mass standards, molecular masses in kilodaltons are indicated; Lane 2, purified His-tagged wild-type; Lane 3, purified His-tagged Δ15; Lane 4, purified His-tagged Δ16.

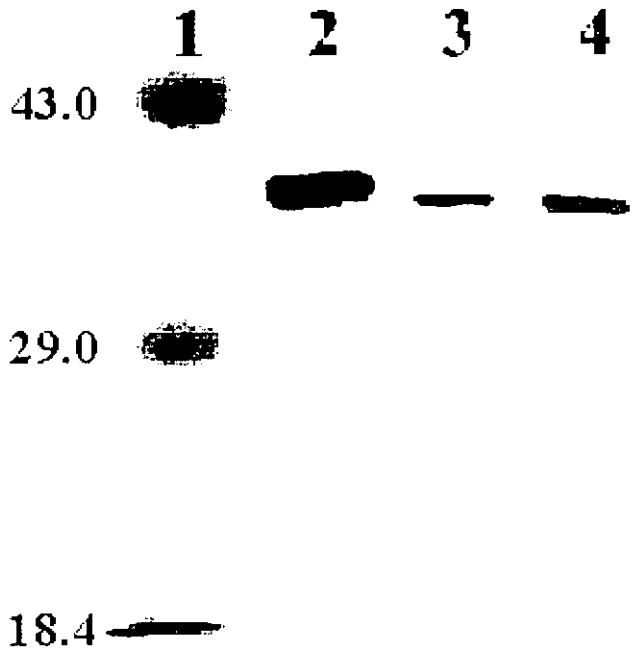

FIGURE 22: Western blot analysis of purified recombinant pyridoxal kinase (WT, Δ15 and Δ16). Lane 1: molecular mass standards; molecular masses in kilodaltons are indicated; Lane 2; 6xHis-PK; Lane 3, 6xHis-Δ15; Lane 4, 6xHis-Δ16.

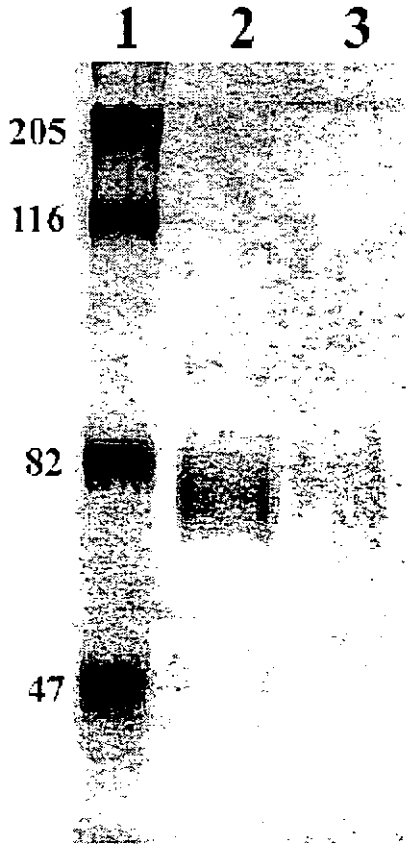

FIGURE 23: 8-15% gradient native gel of wild-type and mutant Δ15. Lane 1, molecular mass standards, molecular masses in kilodaltons are indicated; Lane 2, purified His-tagged wild-type; Lane 3, purified His-tagged Δ15.

3.5 KINETIC PARAMETER OF PURIFIED KINASE

Recombinant pyridoxal kinase, possesing a histidine tag attached to the N-terminus, displays catalytic parameters similar to those of the native pig brain pyridoxal kinase (Table XI). The steady-state kinetic parameters of deleted mutants in cell lysate and purified form are summaried in Table XI. There are slightly different in the K_m value for the substrate of recombinant pyridoxal kinase in different purity. The purified Δ15 mutant displayed K_m values for pyridoxal and ATP slightly different from those of the wild-type enzyme. The Δ15 mutant exhibited 65 % reduced K_m for ATP but two fold increase in K_m for pyridoxal when compared to the wild-type enzyme. There is less and no affect in the kinetic properties of pyridoxal kinase in unpurified state. This supported by the change of kinetic parameters that was in agreement with that measured in the crude lysate. The k_{cat} of the mutant Δ15 was reduced by 40 % when compared to the wild-type enzyme. Remarkably, when one more amino acid (arginine) was deleted from the primary sequence (mutant Δ16), catalytic activity was unstable and totally lost after purification. The K_m for ATP and pyridoxal were measured in cell lysate. There is dramatic decrease in both K_m. 59 % and 7 % K_m for ATP and pyridoxal measured in mutant Δ16 when compared to the wild-type enzyme. It should be emphasized that mutant proteins had indeed been expressed in *E.coli.* No catalytic activity was found in the recombinant protein.

TABLE XI: Kinetic parameters associated with pig brain pyridoxal kinase and His-tag recombinant pyridoxal kinase

	K_m (ATP) in μM		K_m (PL) in μM		k_{cat}
	cell lysate	purified	cell lysate	purified	purified
Pig brain PK	---	12	---	25	0.05
Wild-type	22	17	24	24	0.05
Δ15	15	6	31	43.2	0.02
Δ16	13	---	1.68	---	---

3.6 CIRCULAR DICHROISM (CD) MEASUREMENTS

The effect of deletion of amino acid residues on the secondary structure of pyridoxal kinase was examined by CD spectroscopy in the far-UV region of the spectrum covering the wavelength range 190-250 nm (Figure 24). All measurements were performed in 10 mM potassium phosphate at pH 7.0 using a protein concentration of 0.5 mg/ml. The CD spectrum of wild-type pyridoxal kinase exhibits a negative band centered at around 222 nm due to the $\eta\pi^*$ transition of the α-helix, and a positive band at around 190 nm due to the perpendicular component of the $\pi\pi^*$ transition. The signal at 222 nm was used to calculate the α-helix content (35 %). The CD spectrum of the catalytically competent mutant (Δ15) gives a signal at 222 nm comparable in magnitude to that of the wild-type enzyme, though the spectrum is slightly displaced towards shorter wavelengths. Interestingly, the CD spectrum of the inactive species (Δ16) differs from that of the wild-type enzyme. As shown in Figure 24, the intensity of the negative band corresponding to α-helix structures has been decreased and the positive band at around 190 nm is no longer detectable. The absence of a negative band at 195 nm corresponding to a random coil conformation strongly suggesting that the catalytically inactive mutant preserves some form of secondary structure.

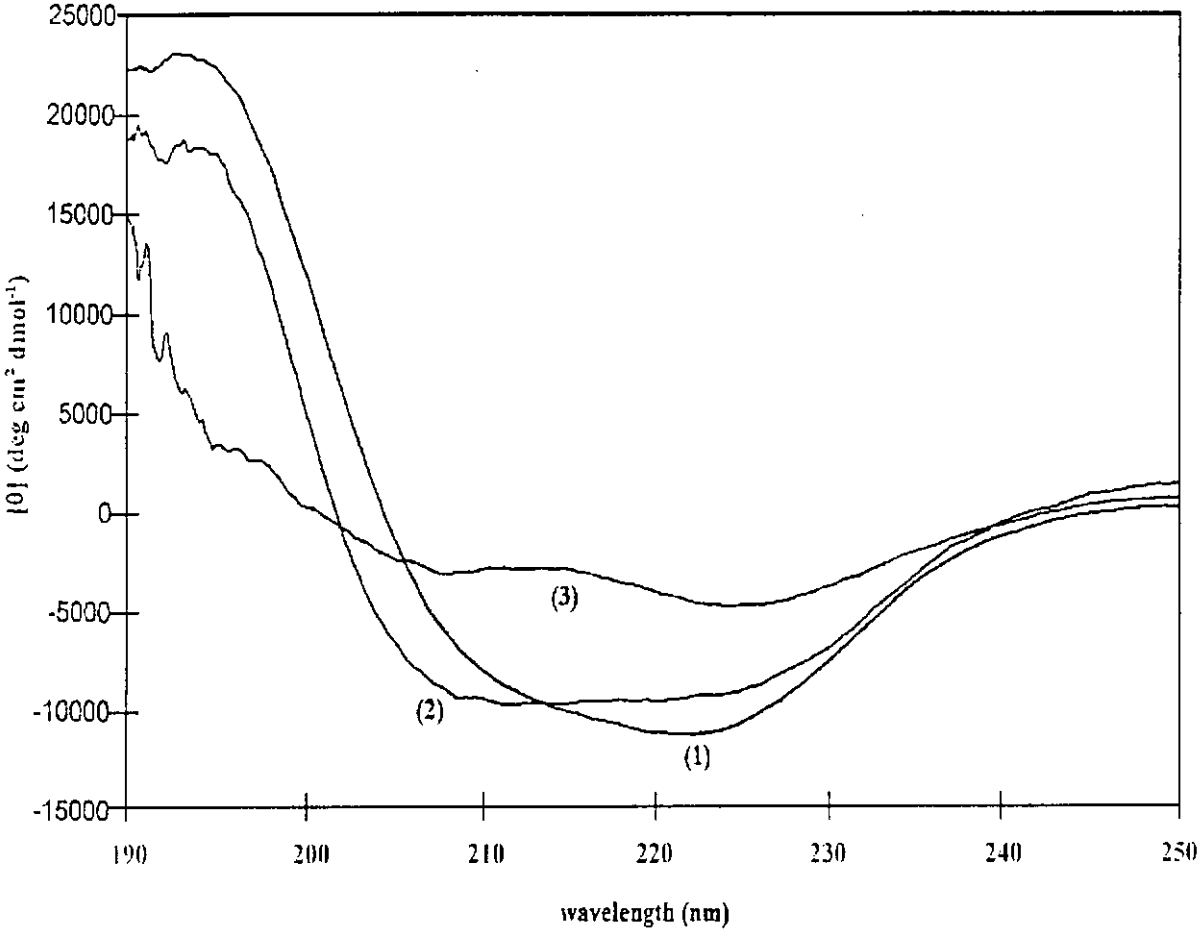

FIGURE 24: Circular dichroism spectra of His-tag recombinant pyridoxal kinase. Wild-type pyridoxal kinase *(curve 1)*, mutant Δ15 *(curve 2)*, and mutant Δ16 *(curve 3)* in 10 mM potassium phosphate, pH7.4 at a protein concentration 0.5 mg/ml.

3.7 BINDING OF TNP-ATP, AN ATP ANALOGUE

To ascertain whether conformational changes of the inactive mutant influence the structure of the ATP binding domain, samples of wild-type and mutated species were titrated with TNP-ATP. The ATP analogue shows very weak emission at 540 nm when excited at 410 nm. Binding of TNP-ATP to the nucleotide site of pyridoxal kinase results in a substantial increase in fluorescence yield detectable over a wide-range of wavelengths (Figure 25). As expected, addition of ATP to the solution containing enzyme and TNP-ATP results in displacement of TNP-ATP from the nucleotide binding site. The mutant (Δ15) endowed with catalytic activity also binds TNP-ATP with 83.4% fluorescence yielded compared that with wild-type enzyme. There is slightly decrease in the fluorescence intensity. This indicated that mutant Δ15 has a small change in the conformation of the ATP domain in agreement with the steady-state kinetic studies that with decreased K_m for ATP . The mutant (Δ16) devoid of catalytic activity has lost the ability to bind TNP-ATP even at concentrations of ligand twenty fold greater than the protein concentration (Figure 26). These results suggested that the structure of the ATP binding domain, localized mean the C-terminal end of the amino acid sequence, has been perturbed as a result of the deletion of amino acid residues pertaining to the N-terminal domain of the protein.

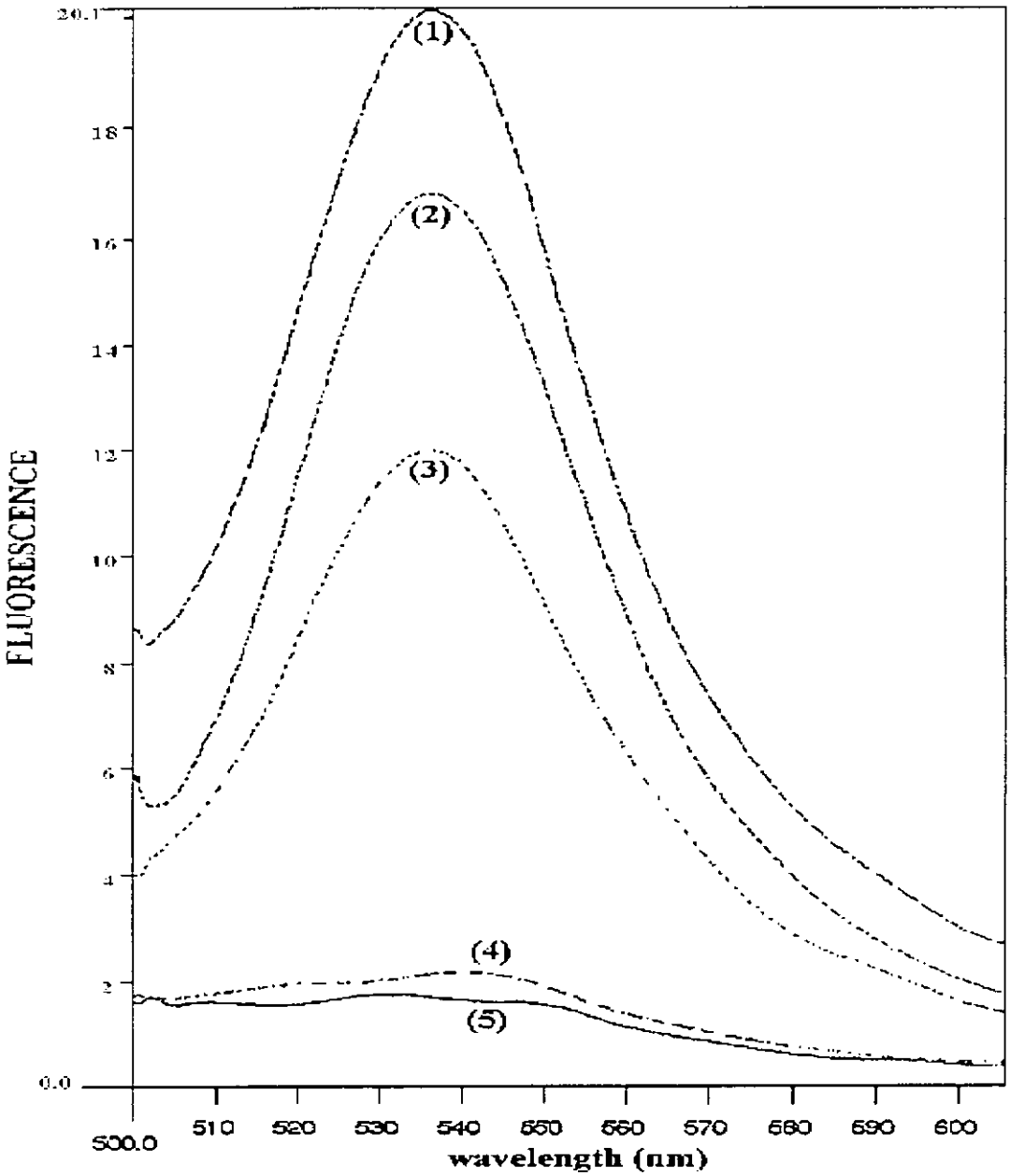

FIGURE 25: Emission spectra of pyridoxal kinase – TNP-ATP complex. Emission spectra of 2.5 μM WT pyridoxal kinase + 7.5 μM TNP-ATP *(curve 1)*, 2.5 μM mutant Δ15 + 7.5 μM TNP-ATP *(curve 2)*, 2.5 μM WT pyridoxal kinase + 7.5μM TNP-ATP + 25 μM ATP *(curve 3)*, 2.5 μM mutant Δ16 + 7.5 μM TNP-ATP *(curve 4)* and 7.5 μM TNP-ATP *(curve 5)*.

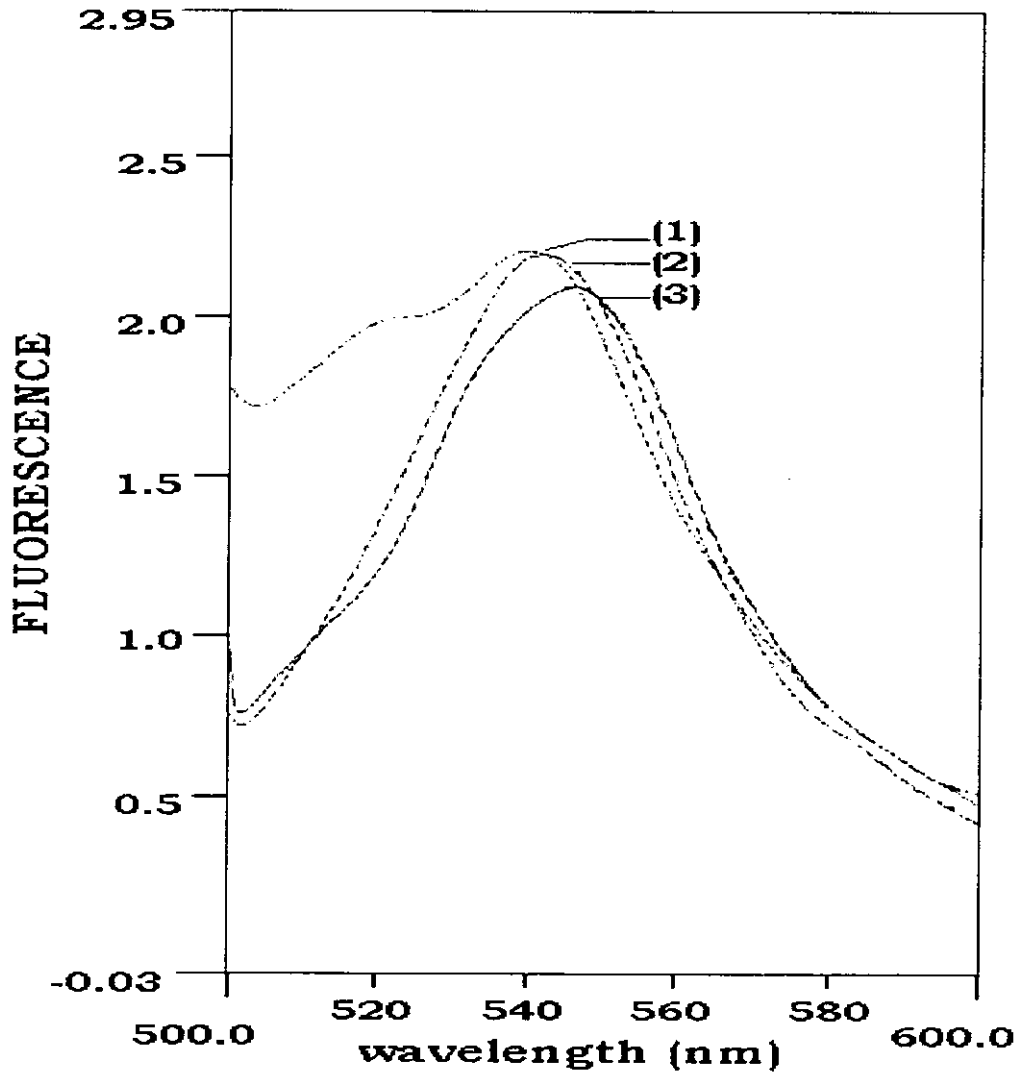

Figure 26: Emission spectra of mutant Δ16 with TNP-ATP. Emission spectra of 2.5 μM mutant Δ16 + 7.5 μM TNP-ATP (curve 1), 2.5 μM mutant Δ16 + 150 μM TNP-ATP (curve 2) and 150 μM TNP-ATP (curve 3).

3.8 STABILITY OF PYRIDOXAL KINASE VARIANTS

The stability of both wild-type and Δ15 mutated pyridoxal kinase against denaturation by GdnHCl at pH7.0 was investigated by fluorescence spectroscopy. All measurements were performed after incubation of the protein solutions for 30 minutes at 25°C in the presence of increasing concentrations of GdnHCl. Control measurements showed that this time of incubation is sufficient to reach equilibrium. The wild-type enzyme contains five tryptophanyl residues, and upon excitation at 295 nm shows a structureless emission band centered at around 345 nm (Figure 27). For the mutants (Δ15 and Δ16), same pattern of fluorescence spectra were observed upon excitation at 295 nm but with about 25 % fluorescence intensity. It is because the mutants have one tryptophanyl residues less than the wild-type enzyme. Addition of increasing concentrations of GdnHCl brings about a decrease in fluorescence intensity emitted at longer wavelength (Figure 28) and a progressive red shift in the band position of the emission spectra. At 2 M GdnHCl, the maximum of emission is centered at 350 nm, indicating exposure of the emitting tryptophanyl groups to the surrounding solvent. Further increase in GdnHCl concentration has no effect in the band position and intensity of fluorescence. The unfolding process is reversible since samples of wild-type enzyme exposed to 2 M GdnHCl regain catalytic activity upon dilution with buffer alone.

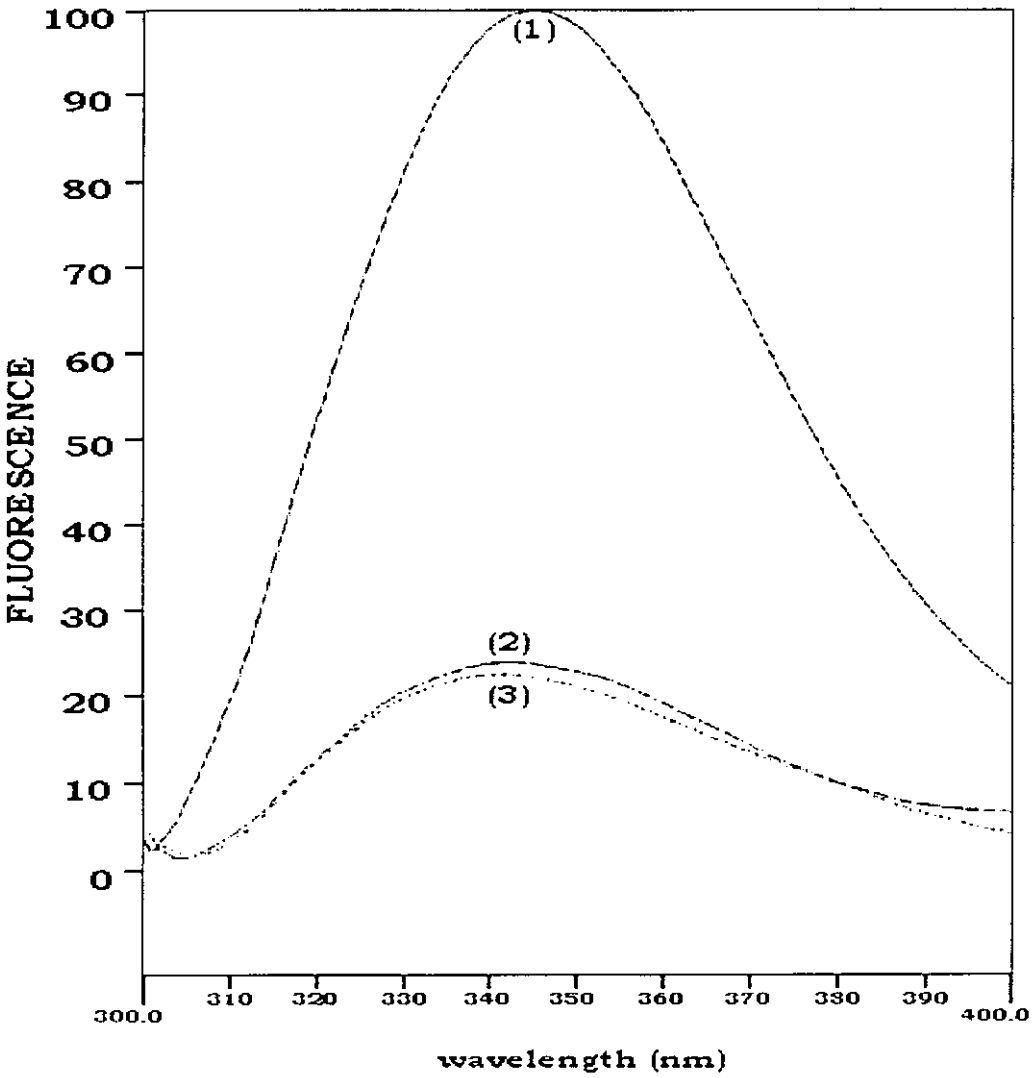

FIGURE 27: **Emission spectra of recombinant pyridoxal kinase upon excitation at 295 nm.** Wild-type enzyme *(curve 1)*, mutant Δ15 *(curve 2)* and mutant Δ16 *(curve 3)*.

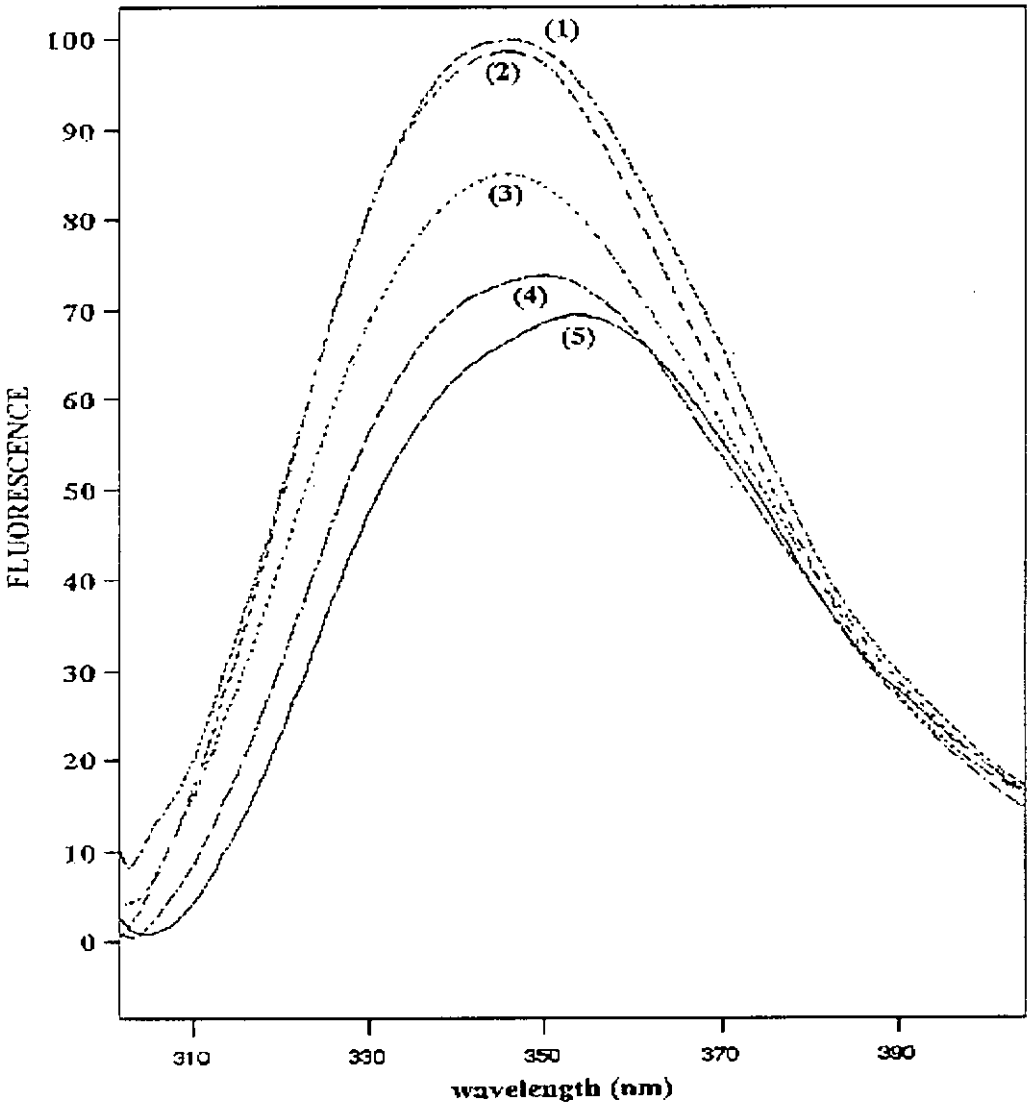

FIGURE 28: Emission spectra of pyridoxal kinase in various concentrations of GdnHCl. The spectra recorded in the presence of 0 M *(curve 1)*, 0.5 M *(curve 2)*, 1 M *(curve 3)*, 1.5 M *(curve 4)* and 2 M *(curve 5)*. The absorbance of the samples at the maximum of excitation (295 nm) were 0.1. The samples were treated with GdnHCl for 30 min at 25°C prior to recording the emission spectra.

In the analysis of the reversible denaturation, a two-state model consisting of equilibrium between folded and unfolded conformations, was assumed. Accordingly, the equilibrium constant (K_e) is related to the fraction of unfolded species (α_u) by the equation

$$K_e = \frac{\alpha_u}{1-\alpha_u} = e^{-\Delta Gu/RT} \quad (2)$$

where $\alpha_u = [F]_N - [F]_{obs} / [F]_N - [F]_U$, $[F]_N$ and $[F]_U$ are the fluorescence intensities of folded and unfolded species, respectively.

The free energy of unfolding was found to vary linearly with GdnHCl concentration, therefore ΔG_{H_2O} was calculated by extrapolating to zero GdnHCl concentration. The denaturation curve of recombinant pyridoxal kinase is indistinguishable from the enzyme isolated from pig brain tissues; therefore the process of unfolding of both proteins is adequately represented by the same free energy ΔG = 4 kcal/mol. The stability of two purified mutants, Δ15 and Δ16, to various concentrations of GdnHCl was also investigated and shown in Figure 29 and Figure 30 respectively. Both the maximum of fluorescence undergoes a red shift of around 5 nm when the GdnHCl concentration reaches a value of 0.5 M. Over the concentration range 0-0.5 M GdnHCl the fluorescence is increased, whereas further increase in denaturing concentration results in quenching of protein fluorescence concomitant with irreversible loss of catalytic activity. This unusual behavior strongly suggests that intermediate species are formed during denaturation of the truncated mutants. Hence, the

overall unfolding reaction should start with the folded conformer (N) and end up with the unfolded species (U) and with intermediate species (I) formed in between the process, i.e. $N \rightarrow I \rightarrow U$.

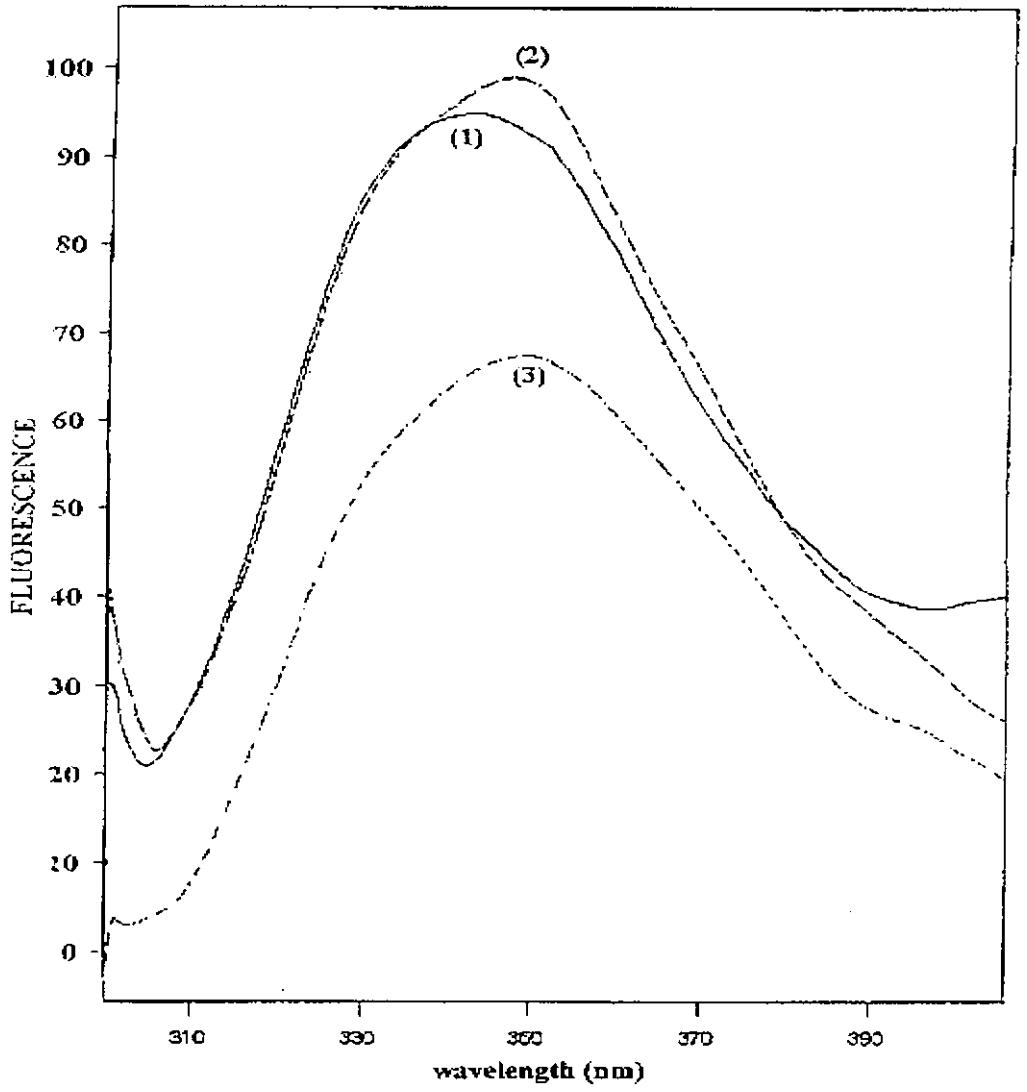

FIGURE 29: Emission spectra of mutant Δ15 in various concentrations of GdnHCl. The spectra recorded in the presence of 0 M *(curve 1)*, 0.5 M *(curve 2)*, and 2 M *(curve 3)*. The absorbance of the samples at the maximum of excitation (295 nm) were 0.1. The samples were treated with GdnHCl for 30 min at 25°C prior to recording the emission spectra.

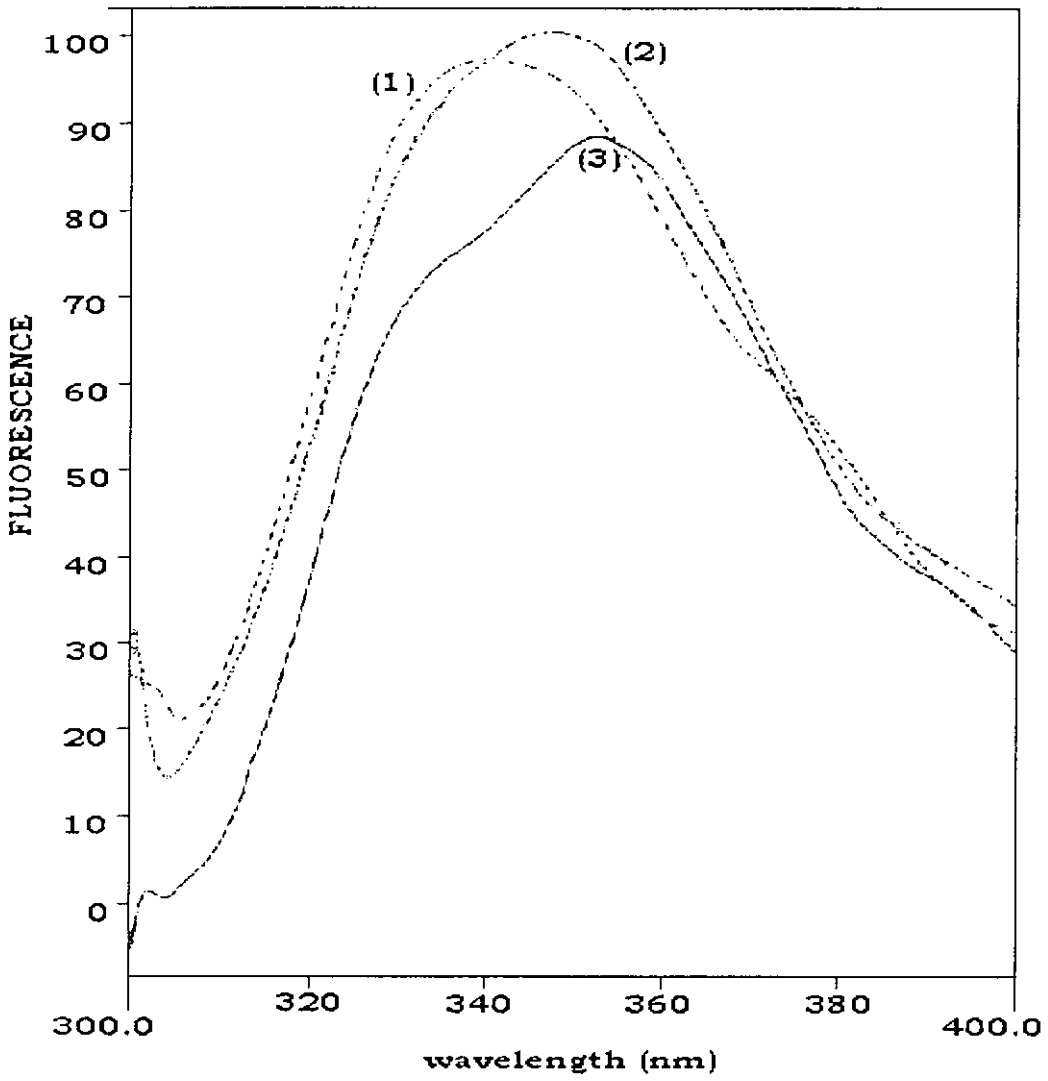

FIGURE 30: Emission spectra of mutant Δ16 in various concentrations of GdnHCl. The spectra recorded in the presence of 0 M *(curve 1)*, 0.5 M *(curve 2)*, and 2 M *(curve 3)*. The absorbance of the samples at the maximum of excitation (295 nm) were 0.1. The samples were treated with GdnHCl for 30 min at 25°C prior to recording the emission spectra.

CHAPTER FOUR

DISCUSSIONS & CONCLUSIONS

IV. DISCUSSIONS & CONCLUSIONS

4.1 DISCUSSIONS

Pyridoxal kinase (EC 2.7.1.35) is an enzyme which catalyze the formation of pyridoxal 5 phosphate (Vitamin B_6) by the transfer of phosphate from ATP to pyridoxal. It is an essential enzyme in the PLP biosynthesis pathway (McCormick *et al.*, 1961). The protein can be successfully purified to homogeneity from porcine brain, bovine brain, sheep brain and sheep liver. (Karawya and Margaret, 1978, Kwok and Churchich, 1979, Kerry *et al*, 1986, Sakurai *et al*, 1993). Pyridoxal kinase is a homodimer. The monomer contains two different domains which are linked by a polypeptide chain (Dominici *et al.*, 1989). Although same experiments had been performed on the structural characterization of pyridoxal kinase, little is known about the architecture of the protein. In recent years, the sequences of pyridoxal kinase from human, porcine (Hanna *et al.*, 1997 and Gao *et al.*, 1998) and rat have been cloned. In the multiple sequences alignment of porcine, human and rat sequences (Figure 4), 87 % sequence identity has been observed. The porcine kinase has the most extended amino acid residues at the N-terminus. In order to investigate the functional role of N-terminal sequence of porcine pyridoxal kinase, a series of truncated mutants were constructed. Interestingly, the extended fragment contains high proportion of glycine residues (MQAGSWVVGGGDSD). Since glycine is the smallest amino acid and undergoes the highest degree of freedom in the conformational change of the protein, it is thought that the extended fragment is probably essential

in the structural conformation or in the mechanism of folding. It is worth to know the structural significance of the extended fragment in the architecture of protein.

Mutants were constructed by polymerase chain reaction. Using this method with specific N-terminal primer, we can specify the deletion region and narrow down the deletion at a controlled manner. The ligation of the PCR product into a pGEM-T vector prior to a restriction step required for another ligation process of the mutated gene to go into the expression vector. This procedure appeared as a redundant experimental step. There are two main reasons for the chosen procedure. Firstly, the PCR product synthesised by Taq polymerase will introduce one extra deoxynucleotides onto it's 3'-end in a template-independent manner. Any one of the four nucleotides can be added when a mixture of all of them is present in the reaction, but preference is given to incorporation of dATP (Clark. 1988). Using this feature to ligate the PCR product into a T–tailing vector, pGEM-T, will increase the efficiency in the ligation process compared to that using the PCR product ligate to the expression vector pAED4 directly. Another reason is that the cDNA cloned into pGEM-T vector is convenient to perform sequencing by using fluorescein labeled M13 universal primers. Using these fluorescein primers, sequencing results are consistent. Although the cDNA ligated into the pAED4 vector could be sequenced using fluorescein labeled dATP, this internal labeling

sequencing method is not efficient when compared with the method that use fluorescein labeled primers.

In the construction of mutant expression vector, the *Hin*dIII-*Sac*I restricted fragment of the cDNA encoding pyridoxal kinase was replaced by a piece of the cDNA fragment from a mutant restricted by the same enzymes. Several restriction sites are available inside the pyridoxal kinase gene for restriction. A major reason for choosing the *Sac*I restriction site is that the restricted fragment can indicate the direction of the gene inserted in the vector. Since a *Sac*I site is located in the pGEM-T vector, it can be used (one is located in the pyridoxal kinase sequence, another is present in the pGEM-T vector) to determine the direction of PCR product. As shown in Appendix XII, PCR products can be inserted into pGEM-T vector in a bidirectional manner. When the N-terminal region is located near the M13-40 primer, three fragments are found after *Hin*dIII-*Sac*I digestion. However, when the N-terminal region of cDNA is close to the M13 reverse primer, only two fragments are found as the 47bp fragment is too small to observe. Thus, an appropriate primer can be selected for sequencing the N-terminal region.

According to the previous studies (Dominici *et al*, 1988, Dominici *et al*, 1989, Churchich *et al*, 1990 and Churchich, 1990), the substrates binding sites were believed to locate near the C-terminal rather than N-terminal of pyridoxal kinase. Nine sets of deletion mutants (Figure 5) were

constructed. If the deleted region did not interact with the substrate binding site located in the C-terminal region, catalytic activity of the mutant protein would not be affected. In fact, experimental results have shown that deletions of several amino acids at the N-terminus of pyridoxal kinase influence the catalytic efficiency of the enzyme. Catalytic activity of pyridoxal kinase was detected in the mutant Δ15 and Δ16. Further deletion of 17, 18, 21, 24, 27, 45 and 61 amino acid residues at the N-terminus were found to contain no detectable level of pyridoxal kinase activity. Although an efficient expression system for porcine pyridoxal kinase was established (Gao *et al*, 1998), the design of these deletion mutants inevitably results in the alteration of DNA sequence in which such changes in the sequence will ultimately affect performance of the present *E.coli* expression system. This is indicated by the reduced level of expression in mutants. The major problem in the reduced expression level of cloned genes is the failure of the polypeptides to reach the native state, leading to their aggregation within the inclusion bodies (Marston, 1986). Generally, inclusion bodies derived from folding intermediaties rather than the native state contain inactive expressed enzymes (Mitraki and King, 1989, Bowden *et al*, 1991, Buchner and Rudolph, 1991 and Kiefhaber *et al*, 1991). Proteins which are active require systematic folding mechanisms during the folding process. Disappearance of several amino acid residues may delay the folding process leading to accumulation of folding intermediates that aggregate to form inclusion bodies (Teschke and King, 1992). In the case of bacterial luciferase which is a heterodimer, the enzyme comprises of α and β

polypeptide that folds and dimerizes in a concerted manner *in vivo*. When the two polypeptide expressed individually, they are difficult to form an active dimers even when the extracts are mixed together. In contrast, when the soluble protein extracts are first treated with denaturant and allowed to refold together, active dimers are built indicating that the subunits must interact during the folding process, and that at least one of the structures formed when the subunits are folded separately is in a conformation that is incapable of interaction. Also, if amino acids at the carboxyl termini of the β subunit are deleted and altered, there is a drastic conditional defect that impairs heterodimer formation, but once formed it is as stable as the wild-type enzyme (Waddle *et al*, 1987 and Sugihara and Baldwin, 1988). Regarding pyridoxal kinase, deletion of N-terminal region of pyridoxal kinase will probably delay the hetero-domain formation process and lead to the aggregation into inclusion bodies. Therefore, the N-terminal region is essential for native structure formation and it interact with other forming structure with respect to the remaining sequence in the formation of native structure during the folding process.

Previous reports (Kwok *et al*, 1987) have shown that the monomeric species of pyridoxal kinase are still catalytically competent. In order to show that the catalytic activity found in the mutant is still existing in the dimeric form, a native gradient gel was performed. From the gel, a protein with a molecular mass of 80 kDa was detected. The kinetic parameter measurement was performed in the three recombinant pyridoxal kinases,

i.e. wild-type, mutants Δ15 and Δ16. In our design of these recombinant pyridoxal kinase, proteins having six histidine residue at the N-terminal were designed. The fact that histidine residues cannot be cleaved from the protein after purification and leaves some uncertainty in the interpretation of the consequences of mutations. Nevertheless, catalytic properties of the expressed wild type enzyme as assessed by kinetic parameter measurement showed that it has similar K_m value for the substrates when compared to the enzyme purified from native pig brain. On the other hand, kinetic parameters measurements of active mutant (Δ15) showed that they have different K_m values for the substrates, ATP and pyridoxal, when compared to that measured in the wild-type. This indicates that conformational change in the substrate binding site may occur leading to alternation of the binding affinity for substrates.

Interestingly, the enzymatic activity of mutant Δ16 is unstable and was totally lost after purification. On the contrary, the enzymatic activity shown in mutant Δ15 was active after purification by following the same procedures. The difference between mutants Δ15 and Δ16 is that one more amino acid (Arg^{16}) was deleted in Δ16 at N-terminus. Thus this Arg^{16} residue appeared to be important in the catalytic mechanism of pyridoxal kinase. The loss of enzymatic activity in mutant Δ16 occurred after purification by nickel-chelating chromatography. Six histidine residues were located upstream the Arg^{16} of mutant Δ16 at the N-terminal. It is possible that the loss of enzymatic activity was due to conformational

changes when the close interaction of histidine residues with the active site domain was broken by histidine residues coupled onto nickel ions during purification. The conformational change cannot be reverted after separating the nickel ions from the hisidine tag. It implies that function of the N-terminal residues and especially Val^{15} is to stabilize the conformational structure of pyridoxal kinase.

Actually, functional role of the N-terminal region of the kinase still remains unclear. Explanations that the deletion either affects the global folding of pyridoxal kinase or the deleted regions of the polypeptide chain represent sites of contact with one of the substrate binding domains are possible. Structural studies on N-terminal deletion mutants Δ15 and Δ16 using a variety of physical and biochemical techniques were performed. Information on conformational heterogeneity as well as stability were collected by studying far-UV CD, TNP-ATP binding, and denaturant-induced unfolding.

Using CD spectroscopy, inactive mutant enzyme (Δ16) displays substantial perturbation of the secondary structure when compared to the wild-type protein. In addition, the emission spectrum of the tryptophanyl residues in the mutated species has been shown to be perturbed by low concentrations of GdnHCl indicating the fragility of the tertiary protein structure in the absence of the essential amino acid Val^{15} at the N-terminus. A red shift of the emitting chromophores in the protein was also observed indicating

exposure of the probe may be a result of the relaxation of the tertiary structure caused by improper folding. Affinity of the analogue TNP-ATP to the mutated protein Δ16 is shown to be lost, suggesting that the C-terminal domain does not adopt the native-like fold when the N-terminal domain is missed. Thus, it is possible that the amino acid residues involved in the N-terminus of the polypeptide chain are essential for the folding pathway and its relationship with the formation of the C-terminal domain should also be considered.

Unfolding studies of the enzyme in the presence of GdnHCl have revealed that denaturation of wild-type pyridoxal kinase proceeds through a concerted process, where folded and unfolded conformers are in equilibrium. On the other hand, the denaturation process of the mutant endowed with catalytic activity (Δ15) shows a biphasic pattern of unfolding, characteristic of a three-state model where an intermediate exists. It is in equilibrium with the folded conformer prior to the formation of unfolded species. Hence, deletion mutants of pyridoxal kinase are not only less stable than the wild-type species, but they also follow different folding pathways. It may be considered that the hydrophobic amino acid residues of the highly conserved section of the N-terminal contribute to stabilization of the whole protein structure. Although the topographical structure of pyridoxal kniase has not yet been reported, the possibility that a section of the N-terminal region is in close relation with the C-terminal domain formation exists.

4.2 CONCLUSIONS

In conclusion, the N-terminal region appeared to stablize the proper folding of pyridoxal kinase and involved in the folding process through folding intermediates in *E.coli* expression system. When the highly conserved section, RVLSIQHV, of the N-terminal was destroyed, the whole protein structure will no longer fold properly leading to the formation of inactive enzyme.

4.3 FUTURE DIRECTIONS

As discussed above, deletion of several amino acids at the N-terminal region resulted in loss of pyridoxal kinase activity and change of the folding pathway. On the contrary, the functional role of C-terminal domain is unknow in spite of several evidences shown that the substrate binding site is located near the C-terminal domain (Dominici *et al*, 1988 and 1989; Churchich *et al*, 1990). Deletion of the amino acids at the C-terminal of pyridoxal kinase should be performed to study the effect on the protein structure and investigate whether a section of the N-terminal region is in close relation with the C-terminal formation. Furthermore, point mutations of the extended N-terminus as well as the highly conserved regions should be performed to ascertain roles of individual amino acid residues in the enzyme.

REFERENCES

Blackshear, P.J. "Systems for polyacrylamide gel electrophoresis". *Methods in Enzymology,* Vol. 104, pp.237-255 (1984)

Bowden, G.A., Paredes, A.M., and Georgiou, G. "Structure and Morphology of Protein Inclusion Bodies in *Escherichia coli*". *Biotechnology*, Vol. 9, pp.725-730 (1991)

Buchner, J. and Rudolph, R., "Routes to Active Proteins from Transformed Micoorganisms". *Current Opinion in Biotechnology*, Vol. 2, pp. 532-538 (1991)

Bradford, M.M. "A rapid and sensitive method for quantitation of microgram quantities of protein utilizing the principle of protein-dye binding". *Analytical Biochemistry,* Vol. 72, pp.248-254 (1976)

Cash, C.D., Maitre, M., Rumigny, J.F., and Mandel, P. "Rapid purification by affinity chromatography of rat brain pyridoxal kinase and pyridoxine-5-phosphate oxidase". *Biochemical & Biophysical Research Communications*, Vol. 96, pp.1755-1760 (1980)

McCormick, D.B., Gregory, M.E. and Snell, E.E. "Pyridoxal phosphokinases. I. Assay, distribution, purification and properties". *Journal of Biological Chemistry,* Vol.256, pp.2076-2084 (1961)

Clark, J.M. "Novel non-templated nucleotide addition reactions catalyzed by procaryotic and eucaryotic DNA polymerases". *Nucleic Acids Research*, Vol.16, pp.9677-9686 (1988)

Churchich, J.E. "Cleavage of Pyridoxal Kinase into Two Structural Domains: Kinetics of Proteolysis Monitored by Emission Anisotropy". *Journal of Protein Chemistry,* Vol. 9, pp.613-621 (1990)

Churchich, J.E., Scholz, G., and Kwok, F. "Activation of pyridoxal kinase by metallothionein". *Biochimica et Biophysica Acta,* Vol. 996, pp.181-186 (1989)

Dominici, P., Kwok, F., and Churchich, J.E. "Proteolytic cleavage of pyridoxal kinase into two structural domains". *Biochimie.*, Vol. 71, pp.585-590 (1989)

Dominici, P., Scholz, G., Kwok, F., and Churchich, J.E. "Affinity Labeling of Pyridoxal Kinase with Adenosine Polyphosphopyridoxal". *Journal of Biological Chemistry*, Vol. 263, pp.14712-14716 (1988)

Gao, Z.G., Lau, C.K., Lo, S.C., Choi, S.Y., Churchich, J.E., and Kwok, F. "Porcine pyridoxal. c-DNA cloning, expression and confirmation of its primary sequence". *International Journal of Biochemistry and Cell Biology,* Vol. 30, pp.1379-1388 (1998)

Hamer, D.H. "Metallothionein". *Annual Review of Biochemistry,* Vol. 55, pp.913-951 (1986)

Hanna, M.C., Turner, A.J. and Kirkness, E.F. "Human pyridoxal kinase. cDNA cloning, expression, and modulation by ligands of the benzodiazepine receptor". *Journal of Biological Chemistry*, Vol. 272, pp.10756-10760 (1997)

Kadowaki, H., Kadowaki, T., Wondisford, F.E. and Taylor, S.I. "Use of polymerase chain reaction catalyzed by Taq DNA polymerase for site-specific mutagenesis". *Gene,* Vol. 76, pp.161-166 (1989)

Karawya, E. and Fonda, M.L. "Purification, Assay, and Kinetic Properties of Sheep Liver Pyridoxal Kinase". *Analytical Biochemistry,* Vol. 90, pp.525-533 (1978)

Kerry, J.A., Rohde, M. and Kwok, F. "Brain pyridoxal kinase: Purification and characterization". *European Journal of Biochemistry,* Vol. 158, pp.581-585 (1986)

Kiefhaber, T., Rudolph, R., Kohler H.H. and Buchner, J. "Protein Aggregation In Vitro and In Vivo: A Quantitative Model of the Kinetic Competition Between Folding and Aggregation". *Biotechnology,* Vol. 9, pp. 825-829 (1991)

Kwok, F. and Churchich, J.E. "Brain Pyridoxal Kinase. Mobility of the Substrate Pyridoxal and Binding of Inhibitors to the Nucleotide Site". *European Journal of Biochemistry,* Vol. 93, pp.229-235 (1979a)

Kwok, F. and Churchich, J.E. "Brain Pyridoxal Kinase: Purification, substrate specificities, and sensitized photodestruction of an essential histidine". *Journal of Biological Chemistry,* Vol. 254, pp.6489-6495 (1979b)

Kwok, F., Scholz, G. and Churchich, J.E. "Brain pyridoxal kinase dissociation of the dimeric structure and catalytic activity of the monomeric species". *European Journal of Biochemistry,* Vol. 168, pp.577-583 (1987)

Laemmli, U.K. "Cleavage of structural proteins during the assembly of the need of bacteriophage T4". *Nature,* Vol. 227, pp.680-686 (1970)

Leklem, J.E., "Vitamin B-6 metabolism and function in humans". In Leklem, J.E. and Reynolds, R.D., eds., *Clinical and Physiological Applications of Vitamin B-6*, A. R. Liss, New York, pp.1-26 (1988)

Lu, T., VanDyke, M. and Sawadogo, M. "Protein-protein interaction studies using immobilized oligohistidine fusion proteins". *Analytical Biochemistry,* Vol. 213, pp.318-322 (1993)

Lumeng, L., Brashear, R.E. and Li, TK. "Pyridoxal 5'-phosphate in plasma: source, protein binding, and cellular transport". *Journal of Laboratory & Clinical Medicine*, Vol. 84, pp.334-343 (1974)

Lumeng, L. and Li, TK. "Mammalian vitamin B-6 metabolism: regulatory role of protein binding and the hydrolysis of pyridoxal 5'-phosphate in storage and transport". In Tryfiates, G.P. ed., *Vitamin B-6 Metabolism and Role in Growth*, Food and Nutrition Press, Westport, pp.27-51 (1980)

Magneson, G.R., Puvathingal, J.M. and Ray, W.J. "The concentrations of free Mg^{2+} and free Zn^{2+} in equine blood plasma". *Journal of Biological Chemistry*, Vol. 262, pp.11140-11148 (1987)

Marston F.A.O. "The Purification of Eucaryotic Polypeptides Synthesized in *Escherichia coli*". ***Biochemical Journal***, Vol. 240, pp. 1-12 (1986)

Messing J., Crea R. and Seeburg P.H. "A system for shotgun DNA sequencing". *Nucleic Acids Research*, Vol. 9, pp.309-321 (1981)

Mitraki, A. and King, J. "Protein Folding Intermediates and Inclusion Body Formation". *Biotechnology*, Vol. 7, pp. 690-699 (1989)

Neary, J.T. and Diven, W.F. "Purification, properties, and a possible mechanism for pyridoxal kinase from bovine brain". *Journal of Biological Chemistry,* Vol. 245, pp.5585-5593 (1970)

Pineda, T. and Churchich, J.E. "Reversible Unfolding of Pyridoxal Kinase". *The Journal of Biological Chemistry,* Vol. 268, pp.20218-20222 (1993)

Sambrook J., Fritsch E.F. and Maniatis T. *Molecular Cloning: A Laboratory Manual*, 2nd ed, Cold Spring Harbor Laboratory Press, USA (1989)

Sauberlich, H.E. "Section IX. Biochemical systems and biochemical detection of deficiency". In Serbrell W.H. and Harris, R.S. eds., *The Vitamins: Chemistry, Physiology, Pathology, Assay,* 2nd ed. Vol. II, Academic Press, New York, pp.44-80 (1968)

Sauberlich, H.E. "Interaction of vitamin B_6 with other nutrients". In Reynolds, R.D. Leklem, J.E. eds. *Vitamin B_6: Its Role in Health and Disease*, A. R. Liss, New York, pp.193-217 (1985)

Scholz, G. and Kwok, F. "Brain Pyridoxal Kinase: Photoaffinity Labeling of Substrate-binding Site". *Journal of Biological Chemistry*, Vol. 264, pp.4318-4321 (1989)

Scholz, G., Kwok, F. and Churchich, J.E. "Binding of a photoaffinity analogue of pyridoxal to pyridoxal kinase". *European Journal Biochemistry,* Vol. 193, pp.479-484 (1990)

Scott, T.C. and Phillips, M.A. "Characterization of *Trypanosoma brucei* pyridoxal kinase: purificaiton, gene isolation and expression in *Escherichia coli*". *Molecular and Biochemical Parasitology,* Vol. 88, pp.1-11 (1997)

Sugihara, J. and Baldwin, T.O. "Effects of 3' End Deletions from the Vibrio barveyi LuxB Gene on Luciferase Subunit Folding and Enzyme Assenbly; Generation of Temperature-sensitive Polypeptide Folding Mutants". *Biochemistry*, Vol. 27, pp. 2872-2880 (1988)

Teschke C.M. and King J. "Folding and assembly of oligomeric proteins in *Escherichia coli*". *Current Opinion in Biotechnology*, Vol. 3, pp. 468-473 (1992)

Vallette, F., Mege, E., Reiss, A. and Adesnik, M. "Construction of mutant and chimeric genes using the polymerase chain reaction". *Nucleic Acids Research,* Vol. 17, pp.723-733 (1989)

Wada, H. and Snell, E.E. "The enzymatic oxidation of pyridoxine and pyridoxamine phosphates". *Journal of Biological Chemistry,* Vol. 236, pp.2089-2095 (1961)

Waddle, J.J., Johnston, T.C. and Baldwin, T.O. "Polypeptide Folding and Dimerization in Bacterial Luciferase Occur by a Concerted Mechanism In Vivo." *Biochemistry*, Vol. 26, pp. 4917-4921 (1987)

Yang, Y., Zhao, G. and Winkler, M. E. "Identification of the pdxK gene that encodes pyridoxine (vitamin B_6) kinase in *Escherichia coli* K-12". *FEMS Microbiology Letters*, Vol. 141, pp.89-95 (1996)

APPENDICES

APPENDIX I

REAGENTS AND SOLUTIONS

A. *Ampicillin (50mg/ml)*

10 g ampicillin (sodium salt)

Dissolve the ampicillin in 200 ml water (final volume) and sterilize by filtration (0.22 μM filter). Dispense into aliquots and store at –20°C.

B. *IPTG (Isopropyl β-D-thiogalactopyranoside) stock solution (0.1M)*

1.2g IPTG

Add water to 50 ml final volume. Filter-sterilze and store at 4°C

C. *LB (Luria-Bertani) medium (per liter)*

10 g Bacto®-Tryptone

5 g Bacto®-Yeast Extract

5 g NaCl

Adjust pH to 7.0 with NaOH.

D. *LB plates with ampicillin*

Add 15 g agar to 1 liter of LB medium. Allow the medium to cool to 50°C before adding ampicillin to a final concentration of 100 μg/ml. Pour 30-35 ml of medium into 85 mm petri dishes. Let the agar harden. Store at 4°C for up to one month or at room temperature for up to one week.

E. LB plates with ampicillin/IPTG/X-Gal

Make the LB plates with ampicillin as above; then supplement with 0.5 mM IPTG and 80 μg/ml X-Gal may be spread over the surface of an LB-ampicillin plate and allowed to absorb for 30 minutes at 37°C prior to use.

F. SOC medium (100ml)

2.0 g Bacto®-Tryptone

0.5 g Bacto®-Yeast Extract

1 ml 1 M NaCl

0.25 ml 1M KCl

1 ml 2M Mg^{2+} stock (1M $MgCl_2 \cdot 6H_2O$/ 1M $MgSO_4 \cdot 7H_2O$), filter-sterilized

1 ml 2M glucose, filter-sterilized

Add Bacto®-Tryptone, Bacto®-Yeast Estract, NaCl and KCl to 97 ml distilled water. Stir to dissolve. Autoclave and cool to room temperature. Add 2M Mg^{2+} stock and 2 M glucose, each to a final concentration of 20 mM. Bring to 100 ml with sterile, distilled water. Filter the complete medium through a 0.2 μm filter unit. The final pH should be 7.0.

G. Solution I

50 mM glucose

25 mM Tris-HCl (pH8.0)

10 mM EDTA (pH8.0)

Solution I can be prepared in batches of approximately 100 ml, autoclaved for 15 minutes at 10 lb/sq. in. on liquid cycle, and stored at 4°C.

H. Solution II

0.2 N NaOH (freshly diluted from a 10 N stock)

1 % SDS

I. Solution III

60 ml	**5M potassium acetate**
11.5 ml	**glacial acetic acid**
28.5 ml	**H_2O**

The resulting solution is 3 M with respect to potassium and 5 M with respect to acetate.

J. TBE electrophoresis buffer

10X stocks solution:

108 g Tris base

55 g Boric acid

40 ml 0.5 M EDTA,

pH8.0

H_2O to 1 liter

0.5X working solution:

0.045 M Tris-borate

0.001 M EDTA

K. X-Gal (5-bromo-4-chloro-3-indolyl-β-D-galactoside) (2 ml)

100 mg X-Gal

Dissolve in 2 ml N,N'-dimethyl-formanide. Cover with aluminum foil and store at –20°C.

APPENDIX II

PK-pAED4 RESTRICTION MAP

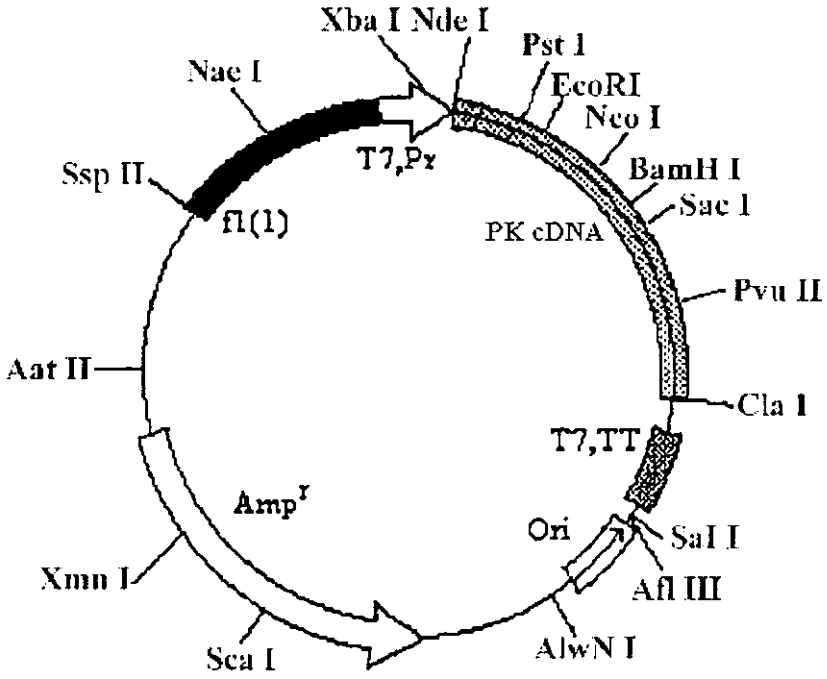

APPENDIX III

DNA MOLECULAR WEIGHT MARKER III (0.12-21.2 kbp)

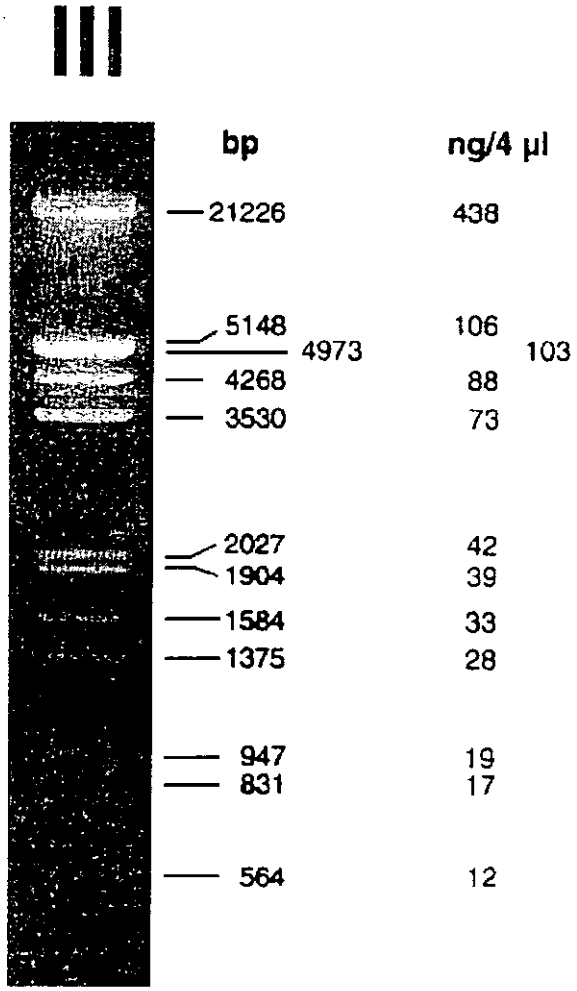

APPENDIX IV

100 BASE-PAIR LADDER

APPENDIX V

RESTRICTION ENZYMES

Restriction enzymes	Units/ml	Inactivation Temp
*Hin*dIII	18,000	85°C
*Sac*I	8,000	65°C
*Pvu*II	5,000	65°C

Unit Definition: **One unit of restriction enzyme will digest 1 μg λDNA in 50 μl assay buffer in 1 hour at 37°C.**

Storage buffer: **10 mM Tris-HCl (pH7.5), 50% glycerol, 300 mM KCl, 1 mM DTT, 0.1 mM EDTA, 300 μg BSA/ml.**

Dilution Buffer: **10 mM Tris-HCl (pH7.5), 50% glycerol, 300 mM KCl, 1 mM DTT, 0.1 mM EDTA, 100 μg BSA/ml.**

Assay Buffer: **1x One-Phor-All Buffer PLUS. OPA+ is supplied at 10x concentration (100 mM Tris-acetate (pH7.5), 100 mM magnesium acetate, and 500 mM potassium acetate).**

APPENDIX VI

PLASMID DNA PURIFICATION BY WIZARD™ *PLUS* MINIPREPS DNA PURIFICATION

A. Cell Resuspension Solution

50 mM Tris-HCl, pH 7.5

10 mM EDTA

100 μg/ml RNase A

B. Cell Lysis Solution

0.2 M NaOH

1 % SDS

C. Neutralization Solution

1.32 M potassium acetate, pH4.8

D. Column Wash Solution

80 mM potassium acetate

8.3 mM Tris-HCl, pH7.5

40 μM EDTA

55 % ethanol

APPENDIX VII

AUTOCYCLE™ SEQUENCING KIT

Components

dNTP Solution	dATP, dCTP, c^{7}dGTP and dTTP in solution
ddATP Solution	ddATP in solution
ddCTP Solution	ddCTP in solution
ddGTP Solution	ddTTP in solution
Taq DNA Polymerase	In buffered glycerol solution
Reaction Buffer	A buffered solution containing $MgCl_2$
DMSO	Dimethyl sulfoxide
A.L.F. M13 –40 Primer	5'-Fluorescein- d[CGCCAGGGTTTTCCCAGTCACGAC]-3' in aqueous soluion (1 pmol/μl; 0.24 A_{260} unit/ ml)
A.L.F. M13 Reverse Primer	5'-Fluorescein- d[TTTCACACAGGAAACAGCTATGAC]-3' in aqueous solution (1 pmol/μl; 0.24 A_{260} unit/ ml)
Stop Solution	Deionized formamide/blue dextran
Mineral Oil	Light, 100% mineral oil; DNase-, RNase- and protease-free
Control DNA	pUC18 DNA in TE buffer (500 μg/ ml)
Enzyme Dilution Buffer	A buffered solution containing Tween 20 and NP-40

APPENDIX VIII

AUTOREAD™ SEQUENCING KIT

Components

T7 DNA Polymerase	**In buffered glycerol solution**
Annealing Buffe:	**A buffered solution containing $MgCl_2$**
Extension Buffer	**A buffered solution containing DTT**
Enzyme Dilution Buffer	**A buffered solution containing glycerol, BSA and DTT**
DMSO	**Dimethyl sulfoxide**
Stop Solution	**Deionized formamide / blue dextran**
Fluore-dATP labelling Mix	**Fluorescein-15-dATP in solution with dCTP, dGTP and dTTP**
T7PR primer	**5'TTA ATA CGA CTC ACT ATA GG3'**

APPENDIX IX

6xHis-PK-pAED4 RESTRICTION MAP

Schematic diagram of pyridoxal kinase cDNA inserted into His-tagged pAED4 expression vector. The pyridoxal kinase cDNA with histidine tag (grayed region) at the N-terminus and separated by a *Hin*dIII restriction site (italic). *Nde*I site (italic), containing a ATG (bolded) start codon, is located at the beginning of histidine-tag.

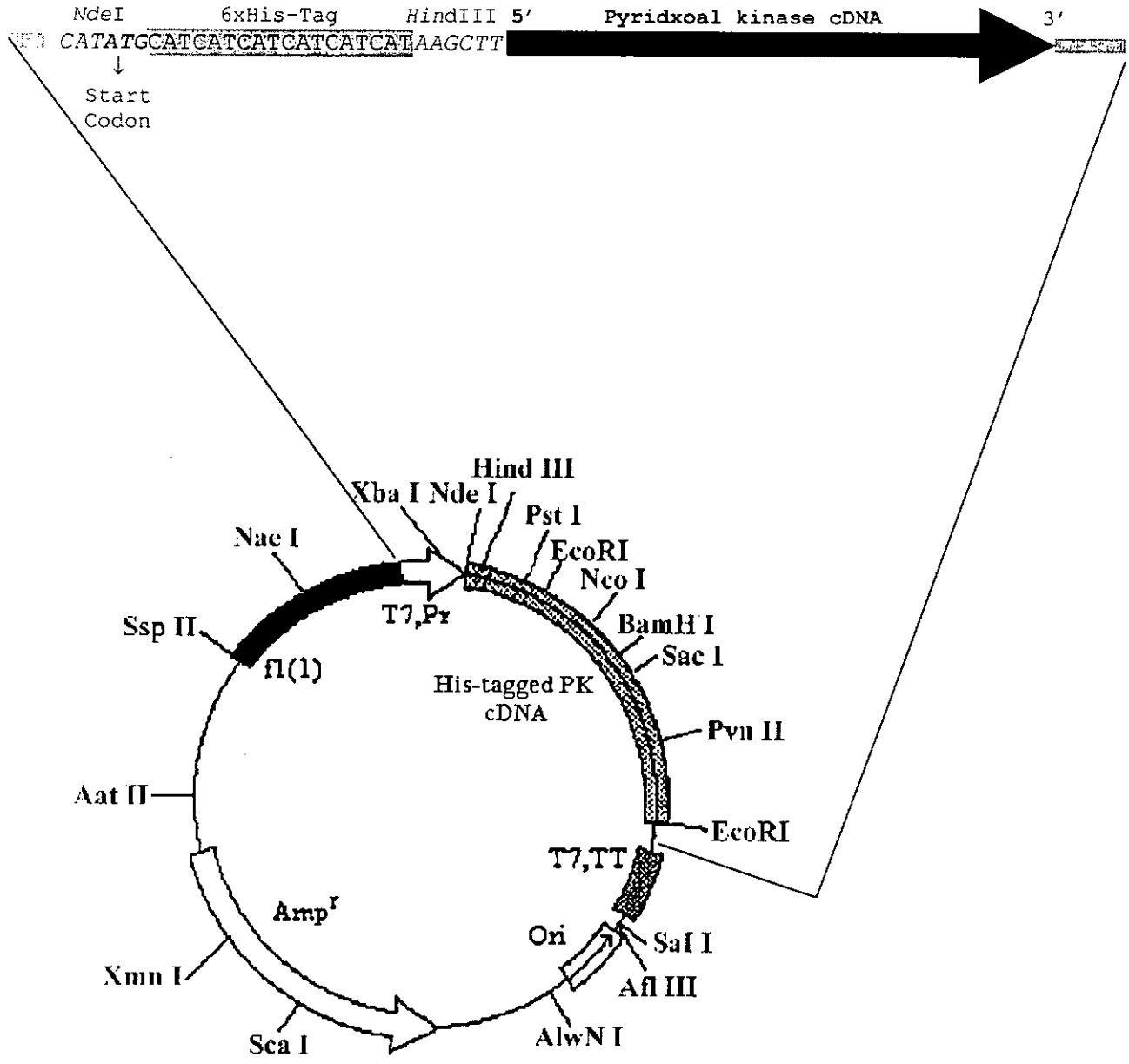

APPENDIX X

REAGENTS AND GEL PREPARATION FOR SDS-PAGE SLAB GELS

I Reagents

A. Acrylamide/bis (30% T, 2.67% C)

87.6 g acrylamide

2.4 g N'-N'-bis-methylene-acrylamide

Make to 300 ml with distilled water. Filter and store at 4°C in the dark.

B. 1.5 M Tris-HCl, pH 8.8

27.23 g Tris base

80 ml distilled water

Adjust to pH 8.8 with 1N HCl. Make to 150 ml with distilled water and store at 4°C.

C. 0.5 M Tris-HCl, pH6.8

6 g Tris base

60 ml distilled water

Adjust to pH 6.8 with 1N HCl. Make to 100 ml with distilled water and store at 4°C.

D. Sample buffer (SDS reducing buffer)

Distilled water	**4.0 ml**
0.5 M Tris-HCl, pH6.8	**1.0 ml**
Glycerol	**0.8 ml**
10 % (w/v) SDS	**1.6 ml**
2-b-mercaptoethanol	**0.4 ml**
0.05 % (w/v) bromophenol blue	**0.2 ml**

E. 5X electrode (Running) buffer, pH8.3

Tris base	**9 g**
Glycine	**43.2 g**
SDS	**3 g**
to 600 ml with distilled water	

Diluted 60 ml 5 X stock with 240 ml distilled water for one electrophoretic run.

II Gel Preparation

	12 % Separatng Gel Preparation	4 % Stacking Gel Preparation
Distilled water	**3.35 ml**	**6.1 ml**
1.5M Tris-HCl, pH 8.8	**2.5 ml**	**---**
0.5M Tris-HCl, pH 6.8	**---**	**2.5 ml**
10% (w/v) SDS stock	**100 µl**	**100 µl**
Acrylamide/Bis (30% Stock)	**4.0 ml**	**1.3 ml**
10% APS (Ammonium persulphate)	**50 µl**	**50 µl**
TEMED	**5 µl**	**10 µl**

APPENDIX XI

SEQUENCE OF THE pGEM-T VECTOR

The sequence supplied below is the part of circular pGEM-5Zf(+) Vector from which the pGEM-T Vector is derived. The pGEM-T Vector has been linearized with EcoR V at base 51 of this sequence (indicated by an asterisk) and a T added to both 3'ends. The added T is not included in this sequence. The M13-40 primer flanked region was underlined. The M13 reverse primer flanked region was grayed. The arrows shown the direction of primers. The *Sac*I restriction site in pGEM-T vector was bolded and italic typed.

```
2901    AAGGGGGATG  TGCTGCAAGG  CGATTAAGTT  GGGTAACGCC  AGGGTTTTCC
                                                →
2951    CAGTCACGAC  GTTGTAAAAC  GACGGCCAGT  GAATTCTAAT  ACGACTCACT
3001    ATA

1       GGGCGAATTG  GGCCCGACGT  CGCATGCTCC  CGGCCGCCAT  GGCCGCGGGA
51      T*ATCACTAGT GCGGCCGCCT  GCAGGTCGAC  CATATGGGAG  AGCTCCCAAC
101     GCGTTGGATG  CATAGCTTGA  GTATTCTATA  GTGTCACCTA  AATAGCTTGG
151     CGTAATCATG  GTCATAGCTG  TTTCCTGTGT  GAAATTGTTA  TCCGCTCACA
                    CAGTATCGAC  AAAGGACACA  CTTT
                                            ←
```

APPENDIX XII

SCHEMATIC DIAGRAM PYRIDOXAL KINASE CDNA INSERTED INTO PGEM-T VECTOR

There are three fragments observed in the *Hin*dIII and *Sac*I restriction enzyme digestion. The size of fragment 2 is depended on each deletion mutant and their size is listed in Table V.

(A)

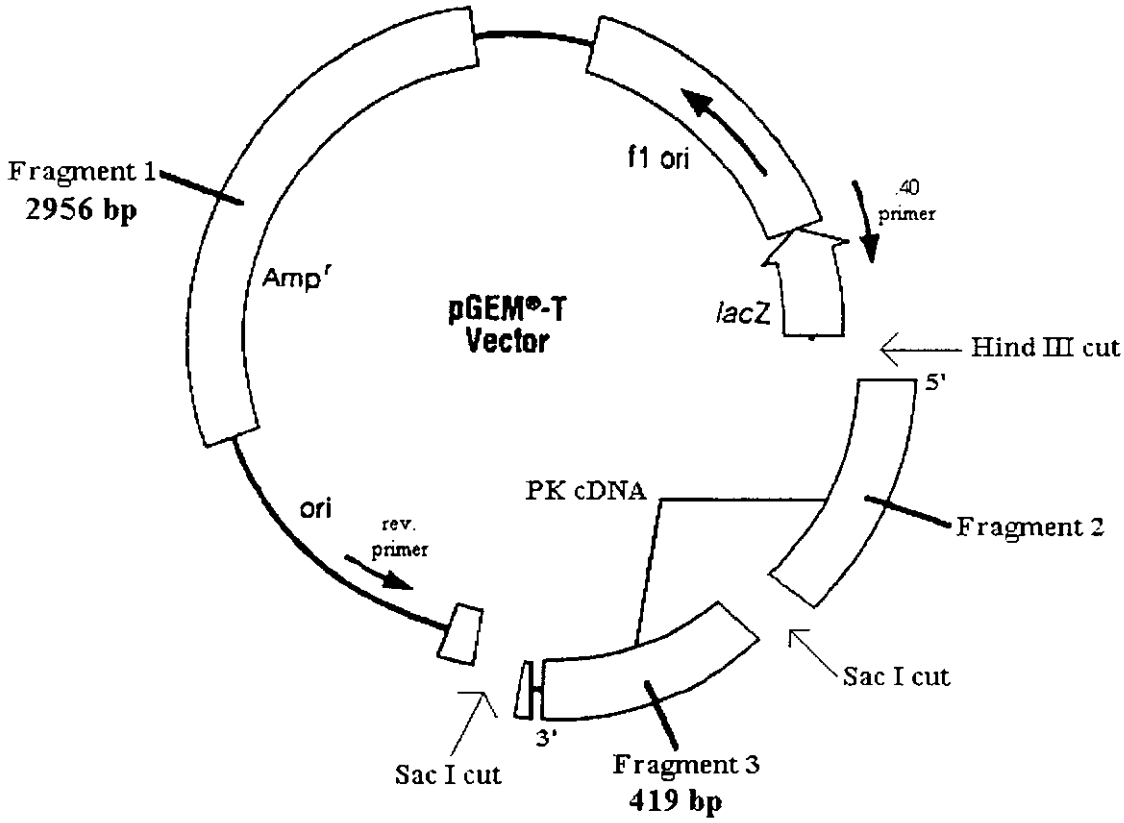

(B)

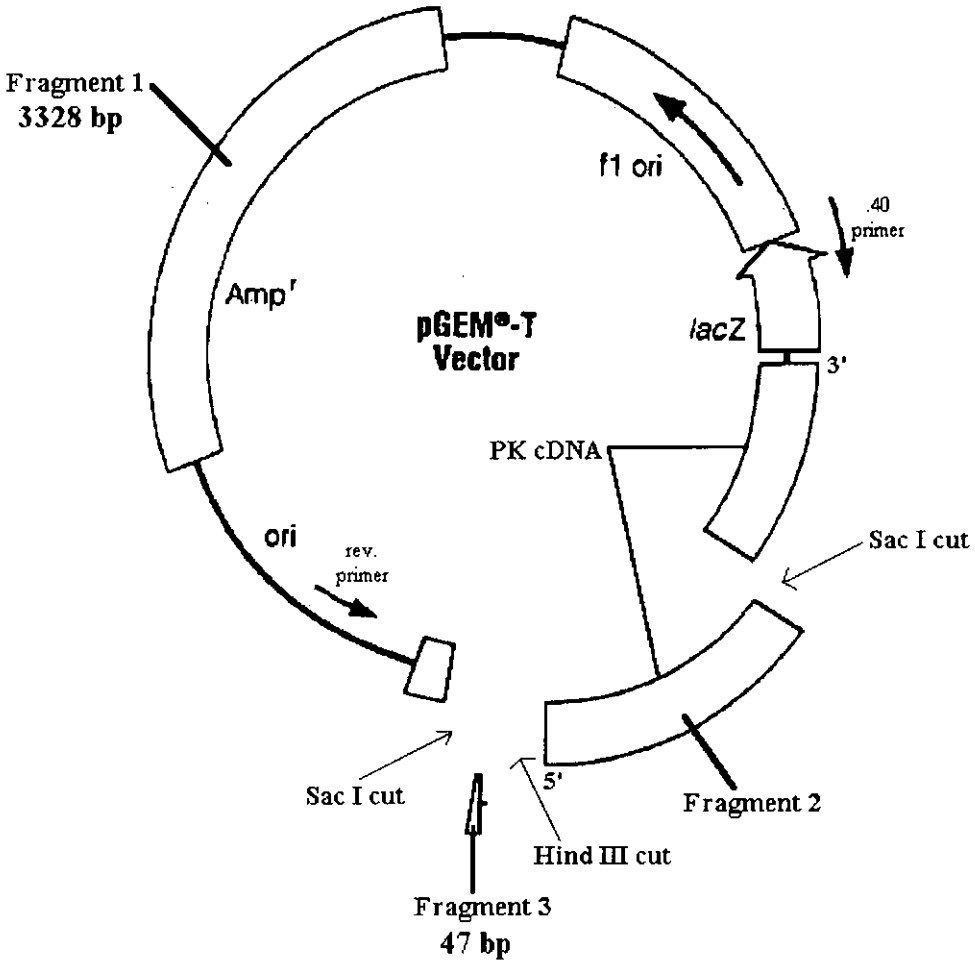
Fragment 1
3328 bp
f1 ori
40
primer
Amp'
pGEM®-T
Vector
lacZ
3'
PK cDNA
ori
rev.
primer
Sac I cut
Sac I cut
5'
Fragment 2
Hind III cut
Fragment 3
47 bp